IMPLANTABLE AMPEROMETRIC GLUCOSE/LACTATE SENSORS WITH NITRIC OXIDE RELEASE/GENERATION COATINGS FOR ENHANCED BIOCOMPATIBILITY AND NEEDLE-TYPE GLUCOSE SENSOR FOR TEAR GLUCOSE MEASUREMENTS

by

Qinyi Yan

A dissertation submitted in partial fulfillment
of the requirements for the degree of
Doctor of Philosophy
(Chemistry)
in The University of Michigan
2011

Doctoral Committee:

Professor Mark E. Meyerhoff, Chair
Professor Zhan Chen
Professor Steven P. Schwendeman
Professor Roseanne J. Sension

DEDICATIONS

This Work is Dedicated To:

My grandma Jinming Wu,
My parents Yunhua Yan and Yicheng Zhang,
My husband Wei Gu, and
My Lord and Savior Jesus Christ.

ACKNOWLEDGEMENTS

First and foremost, I would like to give my sincerest thanks to my mentor, Dr. Mark E. Meyerhoff. His insightful ideas, patient guidance and life-impacting mentoring have helped me through all my graduate study years. I am especially grateful for his advice, encouragement and inspiration during the difficult times of research. I will always be proud of being a Meyerhoff Group member and cherished with all the moments doing scientific research in this lab under his guidance.

I would also like to thank my doctoral committee: Dr. Zhan Chen, Dr. Roseanne J. Sension and Dr. Steven P. Schwendeman. I appreciate all the helpful advice and encouragement from my candidacy exam to my data meeting and final defense. Special thanks to Dr. Schwendeman for his support and generosity in the work related to poly(lactide-*co*-glycolide) (PLGA). I would especially like to thank Yajun Liu in Dr. Schwendeman's lab for her patient help in the PLGA project.

I would like to acknowledge my collaborator Terry Major from the Extra-Corporeal Membrane Oxygenation (ECMO) lab in the Department of Surgery at the University of Michigan Medical School. I would not have collected fruitful results without Terry's nice and patient collaboration in doing animal surgeries. I also

appreciate Terry's helpful advice in my manuscript writing. Sincere thanks also go to my collaborators at Eye Lab Inc.: Dr. Bruce E. Cohan, Zvi Flanders and Hannah Peshkin. Thank you very much for providing me with the opportunity to work on the great tear glucose project, for the good of people in need.

I owe thanks to many former and current graduate students as well as post-docs in the Meyerhoff Lab: Dr. Hyoungsik Yim, Dr. Melissa Reynolds, Dr. Megan Frost, Dr. Jason Bennett, Dr. Mariusz Pietrzak, Dr. Fenghua Zhang, Dr. Kun Liu, Dr. Kebede Gemene, Dr. Lajos Höfler, Dr. Arun Agarwal, Dr. Abdul Rehman, Dr. Gary Jensen, Dr. Jhindan Mukherjee, Dr. Wansik Cha, Dr. Zhengrong Zhou, Dr. Hairong Zhang, Dr. Sangyeul Hwang, Dr. Youngjea Kang, Dr. Yiduo Wu, Dr. Dongxuan Shen, Dr. Biyun Wu, Dr. Lin Wang, Dr. Jun Yang, Dr. Laura Zimmerman, Natalie Walker, Wenyi Cai, Bo Peng, Teng Xue, Andrea Bell, Liz Brisbois, Alex Wolf, Si Yang and Chuncui Huang, Hisham Abd-Rabboh and Ayman Eldourghamy. Thank you all for your thoughtful advice in my research as well as helping me sharpen my presentation skills plus proofreading my proposals, papers and thesis. Special thanks to Hairong Zhang as she guided and helped me with my rotation project. An extra-special thank you to Laura Zimmerman, who has not only been a perfect labmate, but also my best American friend who always teaches me American culture and makes me laugh.

Thanks also go to Wei Dai and Su Chen, my roommates for three years, for all their support and caring for me. Thank you Hangtian Song and Di Gao, who have given me help in research as well as friendship and support. Credits go to Gang Su as well,

who is in the Bioinformatics program at the University of Michigan, for his kind and professional advice and suggestions for my data analysis. I would also like to thank all the undergraduate students who did research projects with me: Lahdan Refahiyat, Adam Justusson, Andrew Robison and Kristen Wiese. You all have given me the precious experience of mentoring in chemistry. Special credits go to Drew who helped me do most of the work in Chapter 4 of this thesis. You've been the most diligent undergraduate student I have had the pleasure to work with.

Next, I would like to extend my thanks to my fellow Team Analytical '05: Chris Avery, Anna Clark, Kate Dooley, Katie Hersberger, Maura Perry and Laura Zimmerman plus her lovely husband Andy Zimmerman, as well as other fellow chemists Meghan Wagner and Matthew Remy. We have been together in classes, teaching, exams, lunch time and game nights. You have taught me so much about the US and I have been enjoying every moment with you guys. Most of us have also been part of the amazing softball team Killa-Joules. You have shown me the real sports team spirit that even when we were behind, there was never a single bad word spit out but encouragement and cheering. I will remember forever the sweat we shed on the diamonds, ice cream after games and the champion trophies that we deserved.

Along with my Ph.D. life in Ann Arbor, I have been blessed to be involved in the life at Ann Arbor Chinese Christian Church (AACCC). I would like to thank my beloved brothers and sisters in Christ who have been loving and supporting me, especially those from Grace Fellowship and FaHoLo Fellowship. I thank you all for your prayers, caring

and encouragement: Brent Hoover, Harold Yan, Hui Wang, Qin Li, Biyun Wu, Su Chen, Zhihua Zhang, Minghuai Wang, Ying Song, Xiaotong Zhang, Yu Qiao, Shengquan Wang, Benbo Song, Yibin Jiang, Wei Zhuang, Zhenzhen Xu, Shanshan Liang, Yilun Wu, Suyi Li, Wei Li, Sha Li, Zeyu Li, Hao Li, Shifang Li, Liuliu Du and Yue Yin. I also owe thanks to my dear mentors and host family Michael and Debbie Carr, for every bible study, prayer, heartfelt talk and family dinner we had together.

In addition, my great gratitude goes to my parents Yunhua Yan and Yicheng Zhang. Thank you for your unconditional love and unshakeable support all the way throughout my twenty-eight years of life, from my first step to learn how to read and write, to my Ph.D. defense, in a country far away from home. I am also incredibly thankful to my dearest husband Wei Gu, for his love, encouragement, inspiration and support. You have been my best friend and the most valuable gift God has ever given me. I always feel that we are so meant to be.

Last but not least, I would like to give my greatest thanks to my Lord and Savior Jesus Christ. Thank you for raising me up from this sinful world and showing me the way of light and hope. Thank you for giving me wisdom that I can use in my scientific research to help people in need. Thank you for giving me the abundant life, enriched by everything and everyone that has appeared. *"I have come that they may have life, and have it to the full." ~ John 10:10*

TABLE OF CONTENTS

LIST OF FIGURES

Figure

LIST OF TABLES

Table

ABSTRACT

IMPLANTABLE AMPEROMETRIC GLUCOSE/LACTATE SENSORS WITH NITRIC OXIDE RELEASE/GENERATION COATINGS FOR ENHANCED BIOCOMPATIBILITY AND NEEDLE-TYPE GLUCOSE SENSOR FOR TEAR GLUCOSE MEASUREMENTS

by

Qinyi Yan

Chair: Mark E. Meyerhoff

One of the greatest technological challenges of implantable biosensors is the biocompatibility problem that arises after implantation. Nitric oxide (NO) is known as a potent anti-thrombus and anti-inflammatory agent released by healthy endothelial cells. Hence, this dissertation research focuses on developing novel NO releasing/generating coatings to enhance the biocompatibility of implantable glucose/lactate sensors. A non-invasive method for detecting tear glucose levels is also proposed as a potential substitute for blood glucose measurements.

Novel NO releasing coatings are developed by doping poly(lactide-*co*-glycolide) (PLGA) with NO donors and top-coating with PurSil which can release NO > 1×10^{-10} mol $min^{-1}cm^{-2}$ for at least 7 days. Intravenous amperometric needle-type glucose/lactate sensors prepared with such coatings have excellent *in vitro* analytical performance. Glucose sensors with NO release show significantly enhanced hemocompatibility when implanted in rabbit veins for 8 h, with minimized thrombus formation on their surfaces and greater accuracy in measuring blood glucose levels, as evaluated using a Clarke error grid analysis.

Nitric oxide generating coatings, including Cu(II)-cyclen polyurethanes, Cu^0 nanoparticle-doped polyurethanes and 100 bilayers of organoselenium-linked polyethyleneimine (SePEI) and alginate (Alg), are employed on glucose/lactate sensors. These coatings all enable the sensors to generate NO from endogenous *S*-nitrosothiols (RSNOs), but there is some influence on the analytical performance of the sensors. Preliminary *in vivo* experiments indicated the possible need for additional RSNOs to generate sufficient NO fluxes.

An amperometric needle-type tear glucose sensor is described and employed in conjunction with a 0.84 mm i.d. capillary tube to collect 4-5 μL tear fluid. The sensor possesses excellent selectivity for glucose over potential electroactive interferent species, including ascorbic acid and uric acid. Further, the new sensor is optimized to achieve very low detection limits of 1.5 ± 0.4 μM of glucose (S/N=3) with a sensitivity of 0.019 ± 0.009 nA/μM (n=4). The glucose sensor is employed to measure tear glucose levels in

anesthetized rabbits over 8 h while also measuring the blood glucose values. A strong correlation between tear and blood glucose levels is found, suggesting that electrochemical measurement of tear glucose concentrations is a potential substitute for blood glucose measurements.

CHAPTER 1

INTRODUCTION

1.1 Overview of Dissertation Research

Biocompatibility has been the major technical challenge in the development of implantable sensors capable of continuously monitoring blood glucose and lactate (See Fig. 1.1 for structures) for people afflicted with diabetes or critically patients in the Intensive Care Unit (ICU) of a hospital. The intravenous thrombus formation and subcutaneous encapsulation by immune cells on the surfaces of implanted sensors greatly compromise the accuracy and reliability of such devices. Nitric oxide (NO) is well-known as a potent anti-thrombus and anti-inflammatory agent that exists endogenously [1-5]. The work described in this thesis is focused on developing biocompatible coatings for implantable glucose/lactate sensors with NO release/generation, based on the hypothesis that NO released/generated on the surfaces of implanted devices will reduce intravascular thrombus formation and subcutaneous inflammatory response. A newly developed glucose sensor intended for detecting glucose levels in tear fluid as a potential non-invasive way to monitor blood glucose will also be described herein.

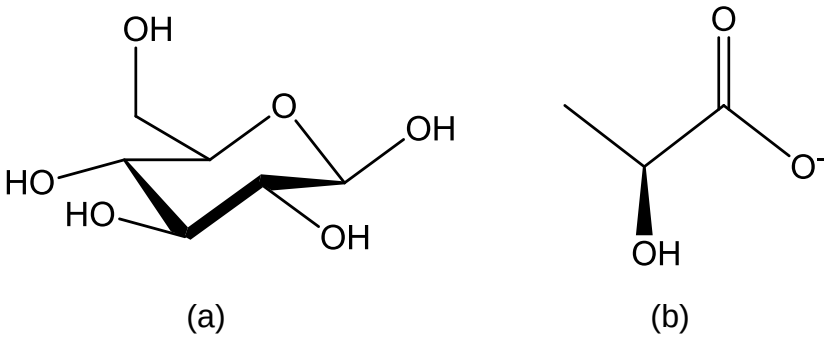

Figure 1.1. Structures of (a) glucose and (b) lactate.

This introductory chapter will discuss the importance of continuous monitoring of glucose/lactate and the current status regarding the development of implantable sensors with specific focus on the challenge of achieving biocompatibility. Then, the incorporation of NO release/generation into sensor coatings will be introduced, specifically in the case of a poly(lactide-*co*-glycolide) (PLGA) matrix. Lastly, the driving force behind the tear glucose measurement will also be discussed.

1.2 Increasing Need of Continuous Glucose/Lactate Monitoring for Diabetic and Critically-Ill Patients

According to the statistics from the World Diabetes Foundation, there are more than 285 million people currently diagnosed with diabetes in the world and the number is increasing every year [6]. For the past few decades, the dominant method for monitoring blood glucose, whether at home or in the hospital environment, has been intermittent measurement of capillary blood glucose, usually coupled with finger pricking. However, such measurements only provide isolated single-time point measurements that cannot fully reflect variations throughout the day and night. While there has recently

been great progress in the development of subcutaneous implantable electrochemical glucose sensors that provide real-time monitoring capability [7], there remain some issues regarding the lag time in response between changes in blood glucose levels and subcutaneous fluid concentrations, and requirements for frequent recalibration with blood levels. For critically ill hospital patients, in particular, there is growing evidence that tight control of blood glucose levels can be of benefit not only to diabetic patients, but also to non-diabetics [8-12]. In this environment, intravenous sensor placement would be the preferred mode to gain the most accurate assessment of real-time blood glucose levels.

Beyond glucose, the accurate monitoring of blood lactate levels is also of great biomedical importance in the critical care setting. Lactate plays a vital role in several biochemical processes that are involved in muscle movement, and it is the key metabolite of the anaerobic glycolytic pathway. In fact, blood lactate levels are now considered one of the most important indicators of the status of critically ill patients, with continuously elevated levels considered a key prognosticator of a poor outcome. Hence, for such patients, the ability to monitor lactate continuously via an intravenous catheter at the patient's bedside would provide a means to assess whether prescribed clinical therapies are working for survival [13-18].

1.3 Current Development of Implantable Glucose/Lactate Sensors and the Biocompatibility Problem

A number of miniaturized electrochemical blood glucose and lactate sensors have been reported in the literature [19-21]. Figure 1.2 shows a common schematic of both glucose and lactate sensor designs and the mechanism of the corresponding substrate measurements. The sensor is composed of a needle-type platinum/iridium (Pt/Ir) wire and wrapped with a silver/silver chloride (Ag/AgCl) reference electrode with glucose/lactate oxidase immobilized on the sensing area. An inner layer of polymers is deposited on the surface of the working electrode at the sensing area to eliminate potential interferences within the biological sample. An outer layer of polyurethane (PU)/polydimethylsiloxane (PDMS) is coated on the whole sensor in order to protect the implanted sensor. This layer also functions to limit the glucose/lactate diffusion rate, to prevent a lower concentration of oxygen (O_2) than the analyte in the enzymatic layer (that would yield non-linear response), so that the overall process is controlled by the diffusion of glucose/lactate rather than the pO_2 tension. Glucose/lactate diffuses into the enzyme layer and hydrogen peroxide (H_2O_2) is liberated from these enzymatic reactions with subsequent oxidation of H_2O_2 at the underlying electrode surface. The resulting anodic current is proportional to the concentration of glucose or lactate in the sample. Several commercial continuous glucose monitoring (CGM) systems based on subcutaneous devices have been developed for diabetic patients [22] (Fig. 1.3 (b)). Girardin et al. recently reviewed both the biochemical perspectives and clinical applications of these designs [23].

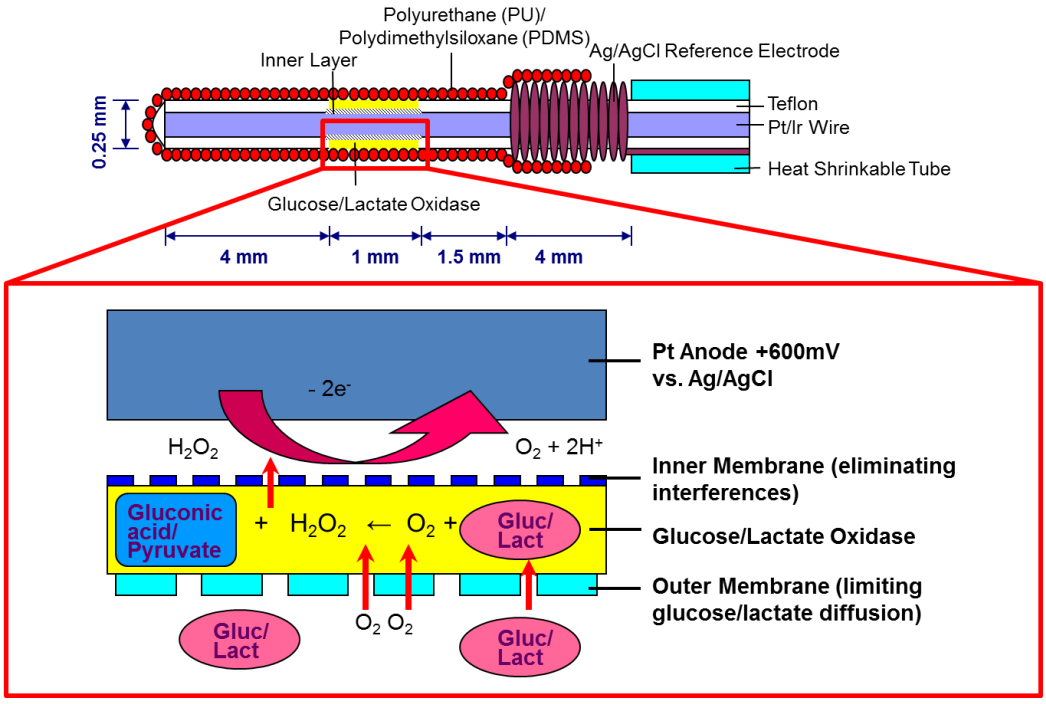

Figure 1.2. Schematic and the amperometric detection mechanism of glucose/lactate sensors.

However, the development of intravenous sensors that can function reliably for extended periods after implantation remains technologically challenging largely due to the biocompatibility issues that arise. When the sensor is implanted in the blood stream, especially within a readily available vein, thrombus formation can occur within minutes, triggered by platelet activation, adhesion and fibrin entanglement with blood cells (Fig 1.3 (a)) [24]. Similarly, implanted devices designed for subcutaneous measurements are also subject to biocompatibility issues, such as an inflammatory response that leads to a fibrotic encapsulation of the devices within a sheath of leukocytes, macrophages, fibroblasts, etc. (Fig 1.3 (b)) [22]. Both situations disturb the physiological environment of the implantation site and may lead to false values of local glucose or lactate concentrations and/or decrease mass transfer of the analyte to the immobilized enzyme

layer of the device. Either case can result in an unreliable analytical output which limits the lifetime and wide clinical use of such implantable sensors [25].

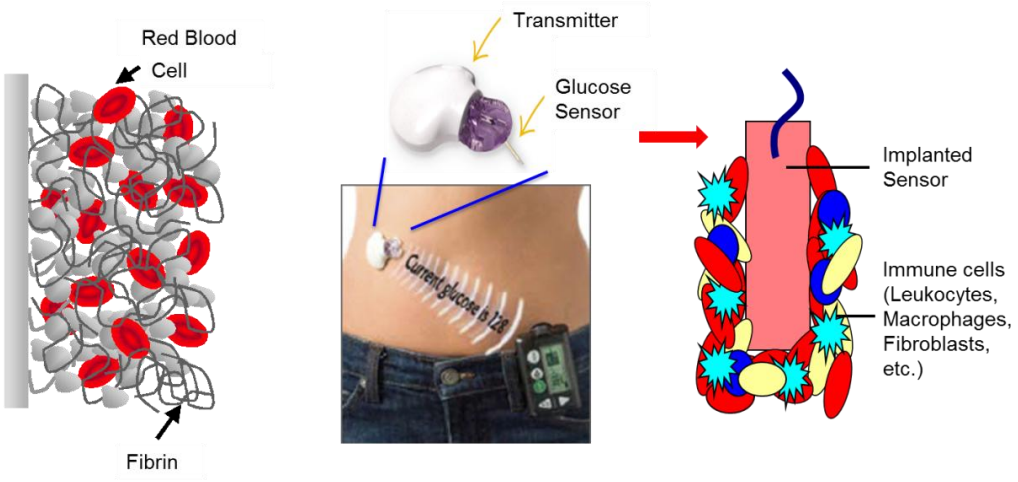

(a) (b)

Figure 1.3. (a) Thrombus formation on the surface of intravenous sensor and (b) immune cell encapsulation of subcutaneous sensor from a commercial CGM system [22].

1.4 Implantable Sensors with NO Release/Generation Polymeric Coatings

To overcome the hurdles discussed above, many researchers have focused on developing more biocompatible polymers for biomedical sensor applications. Several proposed approaches include the use of hydrogels, surfactants and other surface-bound species in the effort to minimize sensor biofouling [26-28]. Because protein adsorption is the first step in the eventual formation of thrombus on the surface of intravascular sensors, decreasing protein adsorption should improve blood compatibility. Unfortunately, none of the approaches that are intended to prevent protein adsorption

completely eliminate thrombus in low flow blood vessels or fully prevent subcutaneous inflammatory responses when tested *in vivo* [24].

The discovery of the anti-platelet and anti-inflammatory properties of NO has provided a new direction for research aimed at solving the fundamental biocompatibility problem of implanted sensors, as well as other blood contacting medical devices [2-5, 29-39]. Indeed, NO is well-known as a potent inhibitor of platelet function [1, 40]. In fact, NO is produced within endothelial cells (ECs) that line the walls of all healthy blood vessels, and serves to prevent clotting by inhibiting platelet activation. This led to the idea of coating intravascular-implanted sensors with polymers that can release or generate NO at physiological concentrations so that adhesion of cells (platelets) and concomitant thrombus formation at the surface of the sensor can be reduced (Fig. 1.4) [32]. Further, NO also inhibits the inflammatory response (reduces neutrophil and macrophage migration to the implant site), and promotes angiogenesis (growth of new blood vessels) [3-5]. These are both important effects that could greatly improve the biocompatibility of sensors implanted subcutaneously.

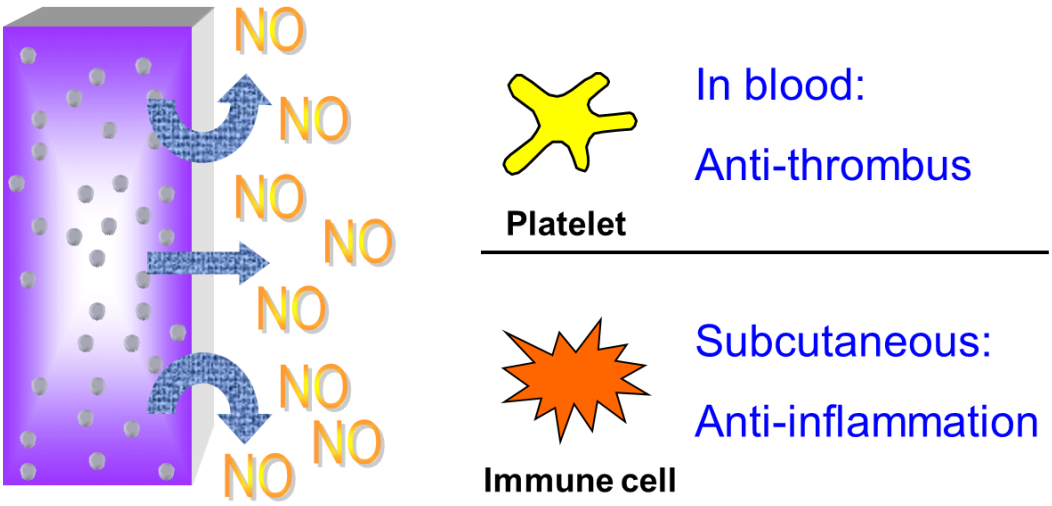

Figure 1.4. Concept of NO release/generation coatings on the surface of sensors implanted in blood to prevent thrombus formation and subcutaneously to reduce inflammation.

Intravascular oxygen sensors with NO release incorporated into silicone rubber coatings have been successfully fabricated as previously reported [33, 41]. Those sensors were implanted in swine arteries for 20 h and the ones with NO release exhibited enhanced hemocompatibility with much less thrombus formation on the sensor surfaces, while the control ones without any NO release formed obvious thrombus. The sensors with NO release also showed improved accuracy in reporting the blood oxygen levels, while the thrombus on the control sensor surfaces influenced the local oxygen concentrations near the sensing area, leading to the deviation from the bulk blood oxygen levels. Intravascular oxygen sensors with NO catalytically generated from endogenous *S*-nitrosothiols (RSNOs) have also been proposed and the *in vivo* experiment data showed similar enhanced hemocompatibility and excellent analytical accuracy of the sensors with NO generation compared to the control ones [36]. As a result, it is promising to

incorporate NO release/generation into implantable glucose/lactate sensors to realize anticipated biocompatibility.

1.4.1 NO Release Coatings Using Poly(lactide-*co*-glycolide) (PLGA)

Herein, we report results of efforts in this direction that make use of a newly formulated NO release coating that consists of a lipophilic diazeniumdiolate species (*N*-diazeniumdiolated dibutylhexanediamine, DBHD/N_2O_2) embedded within a layer of poly(lactide-*co*-glycolide) (PLGA), which is then covered by an outer layer of PurSil (polyurethane/dimethylsiloxane copolymer). DBHD/N_2O_2 readily releases NO upon contact with water by a proton driven mechanism [42] (Fig. 1.5). PLGA undergoes a slow hydrolysis process to generate lactic acid and glycolic acid [43] (Fig. 1.6). Therefore, the use of PLGA as a matrix for the diazeniumdiolate NO donor provides an added source of protons to promote extended NO release, without the need for using tetraphenylborate derivative additives as described in previous work [42], the presence of which was found herein to inhibit enzymatic activity of both glucose and lactate oxidases.

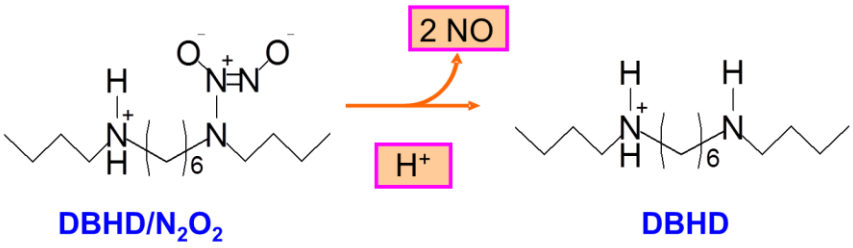

Figure 1.5. Proton driven reaction mechanism of NO release from DBHD/N_2O_2.

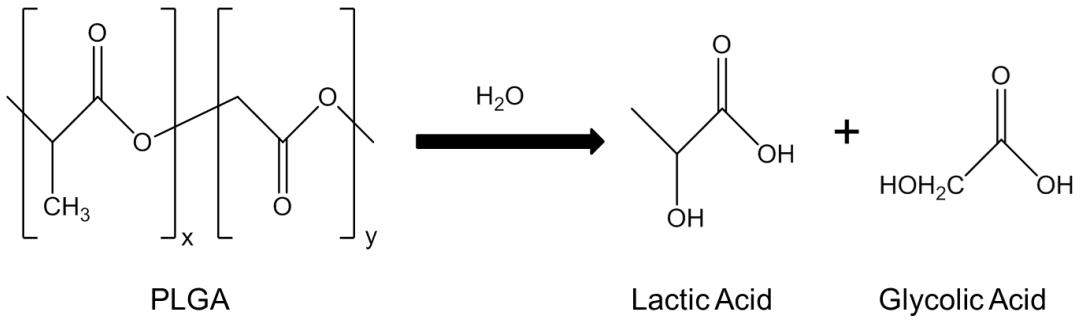

Figure 1.6. Hydrolysis of PLGA to form lactic acid and glycolic acid.

1.4.2 NO Generating Coatings

On the other hand, the NO release application on implantable sensors has its limits as the reservoir of the NO donor will be depleted over time. The diazeniumdiolates-doped PLGA matrix layer used to prepare glucose or lactate enzyme electrodes is typically rather thin (~30 μm from Fig. 3.4 in Chapter 3), thus the lifetime of NO release that can be achieved is limited by the amount of the NO donor loaded within the polymer coating. The thickness of the coating cannot be further increased, because this would greatly influence the glucose/lactate diffusion which will impact the sensor performance (e.g., reduce sensitivity, slow response times, etc.).

S-Nitrosothiols (RSNOs) are another class of NO donor species which are constantly produced in the body as a replenishing NO reservoir. They have been proven useful for developing polymeric coatings that release or generate low levels of NO [44, 45]. One mechanism to generate NO from RSNOs is via catalytic reactions with either Cu(II) [46] or organoselenium (RSe) species [47]. Hence, an attractive alternative to

using NO release polymers to make implantable sensors more biocompatible is to utilize polymeric coatings that can catalytically generate NO, locally at the surface of the implanted device, from the reservoir of RSNOs that already exists within blood. Figure 1.7 illustrates the concept of how polymeric coatings doped with immobilized Cu(II) complexes or RSe sites coated on catheter type sensors will generate NO locally from endogenous RSNO species in blood.

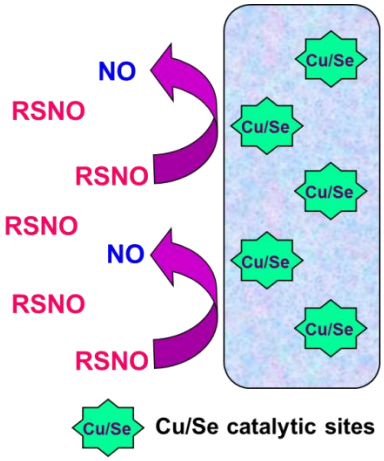

Figure 1.7. NO generating coatings with Cu/Se catalytic sites to generate NO from endogenous RSNO species.

Some important physiological RSNOs are *S*-nitrosoglutathione (GSNO) (Fig. 1.8 (a)), *S*-nitrosocysteine (CysNO) (Fig. 1.8 (b)) and *S*-nitrosoalbumin (AlbSNO) (Fig. 1.8 (c)). The estimated level of the primary endogenous RSNOs present in blood plasma is a subject of great debate, ranging from 10 nM to 7 μM [48]. However, recent studies in our lab using newly developed RSNO sensors suggest that levels in the μM range are likely, based on rapid measurements in whole blood of rabbits and pigs [49]. As a result, it is likely that there are enough endogenous RSNO species in blood to generate

physiological levels of NO from NO generating polymeric coatings. For subcutaneous applications, research is still needed to determine the RSNO levels in subcutaneous fluid.

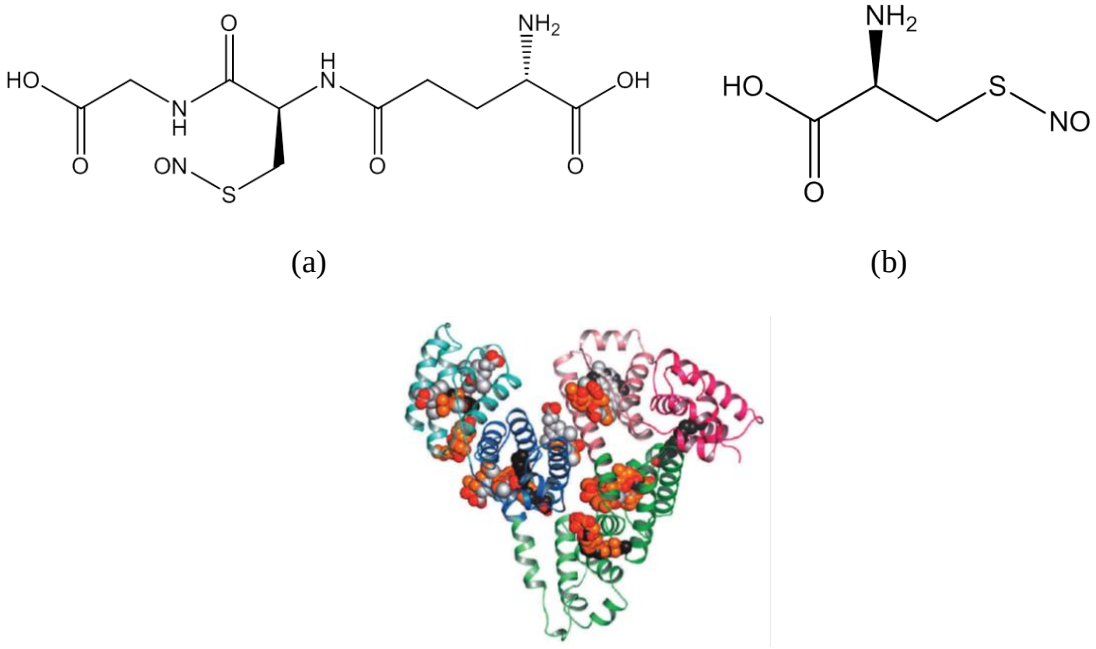

Figure 1.8. Structures of (a) GSNO, (b) CysNO and (c) AlbSNO (NO at Cys34).

In the case of Cu(II) mediated generation of NO, Cu(II) is first reduced to Cu(I) by an appropriate free thiol (RSH), such as cysteine (Cys) or glutathione (GSH), as well as ascorbate in blood or even extracellular fluid (eq 1.1). Then, Cu(I) readily reduces RSNO to NO and RSH [50, 51] (eq 1.2). Recent research in this group has demonstrated that this catalytic mechanism can be incorporated into polymers using immobilized Cu(II)-ligand complexes as catalytic sites [52-54], or small microparticles of Cu^{o} that can corrode to produce trace levels of Cu(II/I) ions that can then react with RSNOs to generate NO [36]. Local reduction of RSNOs to NO and thiolate anions will

provide the further reducing equivalents to assist in regenerating the Cu(I) sites. The Cu^0 strategy was used previously to examine the performance of catheter type electrochemical oxygen sensors implanted in arteries of pigs for up to 20 h, and the sensors that possess copper coatings (doped with Cu^0 nanoparticles) exhibited enhanced biocompatibility in terms of reduced thrombus, as well as improved analytical performance of accurately reporting blood oxygen levels [36]. It is potentially feasible to coat implantable glucose and lactate sensors with polymeric films containing Cu catalysts to generate NO from endogenous RSNO species for extended time periods when in contact with blood, and possibly subcutaneous fluid.

$$Cu^{2+} + RS^- \rightleftharpoons Cu^+ + 1/2\ RS\text{-}SR \qquad (1.1)$$

$$Cu^+ + RSNO \rightleftharpoons Cu^{2+} + RS^- + NO \qquad (1.2)$$

Another catalytic pathway that can be used to generate NO *in vivo* is via RSe species. Previously, it has been demonstrated that NO generation from various RSNO species can occur catalytically using covalently linked diselenide species (RSe-SeR) to polymers such as cellulose filter paper and polyethylenimine (PEI) [47, 55]. Such RSe-derivatized polymers generate NO from RSNO species in the presence of an appropriate thiol reducing agent (e.g., GSH) (eq 1.3 - 1.5). Recently, a new generic and easy approach to incorporate NO generation on almost any surface has been reported [56]. Such NO generating coatings are created via a layer-by-layer (LbL) deposition process in which diselenodiproprionic acid (SeDPA) is covalently linked to PEI creating a polycationic polymer with Se sites that can catalytically liberate NO from RSNOs [56].

It has been found that 100 bilayers of the SePEI and alginate (Alg) as the counter polyanion yields 10 μm thick coatings on almost any substrate, with NO flux levels of $\geqslant 1\times10^{-10}$ mol cm^{-2} min^{-1} in the presence of 1 μM of RSNO substrate, the concentration likely present in fresh whole blood. It is therefore potentially possible to use this LbL approach to create NO generating coatings on needle-type glucose and lactate sensors to enhance the biocompatibility of such implantable devices.

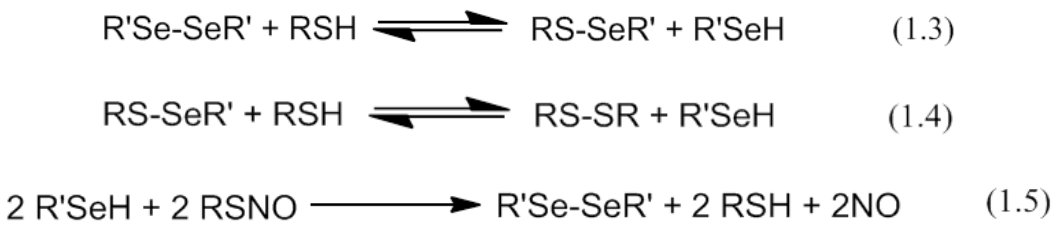

1.5 NO Detection Method Using NO Analyzer (NOA)

Continuous monitoring of released/generated NO flux directly from a device coating surface is feasible by direct measurement of NO using a chemiluminescence NO analyzer (NOA). This method has very low detection limit (ppb NO) and excellent temporal resolution (seconds). Indeed, NO reacts with ozone (O_3) to generate excited state nitrogen dioxide (NO_2*) which then relaxes to the ground state with the emission of light in the red and infrared region (~640 – 3000 nm) (eq 1.6 and 1.7). A photomultiplier tube (PMT) detects the emitted photons in the 640 – 900 nm range.

$$NO + O_3 \longrightarrow NO_2^* + O_2 \qquad (1.6)$$

$$NO_2^* \longrightarrow NO_2 + h\nu \qquad (1.7)$$

Figure 1.9 illustrates the NOA experimental setup. Basically, the NO produced within a test solution in which the coated device (e.g., sensor) is placed is purged into the NOA reaction chamber by bubbling with nitrogen (N_2) carrier gas. The output signal is expressed in the unit of ppb level ([NO]/[N_2]) and can be converted to the unit of 10^{-10} mol min^{-1} cm^{-2} by integrating the ppb/ppm signals, which is used as the standard NO surface flux unit in this dissertation.

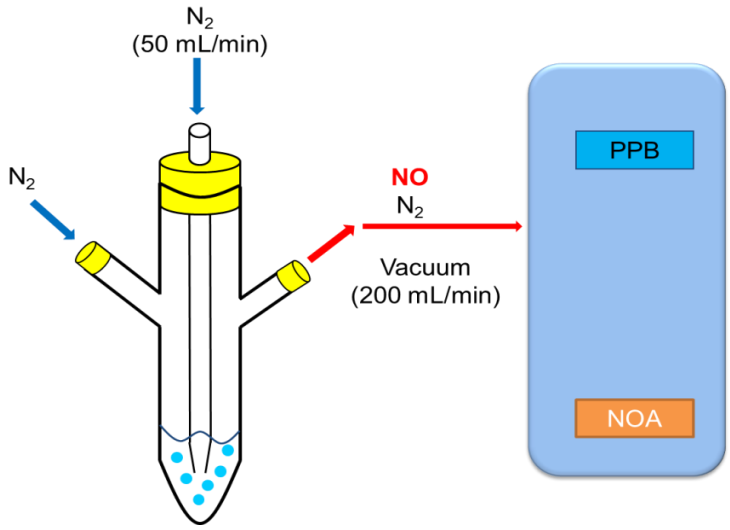

Figure 1.9. NOA setup for detection of NO released/generated from coated devices in the reaction cell.

1.6 Tear Glucose Measurement as a Potential Non-Invasive Substitute for Blood Glucose Measurement

As tight glycemic control is critical to the medical care of diabetic patients as well as to prevent complications such as cardiovascular disease [57], it is often recommended that blood glucose levels be measured several times a day, which usually requires finger pricking coupled with measurement using a strip-test type glucometer. However, in practice, patients may not follow these recommendations, and this might be largely due to the accumulated pain from the repeated finger pricks and blood collection.

Studies have been carried out to find a less invasive means to monitor blood glucose levels including infrared spectroscopy and fluorescence [58], a GlucoWatch design that uses the electro-osmotic flow of subcutaneous fluid to the surface of the skin and detection of glucose in the fluid by e-chem sensor [59], and measurement of tissue metabolic heat conformation [60]. Testing glucose concentrations in tear fluid has also been suggested [61]. If and when a close correlation between tear and blood glucose levels can be clearly shown, the tear glucose testing approach would provide a unique possibility of developing a relatively simple non-invasive method of detecting glucose concentration. In this thesis work, a novel needle-type amperometric tear glucose sensor coupled with a capillary design is explored as a new approach to achieve this goal.

1.7 Statement of Dissertation Research

The purpose of the research described in this dissertation is to develop biocompatible coatings for implantable glucose/lactate sensors with NO release/generation. A new polymeric matrix of PLGA to sustain long-term NO release is proposed and optimized. Different NO generating coatings are also applied onto sensors to study the compatibility between NO generation and the sensing chemistry. A novel tear glucose sensor is also examined as a potential substitute to traditional invasive ways to monitor blood glucose levels.

Chapter 2 describes the development of the new NO release system using a PLGA matrix. Different types of PLGA are studied to find the optimal one to sustain a prolonged NO release (when doped with appropriate NO donors) as well as to maintain a reasonable flux. The optimal ratio of PLGA and NO donor is also established. A prolonged NO release profile was found using PLGA as the polymer matrix. To further understand the protein adsorption properties of such new NO release coatings, an *in vitro* fibrinogen adsorption immunofluorescence assay is carried out.

Chapter 3 discusses the application of the new NO release polymeric coatings using PLGA on implantable glucose/lactate sensors. The analytical performance of these devices is tested with NO release to compare with control sensors prepared without NO release. Animal experiments are carried out to evaluate the anti-thrombotic properties of the NO release glucose sensor by implanting sensors into rabbit veins for 8

h. The thrombus formation was observed after the sensors were explanted and the glucose sensor data are correlated to a standard *in vitro* glucose measurement in blood samples using a bench-top Radiometer instrument. The work described in Chapters 2 and 3 has been published as a full paper in *Biosensors and Bioelectronics* (2011) [62].

Chapter 4 studies NO generating coatings for implantable glucose/lactate sensors. Cu(II)-cyclen polyurethane, polyurethane doped with Cu^0 nanoparticles and Se-LbL are each used as the NO generating coating and the influence of NO generating chemistry on glucose/lactate sensing chemistry is examined. Preliminary animal experiments using the Se-LbL coatings are also carried out to evaluate the anti-thrombotic properties of the SePEI/Alg coatings in the presence of physiological levels of RSNOs in the blood stream.

Chapter 5 proposes a novel tear glucose measurement sensor with a capillary configuration. The correlation between tear and blood glucose over an 8 h period is examined by using a rabbit model. The feasibility of using tear glucose concentrations to predict blood glucose levels is also studied. A US patent for this work has been filed and a full manuscript is to be submitted.

Chapter 6 provides a summary of all the results and future directions of this dissertation work. The use of sulfonated polyurethane as a potential NO release matrix is discussed. Further development of biocompatible and biodegradable NO release polymeric coatings using RSNO in PLGA is also suggested. In addition, the next generation of the tear glucose sensor is also previewed.

1.8 References

1. Riddell, D.R.; Owen, J.S., **1999**, in *Vitamins and Hormones - Advances in Research and Applications*, Vol. 57, Academic Press Inc, San Diego, pp. 25-48.

2. Wallis, J.P. *Transfus. Med.* **2005**, 15(1), 1-11.

3. Guzik, T.J.; Korbut, R.; Adamek-Guzik, T. *J. Physiol. Pharmacol.* **2003**, 54(4), 469-487.

4. Moncada, S.; Palmer, R.M.J.; Higgs, E.A. *Pharmacol. Rev.* **1991**, 43(2), 109-142.

5. Bogdan, C. *Nat. Immunol.* **2001**, 2(10), 907-916.

6. http://www.worlddiabetesfoundation.org/composite-35.htm.

7. Waeger, P.; Hummel, M. *Diabetes Stoffwech. H.* **2008**, 17(5), 385-391.

8. Kondepati, V.R.; Heise, H.M. *Anal. Bioanal. Chem.* **2007**, 388(3), 545-563.

9. Bochicchio, G.V.; Scalea, T.M. *Serono. Sym.* **2008**, 42, 261-275.

10. Lonergan, T.; Le Compte, A.; Willacy, M.; Chase, J.G.; Shaw, G.M.; Wong, X.W.; Lotz, T.; Lin, J.; Hann, C.E. *Diabetes Technol. The.* **2006**, 8(2), 191-206.

11. Vanhorebeek, I.; Langouche, L.; Van den Berghe, G. *Chest* **2007**, 132(1), 268-278.

12. Schetz, M.; Vanhorebeek, I.; Wouters, P.J.; Wilmer, A.; van den Berghe, G. *J. Am. Soc. Nephrol.* **2008**, 19(3), 571-578.

13. Holloway, P.; Benham, S.; St John, A. *Clin. Chim. Acta* **2001**, 307(1-2), 9-13.

14. Shapiro, N.I.; Howell, M.D.; Talmor, D.; Nathanson, L.A.; Lisbon, A.; Wolfe, R.E.; Weiss, J.W. *Ann. Emerg. Med.* **2005**, 45(5), 524-528.

15. Shapiro, N.I.; Howell, M.D.; Talmor, D. *Ann. Emerg. Med.* **2005**, 46(6), 562-562.

16. Shapiro, N.I.; Fisher, C.; Donnino, M.; Cataldo, L.; Tang, A.; Trzeciak, S.; Horowitz, G.; Wolfe, R.E. *J. Emerg. Med.* **2010**, 39(1), 89-94.

17. Arnold, R.C.; Shapiro, N.I.; Jones, A.E.; Schorr, C.; Pope, J.; Casner, E.; Parrillo, J.E.; Dellinger, R.P.; Trzeciak, S.; Emergency Med Shock Res Network, E.M. *Shock* **2009**, 32(1), 35-39.

18. Valenza, F.; Aletti, G.; Fossali, T.; Chevallard, G.; Sacconi, F.; Irace, M.; Gattinoni, L. *Crit. Care* **2005**, 9(6), 588-593.

19. Bindra, D.S.; Zhang, Y.N.; Wilson, G.S.; Sternberg, R.; Thevenot, D.R.; Moatti, D.; Reach, G. *Anal. Chem.* **1991**, 63(17), 1692-1696.

20. Yang, Q.L.; Atanasov, P.; Wilkins, E. *Biosens. Bioelectron.* **1999**, 14(2), 203-210.

21. Hu, Y.B.; Zhang, Y.N.; Wilson, G.S. *Anal. Chim. Acta* **1993**, 281(3), 503-511.

22. http://www.minimed.com/products/guardian/components.html.

23. Girardin, C.M.; Huot, C.; Gonthier, M.; Delvin, E. *Clin. Biochem.* **2009**, 42(3), 136-142.

24. Frost, M.; Meyerhoff, M.E. *Anal. Chem.* **2006**, 78(21), 7370-7377.

25. Frost, M.C.; Meyerhoff, M.E. *Curr. Opin. Chem. Biol.* **2002**, 6(5), 633-641.

26. Wisniewski, N.; Reichert, M. *Colloid Surf. B-Biointerfaces* **2000**, 18(3-4), 197-219.

27. Tada, S.; Inaba, C.; Mizukami, K.; Fujishita, S.; Gemmei-Ide, M.; Kitano, H.; Mochizuki, A.; Tanaka, M.; Matsunaga, T. *Macromol. Biosci.* **2009**, 9(1), 63-70.

28. Deligkaris, K.; Tadele, T.S.; Olthuis, W.; van den Berg, A. *Sensor. Actuat. B-Chem.* **2010**, 147(2), 765-774.

29. Frost, M.C.; Batchelor, M.M.; Lee, Y.M.; Zhang, H.P.; Kang, Y.J.; Oh, B.K.; Wilson, G.S.; Gifford, R.; Rudich, S.M.; Meyerhoff, M.E. *Microchem. J.* **2003**, 74(3), 277-288.

30. Fleser, P.S.; Nuthakki, V.K.; Malinzak, L.E.; Callahan, R.E.; Seymour, M.L.; Reynolds, M.M.; Merz, S.I.; Meyerhoff, M.E.; Bendick, P.J.; Zelenock, G.B.; Shanley, C.J. *J. Vasc. Surg.* **2004**, 40(4), 803-811.

31. Frost, M.C.; Meyerhoff, M.E., **2004**, in *Oxygen Sensing*, Vol. 381, pp. 704-715.

32. Frost, M.C.; Reynolds, M.M.; Meyerhoff, M.E. *Biomaterials* **2005**, 26(14), 1685-1693.

33. Frost, M.C.; Rudich, S.M.; Zhang, H.P.; Maraschio, M.A.; Meyerhoff, M.E. *Anal. Chem.* **2002**, 74(23), 5942-5947.

34. Gifford, R.; Batchelor, M.M.; Lee, Y.; Gokulrangan, G.; Meyerhoff, M.E.; Wilson, G.S. *J. Biomed. Mater. Res. A* **2005**, 75A(4), 755-766.

35. Wu, Y.D.; Meyerhoff, M.E. *Talanta* **2008**, 75(3), 642-650.

36. Wu, Y.D.; Rojas, A.P.; Griffith, G.W.; Skrzypchak, A.M.; Lafayette, N.; Bartlett, R.H.; Meyerhoff, M.E. *Sensor. Actuat. B-Chem.* **2007**, 121(1), 36-46.

37. Shin, J.H.; Marxer, S.M.; Schoenfisch, M.H. *Anal. Chem.* **2004**, 76(15), 4543-4549.

38. Oh, B.K.; Robbins, M.E.; Nablo, B.J.; Schoenfisch, M.H. *Biosens. Bioelectron.* **2005**, 21(5), 749-757.

39. Eroy-Reveles, A.A.; Mascharak, P.K. *Future Med. Chem.* **2009**, 1(8), 1497-1507.

40. D'Atri, L.P.; Malaver, E.; Romaniuk, M.A.; Pozner, R.G.; Negrotto, S.; Schattner, M. *Curr. Med. Chem.* **2009**, 16(4), 417-429.

41. Frost, M.C.; Rudich, S.M.; Zhang, H.P.; Maraschio, M.A.; Meyerhoff, M.E. *Anal. Chem.* **2003**, 75(4), 1037-1037.

42. Batchelor, M.M.; Reoma, S.L.; Fleser, P.S.; Nuthakki, V.K.; Callahan, R.E.; Shanley, C.J.; Politis, J.K.; Elmore, J.; Merz, S.I.; Meyerhoff, M.E. *J. Med. Chem.* **2003**, 46(24), 5153-5161.

43. Schwendeman, S.P. *Crit. Rev. Ther. Drug* **2002**, 19(1), 73-98.

44. Hogg, N. *Free Radical Bio. Med.* **2000**, 28(10), 1478-1486.

45. Al-Sa'doni, H.; Ferro, A. *Clin. Sci.* **2000**, 98(5), 507-520.

46. Williams, D.L.H. *Accounts Chem. Res.* **1999**, 32(10), 869-876.

47. Cha, W.; Meyerhoff, M.E. *Biomaterials* **2007**, 28(1), 19-27.

48. Giustarini, D.; Milzani, A.; Colombo, R.; Dalle-Donne, I.; Rossi, R. *Clin. Chim. Acta* **2003**, 330(1-2), 85-98.

49. Wu, Y.D.; Cha, W.S.; Zhang, F.H.; Meyerhoff, M.E. *Clin. Chem.* **2009**, 55(5), 1038-1040.

50. Askew, S.C.; Butler, A.R.; Flitney, F.W.; Kemp, G.D.; Megson, I.L. *Bioorg. Med. Chem.* **1995**, 3(1), 1-9.

51. Dicks, A.P.; Beloso, P.H.; Williams, D.L.H., **1997**, in *Journal of the Chemical Society-Perkin Transactions 2*, pp. 1429-1434.

52. Oh, B.K.; Meyerhoff, M.E. *J. Am. Chem. Soc.* **2003**, 125(32), 9552-9553.

53. Hwang, S.; Cha, W.; Meyerhoff, M.E. *Angew. Chem. Int. Edit.* **2006**, 45(17), 2745-2748.

54. Hwang, S.; Meyerhoff, M.E. *Biomaterials* **2008**, 29(16), 2443-2452.

55. Cha, W.; Meyerhoff, M.E. *Langmuir* **2006**, 22(25), 10830-10836.

56. Yang, J.; Welby, J.L.; Meyerhoff, M.E. *Langmuir* **2008**, 24(18), 10265-10272.

57. Mattila, T.K.; de Boer, A. *Drugs* **2010**, 70(17), 2229-2245.

58. do Amaral, C.E.F.; Wolf, B. *Med. Eng. Phys.* **2008**, 30(5), 541-549.

59. Potts, R.O.; Tamada, J.A.; Tierney, M.J. *Diabetes-Metab. Res.* **2002**, 18, S49-S53.

60. Cho, O.K.; Kim, Y.Y.; Mitsumaki, H.; Kuwa, K. *Clin. Chem.* **2004**, 50(10), 1894-1898.

61. Baca, J.T.; Finegold, D.N.; Asher, S.A. *Ocul. Surf.* **2007**, 5(4), 280-293.

62. Yan, Q.; Major, T.C.; Bartlett, R.H.; Meyerhoff, M.E. *Biosens. Bioelectron.* **2011**, doi:10.1016/j.bios.2011.04.026.

CHAPTER 2

NITRIC OXIDE RELEASE USING A POLY(LACTIDE-CO-GLYCOLIDE) MATRIX

2.1 Introduction

As discussed in Chapter 1, considerable effort has been focused on developing more biocompatible materials for intravascular and subcutaneous sensors as well as other medical devices. Nitric oxide (NO) has shown its potent inhibition to platelet activation and anti-inflammation functions. In fact, the physiological NO flux from endothelial cells that line the blood vessels is estimated to be in the range of $0.5 – 4.0 \times 10^{-10}$ mol $min^{-1}cm^{-2}$ [1]. Previous studies and initial results [2, 3] have shown promising biomedical application of NO release materials on implantable glucose sensors for improved biocompatibility in subcutaneous tissue, but the NO release lasted for only 1 to 3 days. The goal of research described in this chapter is to develop new polymeric coatings which prolong NO release to at least one week at physiologically relevant levels in order to realize enhanced biocompatibility and potential extended implantation times for intravascular chemical sensors (e.g., glucose sensors) and other biomedical devices.

Initially, diazeniumdiolated dibutylhexanediamine (DBHD/N_2O_2) was doped as the NO donor in the outer polymeric PurSil (a copolymer of polyurethane and dimethylsiloxane, see Fig. 2.1 (a)) layer of the glucose sensor (see Fig. 1.2 in Chapter 1), similar to the approach reported previously for subcutaneous glucose sensor experiments [2]. Potassium tetrakis(4-chlorophenyl)borate (KTpClPB) (Fig. 2.1 (b)) was first used as a lipophilic counter ion to stabilize the pH level within the NO release polymers. The increase in the basic environment, due to free amines produced after NO release, further slows the decomposition of the remaining diazeniumdiolates to release NO; however, as shown previously, the addition of the borate derivative helps buffer the organic phase, keeping the pH low [4] (via hydroxide and potassium ions diffusing out from the polymer matrix, with borate becoming the counteranion to the protonated amine of DBHD). Figure 2.1 (c) shows the difference in NO release profile with and without KTpClPB doped in the polymer with the same amount of DBHD/N_2O_2. When the borate was added into the NO release polymer matrix, the released NO remained at a relatively steady flux, while without the borate the NO flux started to shut down within 30 min, due to the increased pH within the polymer preventing DBHD/N_2O_2 from further decomposing.

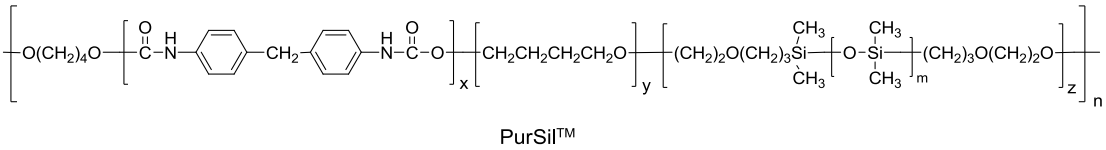

PurSil™

(a)

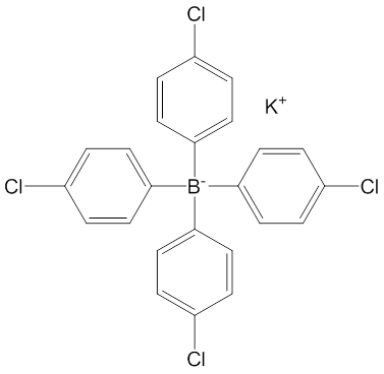

(b)

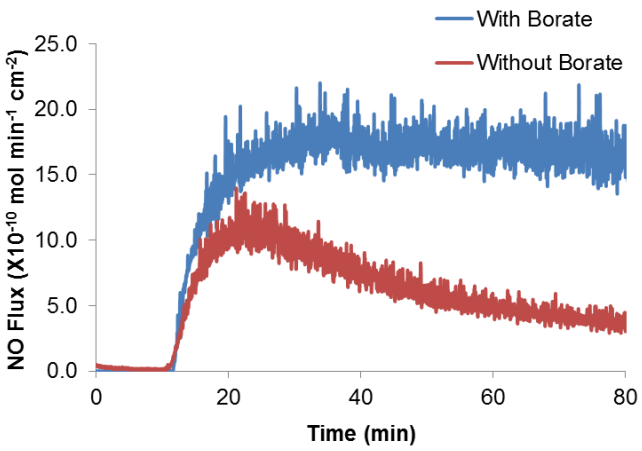

(c)

Figure 2.1. Structures of (a) PurSil and (b) KTpClPB. (c) NO release comparison with and without the doped tetraphenylborate species.

Unfortunately, when either glucose oxidase or lactate oxidase was in contact with the membrane containing the borate derivative for some time (days), both enzymes lost essentially all activity. Control experiments were performed by fabricating glucose sensors that were coated with polymers containing only DBHD/N_2O_2, only borate or both borate and DBHD/N_2O_2. Results showed that glucose sensors with only DBHD/N_2O_2 maintained their catalytic activity, while the sensors with borate or with both species lost response to glucose. This result suggests that the borate derivative, not the NO releasing diazeniumdiolate, deactivated the enzyme preventing the response of the glucose sensor when using outer NO release membranes containing these species. The loss of enzyme

activity was possibly due to the generation of potentially toxic radical species from the cleavage of the carbon-boron bond during the proton-induced or oxidative degradation of the KTpClPB species [5].

To overcome the borate deactivation effect on the enzyme activity, preliminary efforts to coat the sensors with an NO releasing PurSil layer, but excluding the sensing area where the enzymes are immobilized were undertaken. It was hoped that the NO release from the surrounding area could prevent thrombus formation on this small opening. However, an initial *in vivo* study showed that thrombus formation still occurred precisely on the 1-mm opening not covered by NO releasing material after 8 h of implantation in rabbit veins (Fig. 2.2). As a result, a substitute for the borate, which can preserve the enzyme activity, was needed to prolong the NO release time while also still exhibiting a similar function to control the pH of the organic layer containing DBHD/N_2O_2.

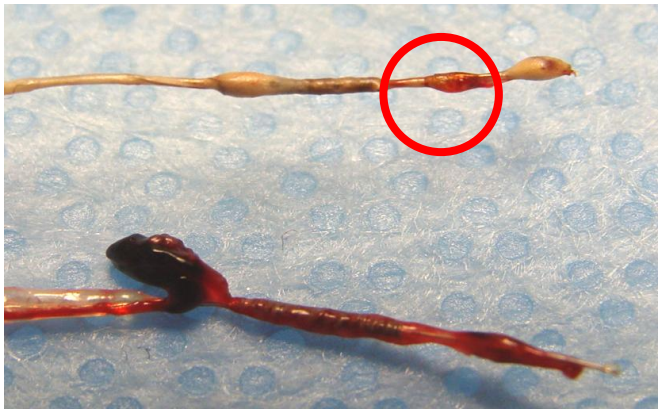

Figure 2.2. Preliminary *in vivo* study of NO release (excluding the sensing area) glucose sensor with borate (top) and control without NO release (bottom) explanted after 8-hour implantation in rabbit veins. Thrombus still formed on the sensing area of the NO release glucose sensor (top red circle).

Some other lipophilic anions were studied as substitutes for KTpClPB, including potassium tetrakis[3,5-bis-(trifluoromethyl)phenyl]borate, dinonylnaphthalene sulfonate (DNNS) and sodium cholate (Fig. 2.3). However, they either deactivated the glucose/lactate oxidase as well, or did not help maintain a steady NO flux like KTpClPB does.

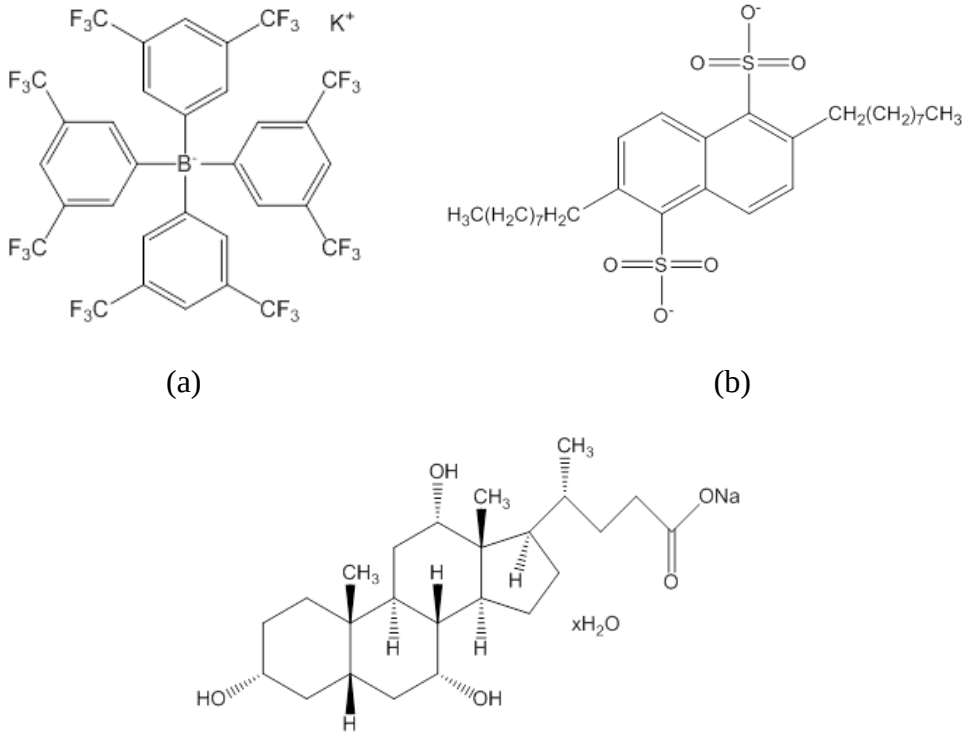

(a) (b)

(c)

Figure 2.3. Structures of (a) potassium tetrakis[3,5-bis-(trifluoromethyl)phenyl]borate, (b) dinonylnaphthalene sulfonate (DNNS) and (c) sodium cholate.

Poly(lactide-*co*-glycolide) (PLGA) is a widely used biodegradable and biocompatible copolymer which has been approved by the U.S. Food and Drug Administration (FDA) in numerous products, especially in drug delivery systems [6].

Further, PLGA is a candidate as a substitute for the toxic tetraphenylborate species to create an NO release coating because PLGA undergoes a slow hydrolysis to produce lactic acid and glycolic acid, and thus can provide an acidic micro-environment ideally suited for proton driven NO release from diazeniumdiolates [7-10]. As the PLGA is hydrolyzed, the lactic and glycolic acids can protonate the free amines produced in the NO release process from the DBHD/N_2O_2 species; thus long-term NO release can be ensured without influencing enzyme activity. There are many types of PLGA with different hydrolysis speeds, controlled by the ratio of lactic and glycolic acid content, molecular weight and the end-cap type (free acid or ester-capped). As a result, in this work different types of PLGA were examined, in order to prolong the sustained NO release at physiologically relevant levels. The optimum PLGA was selected as the base material to create new NO releasing inner polymer coatings for both glucose and lactate sensors. As hypothesized, PLGA did not have any negative influence on either the glucose or lactate oxidase activities which will be discussed in detail in Chapter 3.

2.2 Experimental

2.2.1 Materials

N,*N*'-dibutyl-1,6-hexanediamine (DBHD), phenolphthalein, dinonylnaphthalene sulfonate (DNNS), sodium cholate, 1-(4-butylphenyl)-2,2,2-trifluoroethanone and poly(DL-lactide-*co*-glycolide) 50:50 (PLGA, RESOMER® RG 502 H) were purchased from Sigma-Aldrich (St. Louis, MO). Sodium chloride (NaCl), potassium chloride

(KCl), sodium phosphate dibasic (Na_2HPO_4), potassium phosphate monobasic (KH_2PO_4), potassium hydroxide (KOH), tetrahydrofuran (THF), dimethylacetamide (DMAc), methanol and acetone were from Fisher Scientific (Pittsburgh, PA). PLGA 85:15, PLGA 50:50 (i.v. 0.60, ester terminated) and PLGA 50:50 (i.v. 0.19, ester terminated) were provided by Alkermes Inc. (Cambridge, MA). Potassium tetrakis(4-chlorophenyl)borate (KTpClPB) and potassium tetrakis[3,5-bis-(trifluoromethyl)phenyl]borate were from Fluka (Ronkonkoma,NY). PurSil 20 80A was from the Polymer Technology Group (Berkeley, CA). DBHD/N_2O_2 was synthesized by treating DBHD with 80 psi NO gas purchased from Cryogenic Gases (Detroit, MI) at room temperature for 24 h, as previously described [4].

2.2.2 Characterization of Different Types of PLGA

NO release PLGA polymers were coated on IV polyurethane catheters (0.67 o.d. × 19 mm, Fisher Scientific, PA). The catheters were first glued on the tip and dried overnight, then 10 μL of 5% (w/v) of 2:1 (w/w) PLGA and DBHD/N_2O_2 in THF were loop cast, covering 1.5 cm of the catheter, and finally coated with another 10 μL of ca. 4% (w/v) PurSil solution in 1:1.5 DMAc and THF. The coated catheters were dried in air overnight and then vacuum dried for 1 day.

PLGA 85:15, PLGA 50:50 (i.v. 0.60, ester terminated), PLGA 50:50 (i.v. 0.19, ester terminated) and PLGA 50:50 RG 502 H (i.v. 0.16-0.24, acid terminated) were examined as matrices containing DBHD/N_2O_2. With the same amount (5 mg) of

DBHD/N_2O_2 incorporated, 10 mg of different types of PLGA were dispersed in 300 μL of THF and 10 μL was coated onto catheters as the NO release matrix and top-coated with 10 μL of ca. 4% (w/v) PurSil solution in 1:1.5 DMAc and THF. The initial NO release was monitored by the NOA for 8 h. As a control, the same amount of DBHD/N_2O_2 was also doped in PurSil but without PLGA. The NO release profiles were compared and the optimal PLGA was chosen for future use.

To optimize the ratio of DBHD/N_2O_2 and PLGA, 5 mg of DBHD/N_2O_2 was doped in 5, 10, 15 and 20 mg of PLGA 50:50 RG 502 H matrix and dispersed in 300 μL of THF. Ten microliters of the suspension were coated onto the catheter and top-coated with PurSil. The NO release was tested using the NOA for 8 h and the profiles of different NO donor to PLGA ratios were compared to determine the optimal ratio of diazeniumdiolate and PLGA to maintain a steady NO flux.

Since NO release from DBHD/N_2O_2 is a proton driven mechanism, the residue acid number in different types of PLGA might also be influencing the initial NO release profile. To determine the acid number, approximately 25 mg of the different PLGA types were dissolved in 5 mL of a 1:1 mixture of acetone and THF. The solution was immediately titrated with 0.01 M KOH in methanol to a stable pink endpoint. Phenolphthalein methanol solution (0.1 wt%) was used as an indicator and 5 mL of acetone/THF (1:1) without PLGA was used as a control.

2.2.3 Nitric Oxide Release *In Vitro*

Nitric oxide released from coated catheters was monitored via chemiluminescence with a Sievers Nitric Oxide Analyzer (NOA) 280i (Boulder, CO). The catheters were immersed into 0.1 M PBS, pH 7.4, at 37℃ and the NO flux data were collected. Long-term NO release was monitored over a 7-d period by collecting data for one hour each day. The catheters were soaked in PBS at 37℃ with continuous nitrogen purging over this 7-d period to ensure that all sensors released NO under the same conditions as when measuring the NO flux using the NOA.

2.2.4 *In Vitro* Fibrinogen Adsorption Immunofluorescence Assay

To study the fibrinogen adsorption on to the NO release polymeric coatings, an *in vitro* fibrinogen adsorption immunofluorescence assay was carried out [11]. A 96-well microtiter plate (Nalge Nunc #437111, Rochester, NY) was coated with NO release and control polymers as shown in Figure 2.4. Reconstituted solution was prepared by adding 100 mL of distilled water to each 4 g vial of Serotec BLOCK ACE (#BUF029, Raleigh, NC). First, 1.5 mL of 44.4 mg/mL human fibrinogen (Calbiochem #341576, La Jolla, CA) was diluted with 22.2 mL Dulbecco's phosphate-buffered saline (dPBS) to make a stock solution of 3 mg/mL. Then, 100 μL of the 3 mg/mL fibrinogen solution was added to each polymer-containing microtiter well and incubated for 1.5 h at 37℃. The plate was washed 8 times using 100 μL of wash buffer each time (10-fold diluted

from reconstituted solution with 0.05% Tween 20 (Calbiochem, La Jolla, CA)) per well. To block nonspecific antibody binding, wells were incubated with 100 µL Blocking buffer (4-fold diluted from reconstituted solution) for 30 min at 37 ℃. The plate was washed an additional 3 times using 100 µL wash buffer per well. A background measurement of the plates was performed at 485/20 nm (excitation) and 528/20 nm (emission). The purpose of pre-read blanks was to correct for well-to-well variability and to subtract the plate background (polymer-coated wells, with preadsorbed proteins) before measuring the fluorescence signals (polymer coated wells, with preadsorbed proteins and antibody). To detect adsorbed fibrinogen, goat anti-human fibrinogen:FITC (MP Biochem #55169 CAPPEL, Solon, OH; 2ml DI water/vial) was diluted (1:10) in Diluent buffer (10-fold diluted reconstituted solution) and 100 µL was added to each well. The antibody was allowed to bind to the surface-adsorbed fibrinogen for 1.5 h at 37 ℃. Then the plate was washed 3 times using 100 µL of Wash buffer per well. The measurements were performed with a fluorescence reader (Synergy 2, Biotek, Winooski, VT). Human fibrinogen adsorption to non-coated polypropylene was used as an internal control to normalize the fluorescence signals of the polymer coated wells.

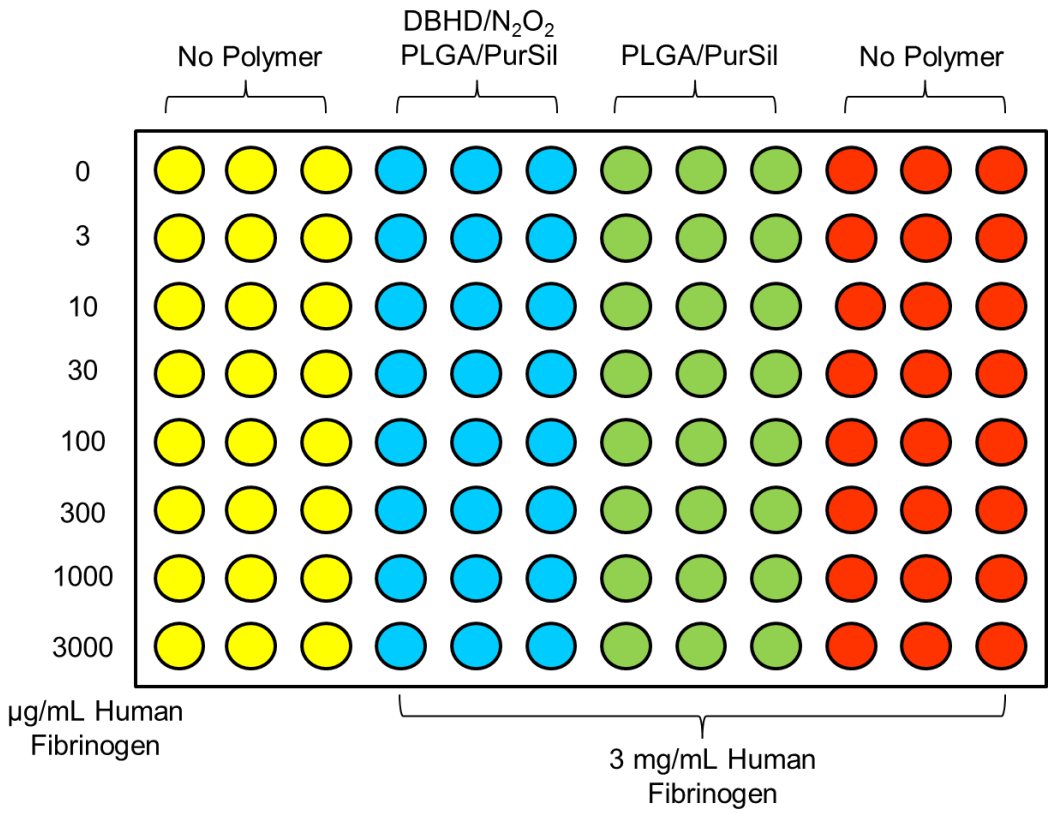

Figure 2.4. *In vitro* fibrinogen adsorption immunofluorescence assay plate configuration.

2.3 Results and Discussion

2.3.1 Comparison of Different Types of PLGA as the NO Release Matrix

The various types of PLGA with different hydrolysis speeds may influence the NO release flux. The higher the glycolide content in PLGA, the faster the hydrolysis rate, so PLGA 50:50 (lactide : glycolide) hydrolyzes faster than PLGA 85:15. The molecular weight (in terms of the inherent viscosity (i.v., dL/g)) of the polymer also has an impact on the hydrolysis speed with a higher i.v. number yielding a slower hydrolysis

speed. The polymer end-cap also plays a role in the hydrolysis speed, as the acid-terminated polymer chain hydrolyzes faster than the ester-terminated polymer. As a result, PLGA 85:15, PLGA 50:50 (i.v. 0.60, ester-terminated), PLGA 50:50 (i.v. 0.19, ester-terminated) and PLGA 50:50 RG 502 H (i.v. 0.16-0.24, acid-terminated) were all used as the matrix of DBHD/N_2O_2 to release NO.

Figure 2.5 shows the NO release profiles of different PLGAs and the control (without PLGA) for the first 8 hours, all with the same amount (5 mg) of DBHD/N_2O_2 doped in 10 mg of the polymers. All showed an initial burst of NO flux at around 30 min after immersion in PBS buffer, and then gradually decreased to a steady NO flux. The burst of NO as well as the later steady NO flux follows the order (from the highest to lowest): PLGA 50:50 (i.v. 0.19) > PLGA 50:50 RG 502 H > PLGA 50:50 (i.v. 0.60) > PLGA 85:15. It should be noted that all the polymers with PLGA have higher NO flux than the control (without PLGA), which indicates that PLGA does control the pH in the polymer matrix by providing a more acidic environment than the control of PurSil, resulting in higher NO flux. The order of NO flux from different PLGAs appears to be consistent with the trend of a faster hydrolysis speed corresponding to a higher NO flux, except that PLGA 50:50 RG 502 H has the highest hydrolysis speed, but the NO flux is lower than that from PLGA 50:50 (i.v. 0.19). To better understand these results, the residual acid numbers of the different types of PLGA were also measured and the results are shown in Table 2.1, combined with the NO flux at the highest burst. From the titration results (n=3), PLGA 50:50 (i.v. 0.19) has a similar residual acid content to PLGA 50:50 RG 502 H, which cannot explain the higher NO burst flux than that from

PLGA 50:50 RG 502 H. On a second thought, PLGA 50:50 RG 502 H is acid-terminated, so it is more hydrophilic and can be predicted to have a higher water uptake in the polymer matrix than PLGA 50:50 (i.v. 0.19) which is ester-terminated. A higher water uptake reduces the acid activity in the PLGA matrix and results in a higher micro pH value [9], which in turns explains the lower initial NO burst from PLGA 50:50 RG 502 H than PLGA 50:50 (i.v. 0.19). As discussed above, PLGA 50:50 RG 502 H was chosen as the best PLGA for prolonged NO release, because it proved to sustain an NO flux at a reasonable range to potentially reduce thrombus formation. Additionally, it had an initial NO flux that was lower than the PLGA 50:50 (i.v. 0.19), further preserving the NO donor reservoir.

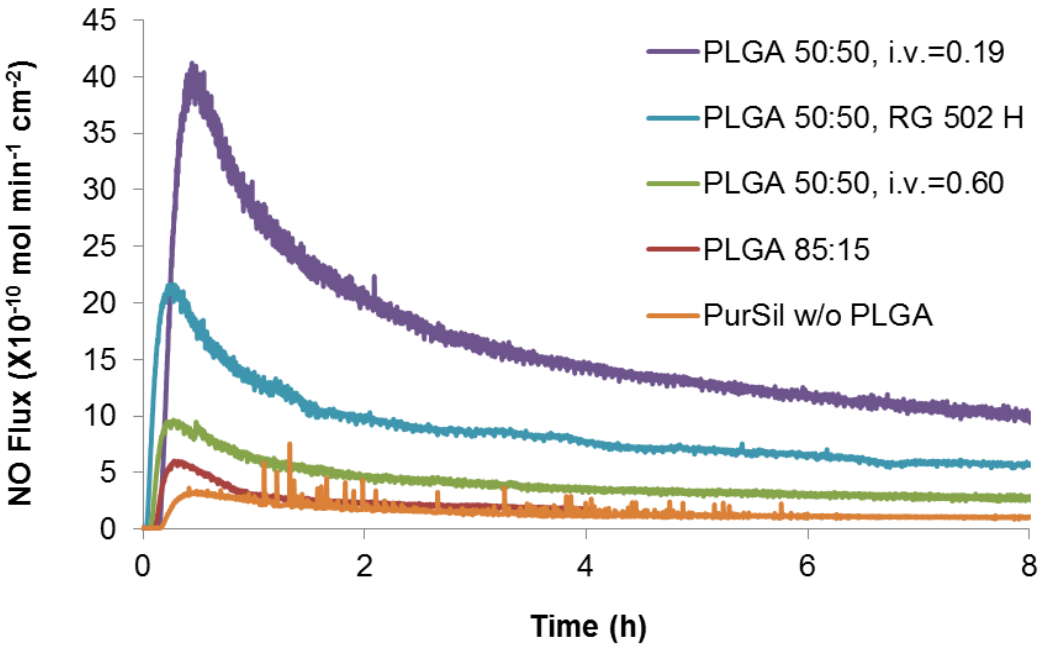

Figure 2.5. NO release profile comparison of different types of PLGA.

Table 2.1. Residual acid number (n=3) and the corresponding NO flux at the burst peak of different types of PLGA.

PLGA	Acid Number (mg KOH/g PLGA)	NO Flux Burst Peak ($\times 10^{-10}$ mol min^{-1} cm^{-2})
50:50 RG 502 H	17.4 ± 1.1	21.5
50:50 i.v. 0.19	18.1 ± 3.0	40.6
50:50 i.v. 0.60	12.5 ± 0.4	9.4
85:15	7.1 ± 0.6	6.0

2.3.2 Optimization of the Ratio of NO Donor and PLGA Matrix

In theory, to sustain a steady NO flux with added lipophilic anions to buffer the pH in the polymeric matrix, the molar ratio of doped anions and DBHD/N_2O_2 should be 1:1. However, as PLGA slowly hydrolyzes to produce the free acids to neutralize the amine groups, it is unknown if the hydrolysis speed will match the NO release process so that enough acid will be produced to maintain an acidic pH in the polymeric environment to prolong further NO release. As a result, it was necessary to carry out experiments where the ratio of PLGA and DBHD/N_2O_2 was varied to determine the optimal amount of PLGA to sustain a steady NO flux.

Figure 2.6 shows the NO release using different amounts of PLGA 50:50 RG 502 H doped with the same amount (5 mg) of DBHD/N_2O_2. It was found that when the amount of PLGA used was more than 10 mg, the steady NO flux did not change much. It was concluded that 5 mg of PLGA may not be enough to buffer the pH after NO is released from the 5 mg of DBHD/N_2O_2, so that the NO release process was slowed down resulting in a lower NO flux. When the weight ratio of PLGA to DBHD/N_2O_2 is greater

than 2:1, the hydrolysis products are able to buffer the pH within the polymer matrix so that a steady NO flux can be maintained within the desired range. It should be noted that for lactate sensors, more PLGA will result in a higher sensing background with more lactic acid produced locally, so the PLGA amount needs to be kept as low as possible while maintaining an acceptable NO flux. As a result, a 2:1 ratio of PLGA and DBHD/N_2O_2 was chosen as the optimal polymer to NO donor ratio to prolong NO release for use with glucose/lactate sensors.

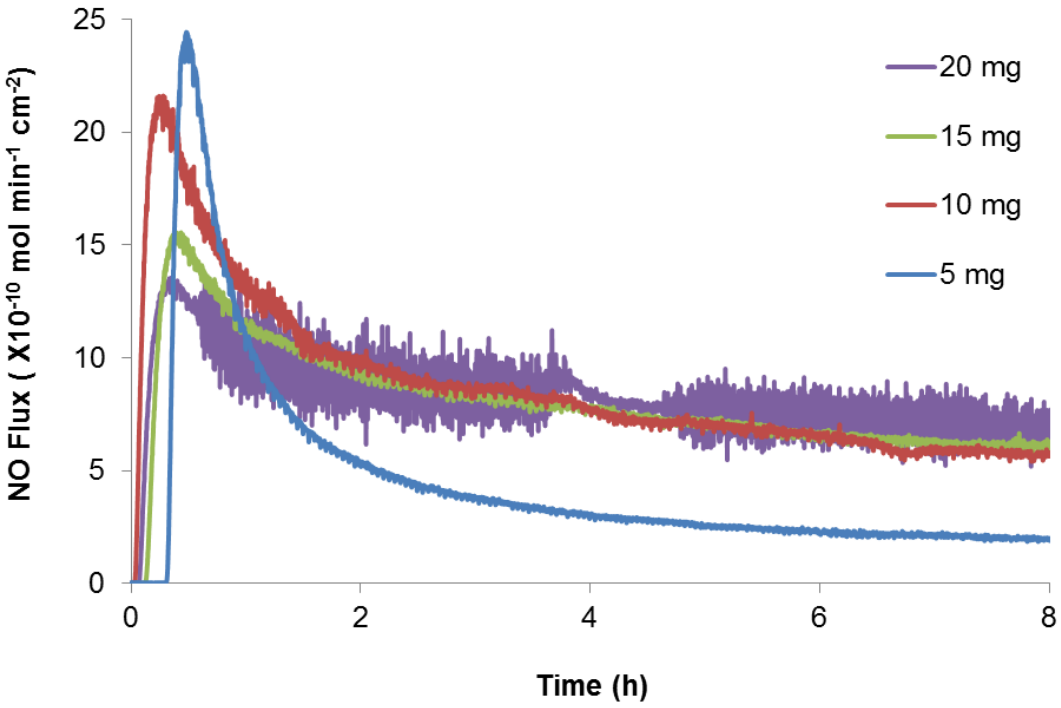

Figure 2.6. NO release for coatings prepared with varying amounts of PLGA in 300 µL of THF doped with 5 mg of DBHD/N_2O_2.

2.3.3 Prolonged NO Release Using PLGA

Figure 2.7 shows the NO release of coated catheters over a one week period of time using PLGA as the matrix in which the DBHD/N_2O_2 is embedded. The NO flux reached an average maximum of 22 $\times 10^{-10}$ mol $min^{-1}cm^{-2}$ approximately 30 min after immersion in PBS. The NO release then decayed exponentially, but continued for more than 7 days at a rate > 1 $\times 10^{-10}$ mol $min^{-1}cm^{-2}$, which is similar to the NO flux produced by endothelial cells in cell cultures [1]. This NO release result is similar to that observed when using tetraphenylborate derivatives as an additive in the PurSil polymer matrix (Fig. 2.8). On the other hand, with the same amount of DBHD/N_2O_2 alone doped into the PurSil polymer without the tetraphenylborate or PLGA, the maximum flux was only 3 $\times 10^{-10}$ mol $min^{-1}cm^{-2}$ and the NO flux diminished to < 1 $\times 10^{-10}$ mol $min^{-1}cm^{-2}$ within several hours (Fig. 2.8). Hence, using a matrix that contained all PLGA for DBHD/N_2O_2 and a top coating of PurSil, provides a bilayer coating that releases NO for more than one week. This is a much longer period than the previously proposed NO release coatings on glucose sensors [2, 12].

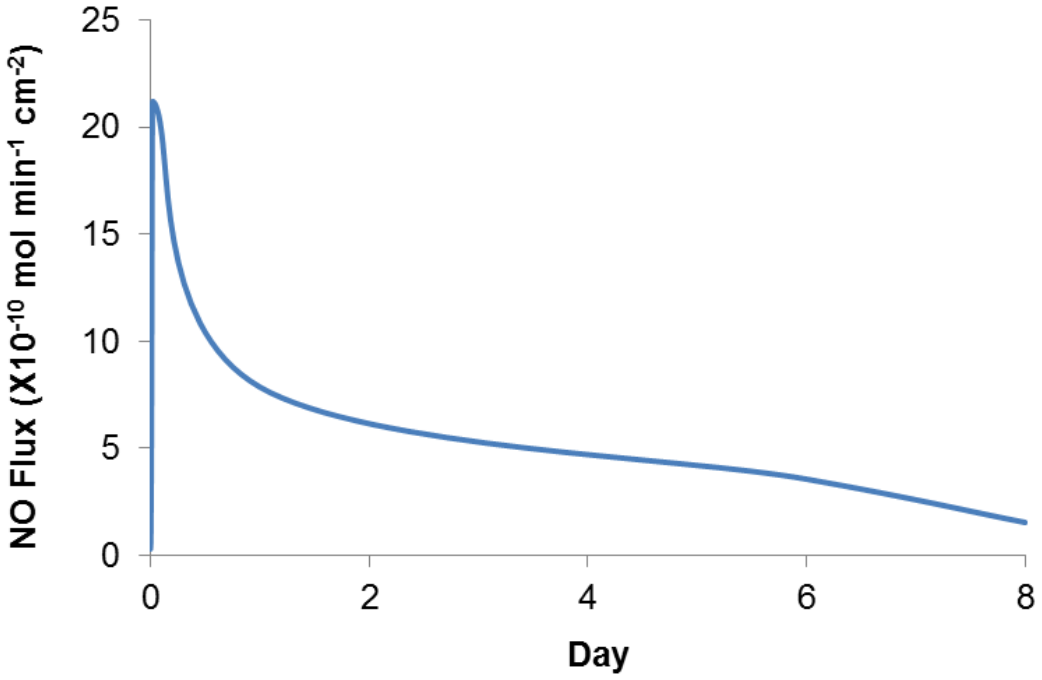

Figure 2.7. NO release of PLGA matrix doped with DBHD/N_2O_2 and top-coated with PurSil for more than one week.

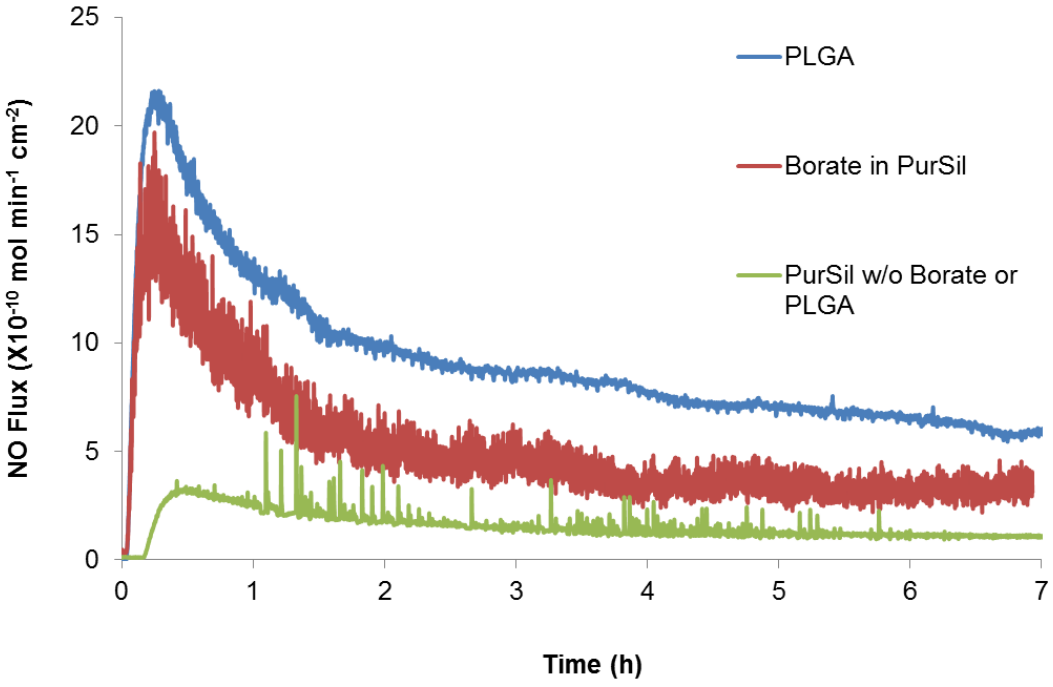

Figure 2.8. NO release profile comparison of the same amount of DBHD/N_2O_2 in PLGA, PurSil with KTpClPB and PurSil only.

2.3.4 Fibrinogen Adsorption of NO Release Polymers

Figure 2.9 shows the fibrinogen adsorption of NO release PLGA/PurSil polymer matrix as well as the control PLGA/PurSil polymer coatings compared to the polypropylene microtiter plate material. It was found that both NO release and control PLGA/PurSil polymeric coatings adsorbed 20 times more fibrinogen than the polypropylene material. The reason that the microtiter plate itself did not adsorb much protein may be due to the smooth surface of the wells from industrial production, while the coated polymers could potentially have rougher surfaces due to the hand-made process, which makes the polymers readily adsorb more proteins. However, NO release coatings still showed excellent anti-thrombus functions from the animal experiments which are reported in detail in Chapter 3. It was concluded that NO does not prevent protein adsorption on polymer surfaces, but the protein adsorption is not the key step in thrombus formation. It is the platelet activation which ultimately triggers the thrombus formation and NO can downregulate the platelet activity. As a result, NO release is crucial to prevent thrombus formation on polymeric surfaces when in contact with blood; the PLGA-based NO release coatings can be applied to multiple medical devices, including implantable sensors, to enhance the biocompatibility of such devices.

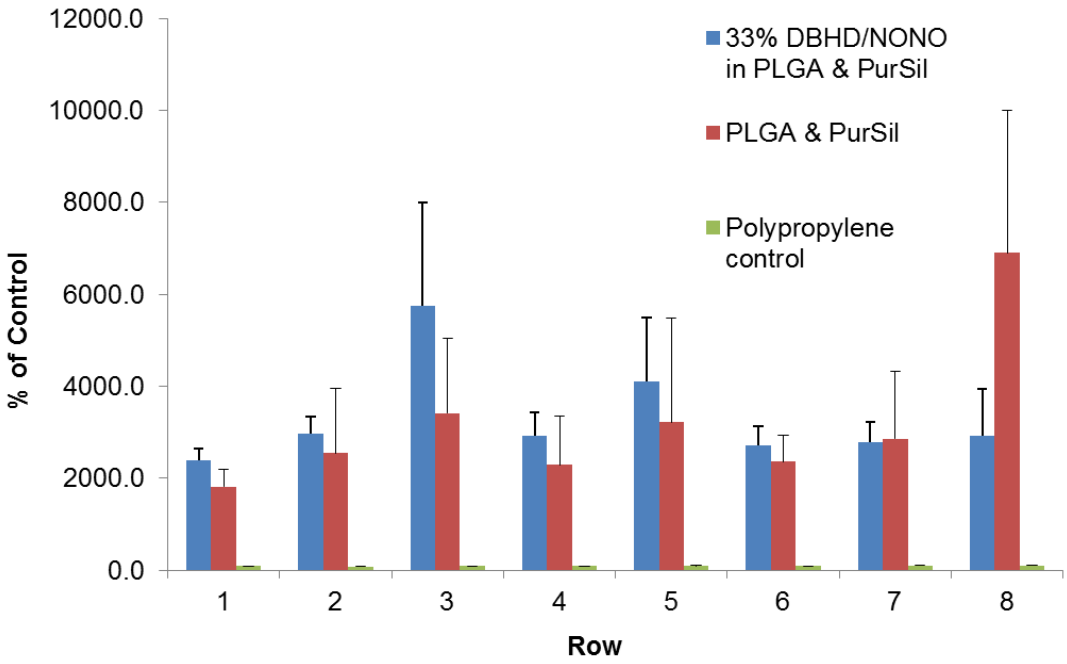

Figure 2.9. Fibrinogen adsorption results of the NO release coatings and control polymers on a microtiter plate.

2.4 Conclusions

Novel nitric oxide releasing coatings containing a lipophilic diazeniumdiolate NO donor species embedded in a PLGA matrix have been successfully developed that can release NO for more than one week at physiologically relevant levels. PLGA 50:50 RG 502 H was selected as the best PLGA to sustain the prolonged NO release at physiological levels for application on glucose and lactate sensors. The 2:1 weight ratio of PLGA and DBHD/N_2O_2 was also chosen as the optimal polymer to NO donor ratio to realize the prolonged NO release. Although the new NO release coatings tend to adsorb proteins on the surface, it can be anticipated that the released NO can still prevent thrombus formation by deactivating platelets, which is further described in Chapter 3.

The new NO release coatings using PLGA have prospective applications as coatings for many other blood-contacting medical devices.

2.5 References

1. Vaughn, M.W.; Kuo, L.; Liao, J.C. *Am. J. Physiol.-Heart Circul. Physiol.* **1998**, 274(6), H2163-H2176.

2. Gifford, R.; Batchelor, M.M.; Lee, Y.; Gokulrangan, G.; Meyerhoff, M.E.; Wilson, G.S. *J. Biomed. Mater. Res. A* **2005**, 75A(4), 755-766.

3. Oh, B.K.; Robbins, M.E.; Nablo, B.J.; Schoenfisch, M.H. *Biosens. Bioelectron.* **2005**, 21(5), 749-757.

4. Batchelor, M.M.; Reoma, S.L.; Fleser, P.S.; Nuthakki, V.K.; Callahan, R.E.; Shanley, C.J.; Politis, J.K.; Elmore, J.; Merz, S.I.; Meyerhoff, M.E. *J. Med. Chem.* **2003**, 46(24), 5153-5161.

5. Nishida, H.; Takada, N.; Yoshimura, M.; Sonoda, T.; Kobayashi, H. *Bull. Chem. Soc. Jpn.* **1984**, 57(9), 2600-2604.

6. Schwendeman, S.P. *Crit. Rev. Ther. Drug* **2002**, 19(1), 73-98.

7. Shenderova, A.; Ding, A.G.; Schwendeman, S.P. *Macromolecules* **2004**, 37(26), 10052-10058.

8. Li, L.; Schwendeman, S.P. *J. Control. Release* **2005**, 101(1-3), 163-173.

9. Ding, A.G.; Shenderova, A.; Schwendeman, S.P. *J. Am. Chem. Soc.* **2006**, 128(16), 5384-5390.

10. Ding, A.G.; Schwendeman, S.P. *Pharm. Res.* **2008**, 25(9), 2041-2052.

11. Major, T.C.; Brant, D.O.; Reynolds, M.M.; Bartlett, R.H.; Meyerhoff, M.E.; Handa, H.; Annich, G.M. *Biomaterials* **2010**, 31(10), 2736-2745.

12. Shin, J.H.; Marxer, S.M.; Schoenfisch, M.H. *Anal. Chem.* **2004**, 76(15), 4543-4549.

CHAPTER 3

INTRAVASCULAR GLUCOSE/LACTATE SENSORS WITH NITRIC OXIDE RELEASE COATINGS

3.1 Introduction

As discussed in Chapter 1, it is desirable to develop intravenous glucose sensors to accurately monitor real-time blood glucose levels for critically ill hospital patients in order to decrease the potential complications for diabetic patients, as well as to gain better outcomes for non-diabetics, both benefitting from tight glycemic control [1-5]. Beyond glucose, it is also important to continuously monitor blood lactate levels, as lactate is one of the most important indicators of survival for critically ill patients [6-11]. Miniaturized implantable glucose and lactate sensors have been developed, but they still face the challenge of biocompatibility which might impair their reliability and extended usage after implantation [12, 13].

To enhance the biocompatibility of such implantable glucose/lactate sensors, it has been proposed to coat these devices with polymers capable of releasing or generating nitric oxide (NO), based on the fact that NO is a potent anti-thrombus and anti-inflammatory agent [14, 15]. Recent research in this laboratory [15-20] and

elsewhere [21-24] has shown that polymers capable of releasing 1-15 × 10^{-10} mol $min^{-1}cm^{-2}$ of NO at the polymer/blood interface can effectively decrease the platelet adhesion and thrombus formation on the surfaces of implanted devices. Further, working in collaboration with Dr. George Wilson's group at the University of Kansas, our laboratory demonstrated that electrochemical glucose sensors prepared with NO releasing outer polymeric membranes greatly decreased the *in vivo* inflammatory response after subcutaneous implantation of sensors in rats for 2 days (when compared to control sensors implanted in the same animals), without degrading the analytical performance of the glucose sensor itself [25]. Schoenfisch and coworkers also modified miniaturized electrochemical glucose sensors with NO releasing xerogels and observed an improvement in biocompatibility over a 3 day period by analyzing the platelet and cell adhesion using *in vitro* assays [23]. To date, there are no reports on the use of NO releasing glucose sensors for making improved intravascular measurements, or the adaptation of this concept for preparing lactate sensors with improved *in vivo* biocompatibility. In this chapter, a novel design for preparing intravascular glucose and lactate sensors with NO releasing polymeric coatings using the PLGA matrix described in detail in Chapter 2 is reported, and real-time *in vivo* data obtained for glucose sensing in the veins of rabbits confirms the reduced thrombus and improved analytical performance of such devices.

3.2 Experimental

3.2.1 Materials

Glucose oxidase (Type VII, From Aspergillus niger), d-(+)-glucose, glutaraldehyde, bovine serum albumin (BSA), iron (III) chloride ($FeCl_3$), 37 % hydrochloric acid (HCl), cellulose acetate, methanol, L-lactate, L-ascorbic acid, uric acid, Nafion (5 wt % solution in a lower aliphatic alcohols/H_2O mix), 1, 3-diaminobenzene, resorcinol, tetrahydrofuran (THF), dimethylacetamide (DMAc), *N*,*N*'-dibutyl-1,6-hexanediamine (DBHD), polyethylenimine (PEI) and poly(DL-lactide-*co*-glycolide) 50:50 (PLGA, RESOMER® RG 502 H) were purchased from Sigma-Aldrich (St. Louis, MO). Sodium chloride (NaCl), potassium chloride (KCl), sodium phosphate dibasic (Na_2HPO_4) and potassium phosphate monobasic (KH_2PO_4) were from Fisher Scientific (Pittsburgh, PA). Platinum/iridium (Pt/Ir) and silver (Ag) wires were products of A-M Systems (Sequim, WA). Lactate oxidase was obtained from Genzyme (Cambridge, MA). Potassium tetrakis(4-chlorophenyl)borate (KTpClPB) was from Fluka (Ronkonkoma, NY). PurSil 20 80A was from the Polymer Technology Group (Berkeley, CA). DBHD/N_2O_2 was synthesized by treating DBHD with 80 psi NO gas purchased from Cryogenic Gases (Detroit, MI) at room temperature for 24 h, as previously described [26].

3.2.2 Fabrication of NO Release Glucose/Lactate Sensors

The design of the needle-type glucose sensor was based on previous publications [25, 27]. Briefly, a 1-mm cavity was cut at 4 mm from one tip of a 10-cm-long Teflon-coated Pt/Ir wire of 0.2 mm outer diameter (see Fig. 3.1). A 15-cm, 0.1-mm o.d. silver/silver chloride (Ag/AgCl) wire was tightly wrapped around the sensor starting 1.5 mm above the opening covering a length of 4 mm. The Ag/AgCl wire was prepared by dipping the Ag wire into a $FeCl_3$/HCl solution. The straight section above the wrapped Ag/AgCl wire was covered with a 5-cm long, 0.4-mm o.d., heat shrinkable polyester tubing (Advanced Polymers, Salem, NH). The 1-mm opening of the sensor was dip-coated with a thin layer of Nafion. Then, an *in situ* electropolymerization coating was applied using a Voltammograph potentiostat (Bioanalytical Systems Inc., W. Lafayette, IN) cycling voltage between 0 and +830 mV at 2 mV/s for 18 h with 1,3-diaminobenzene and resorcinol [28] to enhance selectivity over interferences that are electroactive, e.g., ascorbate, urate, and acetaminophen. One microliter of glucose oxidase solution with BSA was then dropped in the cavity along the wire. This layer was dried for 30 min and then crosslinked by adding 1 μL of 2% (vol/vol) glutaraldehyde solution and allowing it to cure in air for 1 h. The sensor was then rinsed with water, and allowed to dry for 1 h. NO release sensors were first loop cast with 2:1 (wt/wt) PLGA and DBHD/N_2O_2 in THF and then ca. 4% (wt/vol) PurSil solution in 1:1.5 DMAc and THF. Control sensors were first coated with PLGA solution in THF without the diazeniumdiolate added, and then coated with the outer PurSil solution layer.

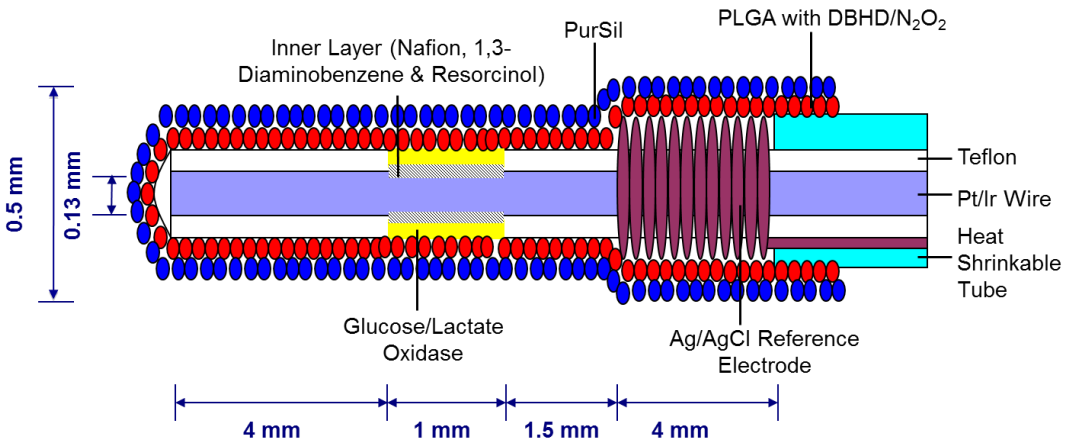

Figure 3.1. Configuration of NO releasing glucose/lactate sensors.

The fabrication of the lactate sensor was the same to that of the glucose sensor, except that the enzyme solution used was lactate oxidase stabilized with 0.7% of PEI, and the crosslinking time was 2 h instead of 1 h.

3.2.3 Analytical Performance of NO Release Glucose/Lactate Sensors

Glucose and lactate sensors were calibrated on a 4-channel potentiostat BioStat (ESA Biosciences Inc., Chelmsford, MA). The sensors were tested at an applied potential of +600 mV vs. Ag/AgCl reference in 0.1 M phosphate buffer saline (PBS), pH 7.4 at 37℃. The buffer was purged with 10% oxygen in nitrogen (Cryogenic Gases, Detroit, MI) to ensure that the sensors can provide a linear response to 15 mM glucose under such low oxygen tension (levels closer to *in vivo* conditions).

The stability of NO release glucose/lactate sensors was tested by calibrating the sensors over one week and monitoring the sensitivity change. The normalized sensitivity of NO releasing glucose/lactate sensors over one week period of time was plotted and the sensitivity percentage was calculated by dividing the sensitivity on each day by that on day 7. To test the repeatability of the NO releasing glucose sensor, the devices were inserted into a 5 mM glucose solution 5 separate times, with washing and allowing the baseline to stabilize in between these multiple measurements. The glucose concentrations were then back-calculated using the calibration curve plotted earlier and the average was taken to evaluate the repeatability of such sensors.

To test the selectivity of NO release sensors over naturally existing interferences such as ascorbic acid, uric acid and other neutral molecules such as acetaminophen, the maximum possible *in vivo* level of interfering species were added into the solution when calibrating the sensors. Using an NO release glucose sensor for an example, the % error was calculated by dividing the current from interferences (0.5 mM for ascorbic acid and 0.2 mM for acetaminophen [29]) by the signal from 5 mM of glucose. The selectivity was monitored for one week to test the stability of the inner polymeric layer for blocking those interferences.

3.2.4 Nitric Oxide Release *In Vitro*

Nitric oxide released from both glucose and lactate sensors was monitored via chemiluminescence with a Sievers Nitric Oxide Analyzer (NOA) 280i (Boulder, CO).

The sensors were immersed into 0.1 M PBS, pH 7.4, at 37℃ and the NO flux data were collected. Long-term NO release was monitored over a 7-day period by collecting flux data for 1 h each day. The sensors were continuously soaked in PBS at 37℃ with nitrogen purging to ensure that all sensors release NO under the same conditions as when measuring NO flux using the NOA.

To measure the NO release coating thickness of the sensors, an NO release glucose sensor was cut in the sensing area and the Ag/AgCl reference electrode wrapped portion. Images were taken at the cross-sections using a Scanning Electron Microscope (SEM, Hitachi S-3200N), and the coating thickness was estimated from these images.

3.2.5 *In Vivo* Protocol for Evaluation of Both Sensor Performance and Biocompatibility

A total of 15 white rabbits (Myrtle's Rabbitry, Thompson's Station, TN) were used in this study to test the glucose sensors only. A protocol as described elsewhere in detail was followed for the *in vivo* experiments except with the maintenance fluid rate adjusted to 3.3 mL/kg/min [22]. One control (without NO release) and two NO release glucose sensors were implanted in the veins of an anesthetized rabbit for 8 h (Fig. 3.2). All the sensors fabricated for the *in vivo* study were first glued into 24-gauge IV polyurethane catheters (0.67 o.d. × 19 mm, Fisher Scientific, PA), and then coated with outer polymers (PurSil) (Fig. 3.2). The electrochemical response of each sensor to blood glucose was monitored via the output current of the sensors. To calibrate the sensors and evaluate the analytical performance regarding sensing glucose, 0.6 mL of

blood was drawn from the rabbits every 30 min to test the blood glucose level using a 700 Series Radiometer blood analyzer (Radiometer America Inc., Westlake, OH). The blood glucose level measured *in vitro* on the Radiometer instrument after 1 h of sensor implantation was used to set a one point calibration for each of the implanted sensors [30, 31], and the continuous output thereafter was compared to the other intermittent blood glucose values. After 8 h, the sensors were explanted and the thrombus formation on each device was documented via digital photography. For a quantitative analysis of the thrombus formation, Image J software (http://rsbweb.nih.gov/ij/index.html) was used to measure the area of the red pixels (thrombus) from the photos, and the results of the control and NO release sensors were compared.

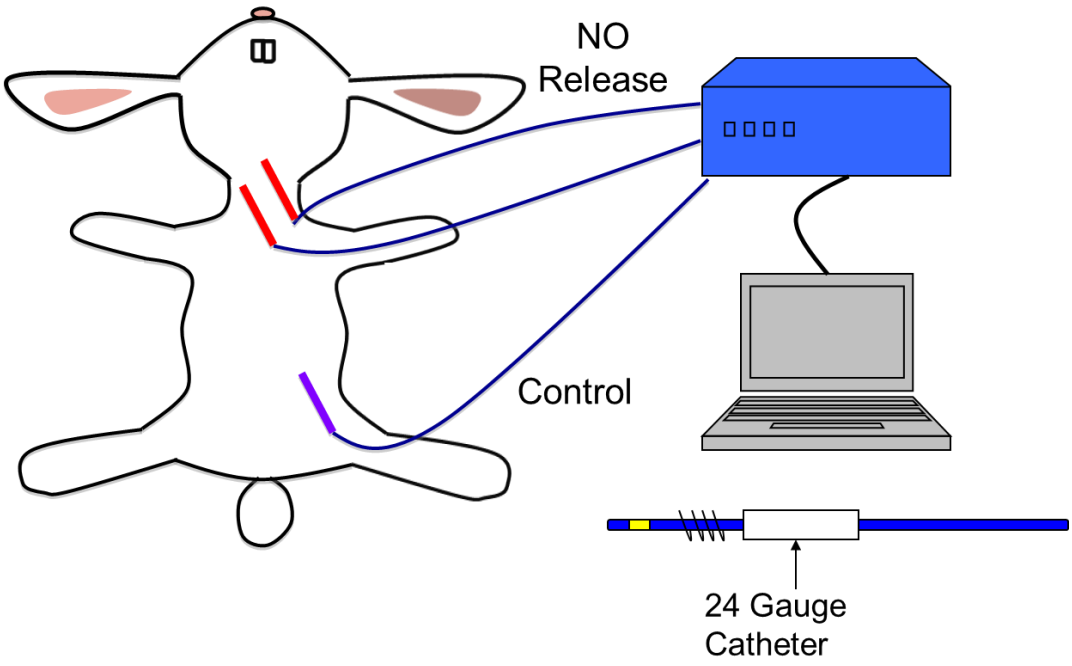

Figure 3.2. *In vivo* experimental configuration of glucose sensors implanted in rabbit veins for 8 h.

3.3 Results and Discussion

3.3.1 Prolonged NO Release of Glucose/Lactate Sensors

Figure 3.3 shows the NO release of glucose/lactate sensors over a one week period of time using PLGA as the matrix in which the DBHD/N_2O_2 is embedded. The NO flux reached an average maximum of 24 $\times 10^{-10}$ mol $min^{-1}cm^{-2}$ (n=4) approximately 30 min after immersion in PBS. The NO release then decayed exponentially, but continued for more than 7 days at a rate > 1 $\times 10^{-10}$ mol $min^{-1}cm^{-2}$, a flux similar to the NO flux produced by endothelial cells in cell cultures [32]. Hence, using a matrix that contained all PLGA for DBHD/N_2O_2 and a top coating of PurSil, provides a bilayer coating that releases NO for more than one week without influencing the enzyme activity. This is a much longer period than the previously proposed NO release glucose sensors [25, 33].

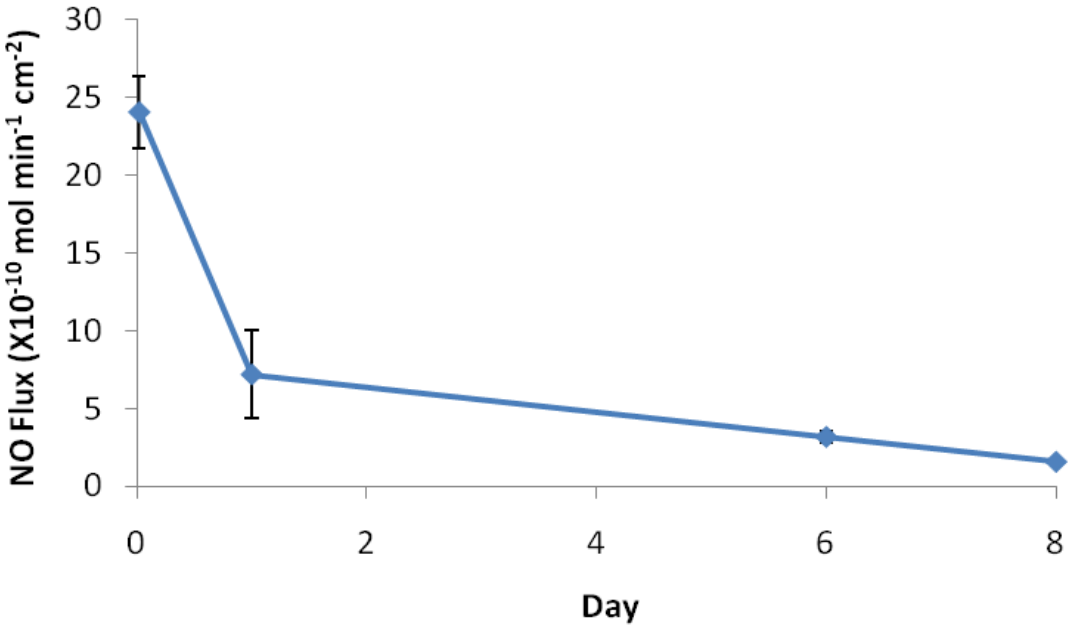

Figure 3.3. NO release of glucose/lactate sensors for over 7 days (n=4).

Figure 3.4 shows the cross-sectional SEM images of the NO release glucose sensor at (a) the sensing area where the enzyme is immobilized and (b) the Ag/AgCl wire wrapped area. It can be seen that both the inner PLGA/DBHD/N_2O_2 coatings and the top PurSil layer were estimated to be ca. 30 μm thick, respectively.

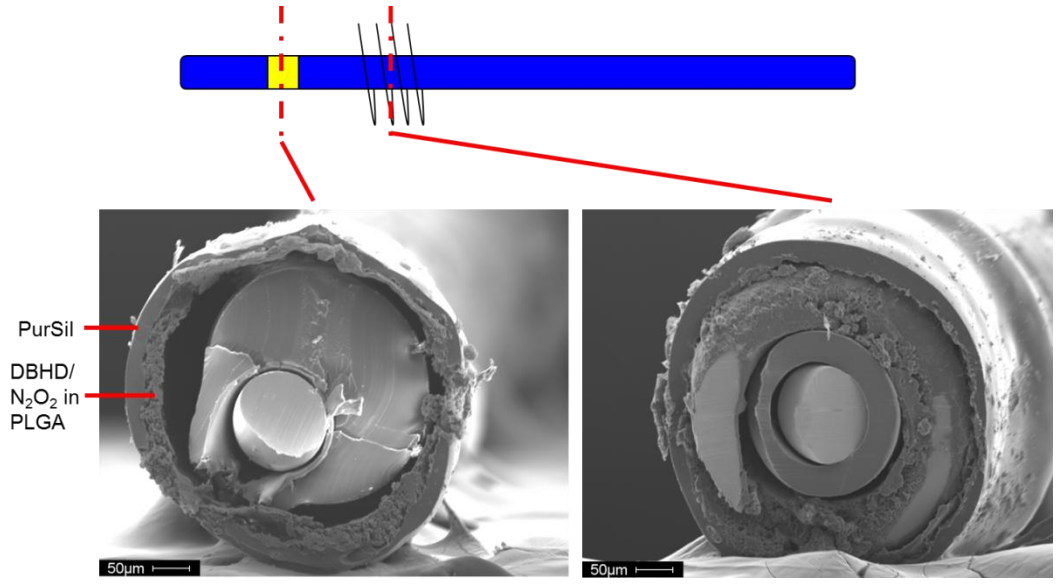

(a) (b)

Figure 3.4. SEM images of cross-sections of the NO release glucose sensor (a) at the sensing area and (b) at the Ag/AgCl wrapped area.

3.3.2 *In Vitro* Performance of NO Release Glucose/Lactate Sensors

In addition to biocompatibility, any enzyme-based sensor aimed at real biological applications must have reasonably stable sensitivity, a wide enough linear range for blood measurements, good response times and an acceptable selectivity over naturally existing interferences. Figure 3.5 shows the typical current measurement of the NO release sensor for (a) glucose and (c) lactate, as well as the plotted calibration curve of the linear concentration range of (b) glucose and (d) lactate. For glucose sensors, 0.5 mM of ascorbic acid, 0.2 mM of acetaminophen and aliquots of 5, 10 and 15 mM of glucose were added into the solution in the order as shown in the figure. For lactate sensors, aliquots of 2, 4 and 6 mM of lactate were used for the calibration.

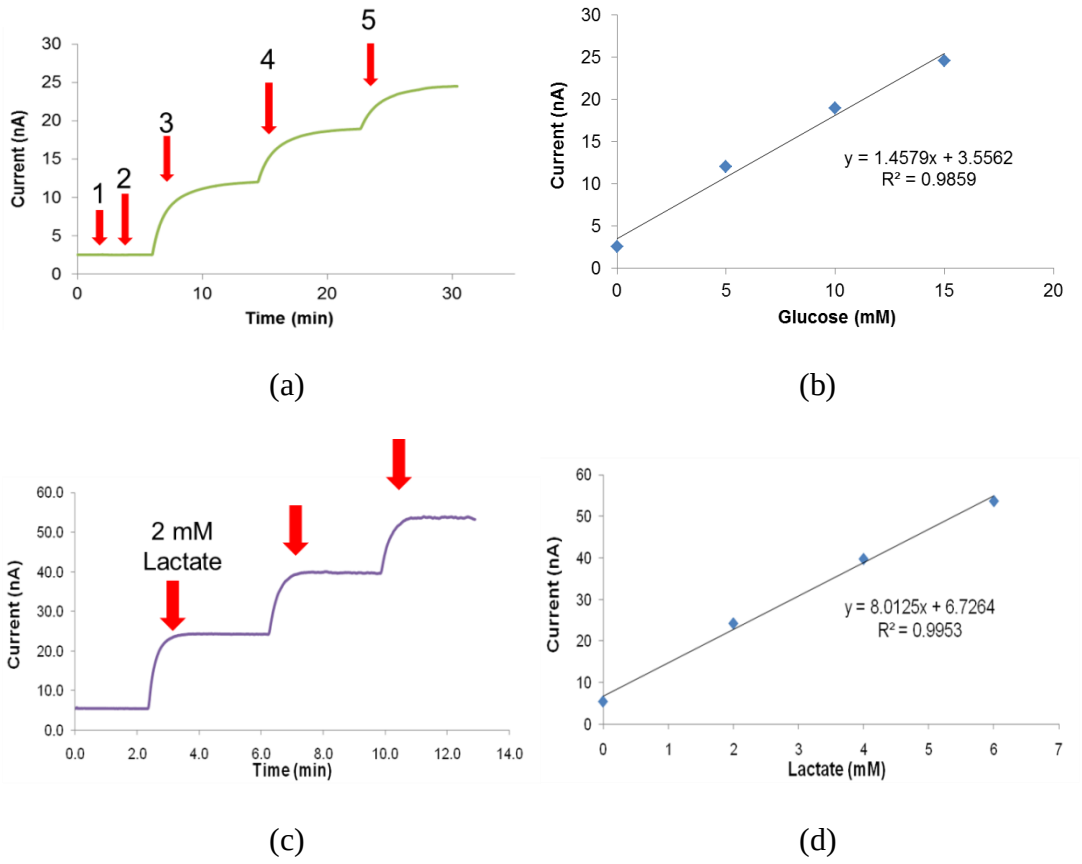

Figure 3.5. Amperometric responses and corresponding calibration curves of NO release sensors for (a), (b) glucose and (c), (d) lactate. For glucose sensor calibration in (a), 0.5 mM of ascorbic acid, 0.2 mM of acetaminophen and aliquots of 5, 10 and 15 mM of glucose were added into the solution in this order as shown in the figure. For lactate sensor calibration in (b), aliquots of 2, 4 and 6 mM of lactate were used for the calibration.

The *in vitro* normalized sensitivity of NO releasing glucose sensors (n=4) over a one week period of time is shown in Figure 3.6 (a). The sensitivity percentage was calculated from dividing the sensitivity on each day by that on day 7. As is shown in Fig. 3.6 (a), the sensitivity increased during the first 3 days because of the conditioning of the outer polymeric coatings (water uptake), and remained relatively stable thereafter.

The NO releasing glucose sensors showed a stable sensitivity from 1.9 to 3.7 nA/mM, had a linear range from 0 to over 15 mM under a 10% level of oxygen (pO_2 of 70 mmHg) which is close to the venous blood oxygen levels, and the steady-state current was reached within 5 minutes.

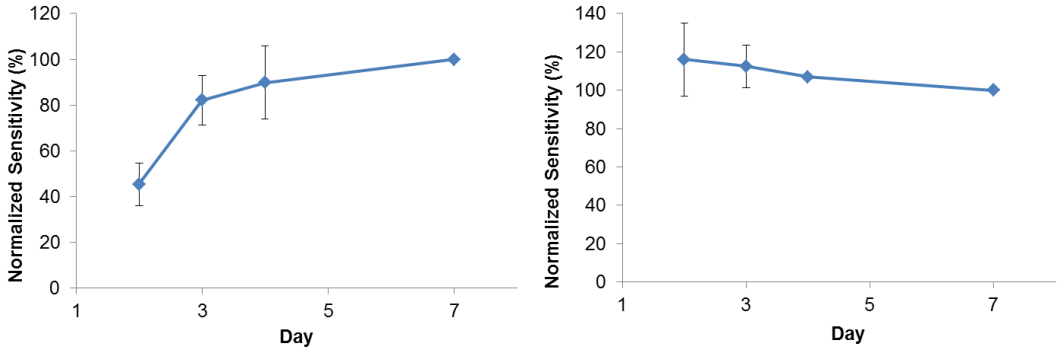

(a) (b)

Figure 3.6. Normalized sensitivity of (a) NO releasing glucose sensors (n=4) and (b) NO releasing lactate sensors (n=3) over one week period of time. The percentage was calculated by dividing the sensitivity values on each day by the sensitivity on day 7.

Figure 3.6 (b) shows the stability of NO release lactate sensors (n=3) over one week in terms of the normalized sensitivity. The sensitivity decreased slightly over time, which is possibly due to the gradual loss in enzyme activity. Indeed, lactate oxidase is known to be a less stable enzyme than glucose oxidase [34]. The NO releasing lactate sensors exhibited a stable sensitivity range from 4.9 to 7.2 nA/mM, had a linear range from 0 to 10 mM lactate and the response time was less than 2 minutes. Both NO releasing glucose and lactate sensors showed acceptable *in vitro* analytical performance over a 7-day period, similar to the designs proposed earlier [27, 35], and were viewed as potentially useful for *in vivo* measurement.

The repeatability of the NO release glucose sensors was tested by inserting the device into 5 mM glucose solutions 5 separate times, with washing and allowing the baseline to stabilize in between these multiple measurements. Figure 3.7 shows the results from the repeated measurements of 5 mM glucose. The glucose concentrations were back-calculated using the calibration curve plotted earlier. The sensor showed an acceptable repeatability with an average of 5.19 ± 0.53 mM measured for the 5 measurements.

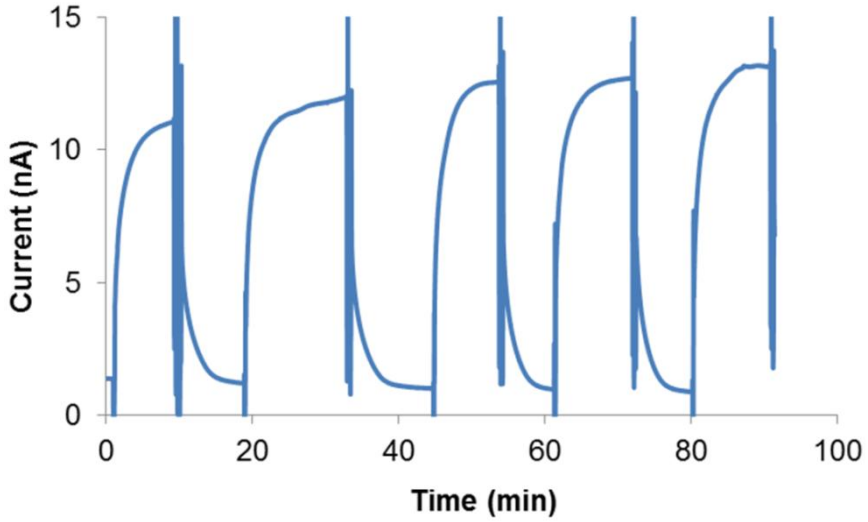

Figure 3.7. Repeat measurements of 5 mM of glucose from the NO release glucose sensor.

When NO release was first introduced to create an implantable glucose sensor, there was some concern about an increase in the background current (due to oxidation of NO at the platinum anode) that could add inaccuracy to the glucose measurement, especially in the case of using a one-point calibration for the *in vivo* application. From the *in vitro* calibration results, NO releasing glucose sensors that possess a flux of ca. 4 ×

10^{-10} mol min^{-1} cm^{-2} had an average background current of 2.3±0.9 nA (n=4) which was only slightly higher than the control sensors without NO release, that had an average of 1.2±0.7 nA (n=4). However, NO releasing sensors had a sensitivity range from 1.9 to 3.7 nA/mM, so the signal-to-background ratio at normal glucose levels (5.5 mM) was between 5 and 10. Furthermore, the background current of NO releasing glucose sensors in the blood stream is expected to be lower than tested *in vitro*, as there are many biological NO scavengers, such as oxyhemoglobin that exist in the blood, that will decrease the flux of NO toward in the inner platinum working electrode of the intravascular sensor. As a result, the background current contributed from NO release is negligible for intravascular applications, especially for the glucose sensor with sensitivity > 2 nA/mM. The NO contribution to the lactate sensor background is greater than the glucose sensor because normal lactate levels can be < 0.5 mM. Nevertheless, for real measurements, especially for patients in the ICU with elevated lactate levels > 2 mM, the current from the NO background is < 20% of the signal that would occur at these levels of lactate. Although undesirable, a two-point calibration can be performed when the sensor background from NO release is contributing significantly to the sensor signal.

When PLGA was first applied to the NO releasing lactate sensor, there was a concern that the lactic acid produced would also increase the background signal. However, the results showed that the increase in background signal was from NO rather than lactate, as the background was similar to that of the NO releasing glucose sensor with the same level of NO release. Indeed, the degradation timeframe of the PLGA

50:50 with an internal viscosity of 0.16 - 0.24 dL/g is known to be 2 - 4 weeks [36]. Thus, the hydrolysis of the PLGA layer coated onto sensors under the PurSil layer occurs at a very slow rate producing very low steady-state levels of lactic acid (likely in the nanomolar range) in the sensing layer of the device, while the physiological levels of lactic acid are in the millimolar range. As a result, PLGA is suitable to use to prolong NO release on lactate sensors without adding inaccuracy to the analytical performance.

The NO release sensors also need to have excellent selectivity over naturally existing interferences such as ascorbic acid, uric acid and other neutral molecules such as acetaminophen, in order to be considered for real clinical application. The electropolymerization of 1, 3-diaminobenzene and resorcinol was applied as the inner layer onto the sensing area with an underlying layer of Nafion [28, 37]. The monomers were electropolymerized at the electrode surface only in the pores of the Nafion layer which created a composite polymer mixture. Figure 3.8 shows the structures of the monomers and the proposed electropolymerized polymer. Figure 3.9 illustrates the cyclic voltammogram of the electropolymerization process. The peak current dropped significantly after 18 h of reaction, indicating the formation of a non-conducting polymer layer on the sensing surface. The selectivity results for NO releasing glucose sensors over major interferent molecules are shown in Table 3.1. Using the NO releasing glucose sensor for an example, the % error was calculated by dividing the current from the maximum possible *in vivo* level of interferences (0.5 mM for ascorbic acid and 0.2 mM for acetaminophen) by the signal from 5 mM of glucose. Even though the selectivity decreased over a one-week period, the % error remained < 3% for ascorbic

acid and < 7% for acetaminophen. This indicated that the sensor could retain a reasonable selectivity over major interferences for at least one week during the NO release time.

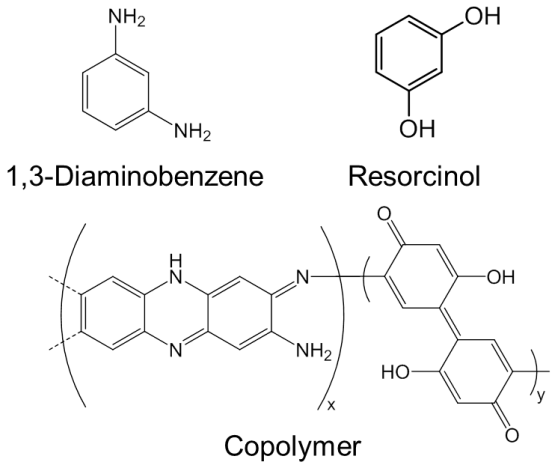

Figure 3.8. Structures of 1,3-diaminobenzene, resorcinol and the corresponding electropolymerized polymers.

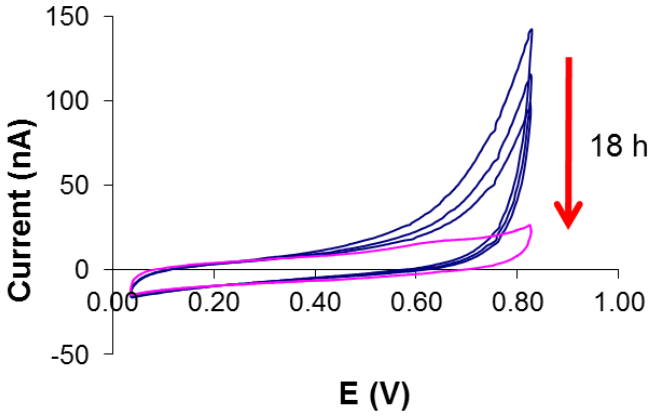

Figure 3.9. Cyclic voltammogram of the 18 h electropolymerization of 1,3-diaminobenzene and resorcinol at Pt/Ir working electrode of glucose/lactate sensors.

Table 3.1. Selectivity of NO releasing glucose sensors over a one-week period (n=4)[a].

Day	3	5	6	7
Ascorbic acid (%)	0	1.10±1.01	2.08±1.09	2.88±1.53
Acetaminophen (%)	1.86±1.38	3.31±1.09	5.35±1.66	6.76±1.67

[a] Selectivity was measured by dividing the current from the maximum possible physiological level of interferences (0.5 mM for ascorbic acid and 0.2 mM for acetaminophen) by the signal from 5 mM of glucose.

3.3.3 Blood-Compatibility and Surface Thrombus Evaluation of NO Release Glucose Sensors

All the control and NO release glucose sensors were conditioned in PBS buffer for 3 days before implantation in rabbit veins to ensure stable sensitivity during the *in vivo* experiments. For NO releasing sensors, the NO flux was checked by the NOA both before and after the *in vivo* implantation, and the NO flux results were similar to the *in vitro* NO release profile, as shown in Figure 3.3. Figure 3.10 shows the NO release flux measurements of 2 individual NO release glucose sensors (a), (c) before and (b), (d) after the 8 h implantation in rabbit veins. From Figure 3.10, it can be seen that the NO releasing glucose sensors were capable of maintaining a steady-state surface flux of $> 4 \times 10^{-10}$ mol min^{-1} cm^{-2} during the entire 8 h of the experiment.

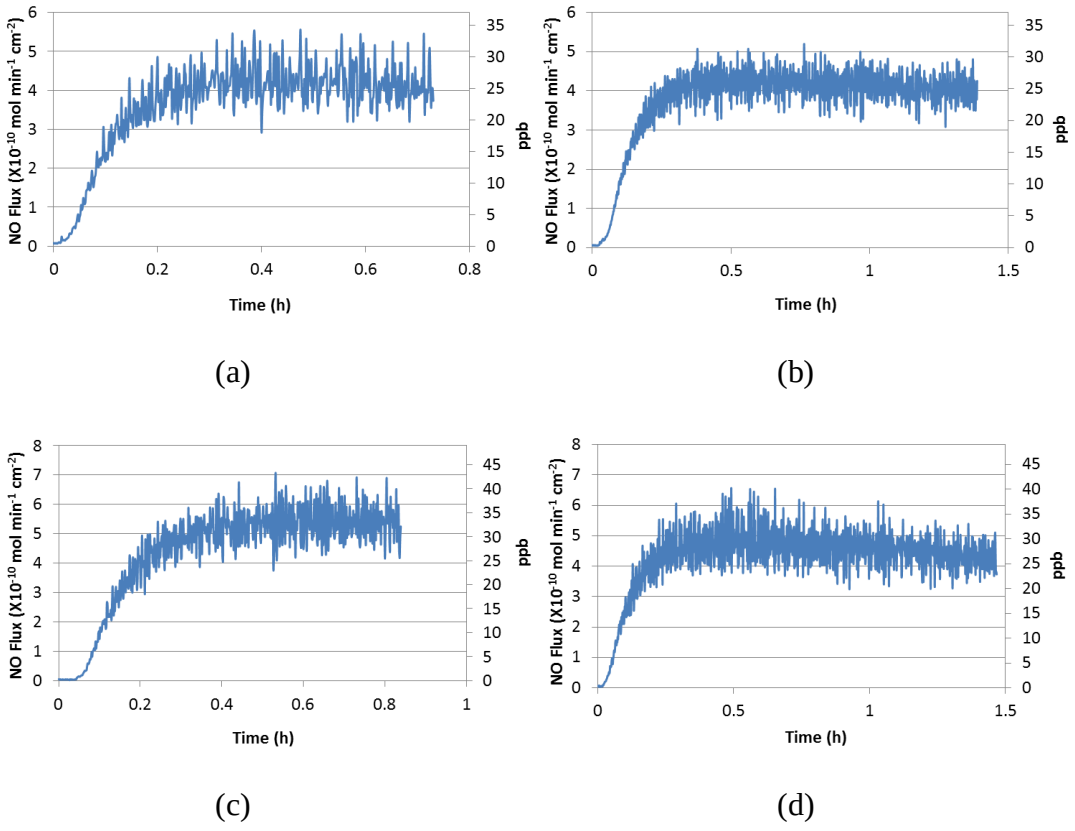

Figure 3.10. NO release of 2 individual glucose sensors (a), (c) before and (b), (d) after 8 h of implantation in rabbit veins.

Figure 3.11 (a) and (b) shows photos of control and NO releasing glucose sensors explanted from rabbit veins after 8 h of implantation. The results from two individual rabbit experiments with three sensors implanted in each were shown in photos (a) and (b). As can be seen from the photos, the bottom two NO releasing sensors in both (a) and (b) showed minimal thrombus formation on the surface, while the one control sensor (top) without NO release formed obvious thrombus on the surface. The copolymer of polyurethane and siloxane, PurSil, with a blank underlying PLGA layer, is clearly thrombogenic.

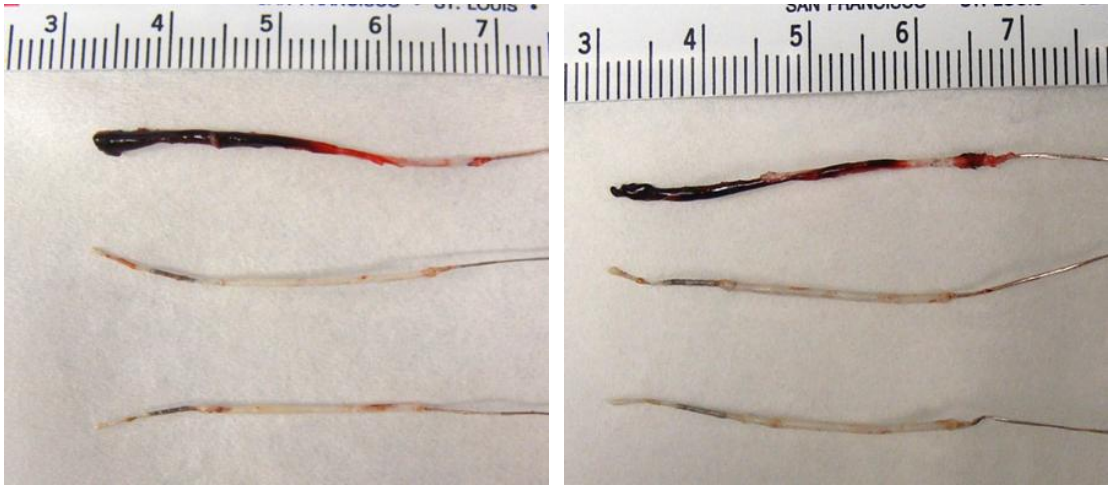

(a) (b)

Figure 3.11. Glucose sensors explanted after 8-h implantation in rabbit veins. Photos (a) and (b) demonstrate the drastic difference in thrombus formation between control (top) and NO releasing (middle, bottom) glucose sensors in two example rabbits.

Using the Image J software, a more detailed statistical analysis of thrombus formation was performed. Figure 3.12 shows an example of extracting the red pixel area from the original picture using Image J. Then the red pixel area was measured indicating the amount of thrombus formed on sensor surfaces. From the picture, the red area of the control glucose sensor reads 0.357 cm^2 while the two NO release glucose sensors read 0.083 and 0.253 cm^2, respectively. NO release sensors formed much less thrombus than the control sensor without any NO release.

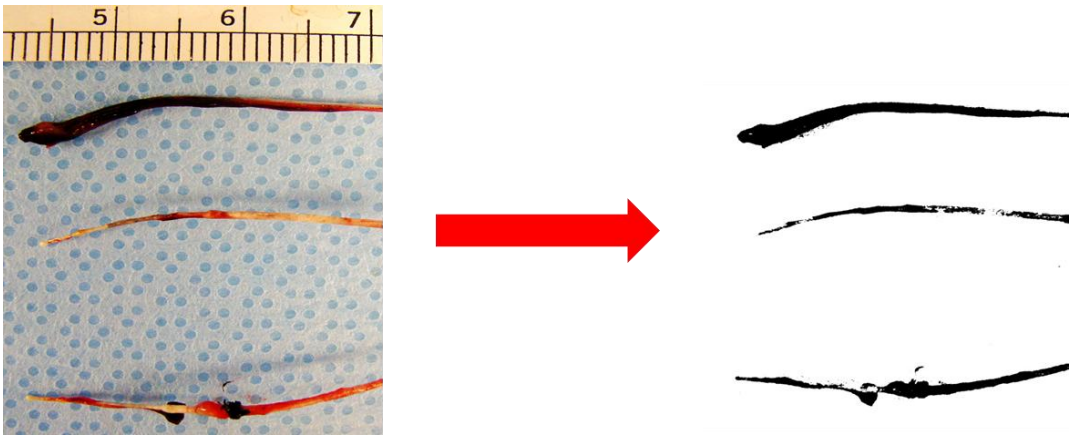

Figure 3.12. Measurement of the red pixel area of explanted sensors using Image J.

Figure 3.13 shows the comparison of the overall thrombus formation between NO releasing (n=30) and control glucose sensors (n=15) in the 15 rabbits used for the *in vivo* testing experiments. Although the deviations were comparatively large, the mean values are statistically different, with NO releasing glucose sensors forming considerably less thrombus than control sensors without NO release ($p<<0.05$). These results confirm the expected anti-thrombus function of NO emission from the surface of the glucose sensors at a surface flux of $> 4 \times 10^{-10}$ mol min^{-1} cm^{-2}.

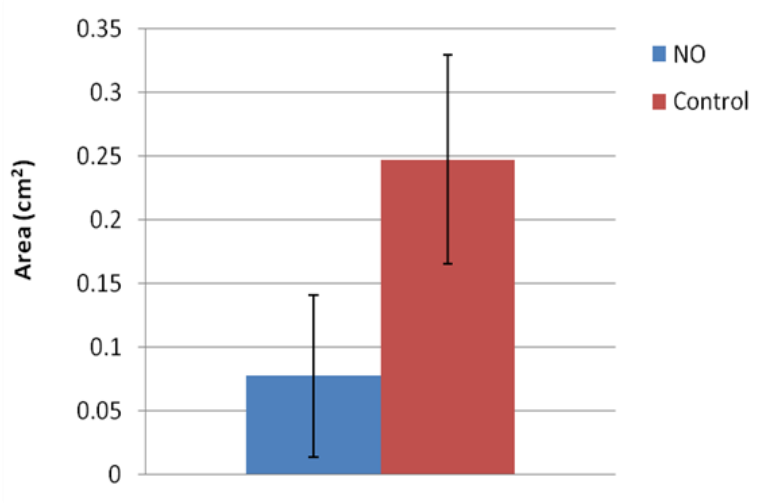

Figure 3.13. Red pixel area in terms of thrombus formation of both control (n=15) and NO releasing glucose sensors (n=30).

It should be noted that from the protein adsorption results in Chapter 2, the NO release coatings tend to adsorb a large amount of proteins such as fibrinogen on the surface. However, from the *in vivo* results described above, the released NO still prevented thrombus formation by deactivating platelets. As suggested in the literature [38], that platelet activation is the key step which ultimately triggers the thrombus formation *in vivo* and NO effectively downregulats platelet activity. As a result, NO release is crucial to prevent thrombus formation on polymeric surfaces in contact with blood.

3.3.4 *In vivo* Glucose Sensor Performance

The implanted NO releasing and control glucose sensors were calibrated by a bench top commercial Radiometer instrument (blood-gas/electrolyte/metabolite analyzer)

using a one-point calibration method described earlier. The calculated blood glucose values of the implanted glucose sensors were also correlated to the Radiometer readings. There was a strong correlation between readings from the *in vivo* and *in vitro* devices, with the correlation coefficient between the glucose readings from the sensors and that from the Radiometer being 0.7742 ($p<<0.05$) ($n=30$) for 15 separate *in vivo* sensor experiments.

Figure 3.14 shows an example of the 8 h continuous monitoring of blood glucose levels reported by NO release and control glucose sensors as well as the bench-top Radiometer instrument. It can be seen that the values from both NO release glucose sensors matched with that from the *in vitro* measurements, while the control glucose sensor showed a deviation starting at around 2 h after implantation. This could be due to the fact that local glucose diffusion was disturbed by the thrombus formation on the implanted control sensor surface, leading to a false current output for a given level of glucose in the blood stream. This result correlated to the thrombus formation results shown in Figure 3.11, that the glucose output readings were reliable when the surfaces of NO release glucose sensors are clean, while the reported blood glucose results showed deviation from the real blood glucose concentrations when the control sensor formed thrombus on the surface.

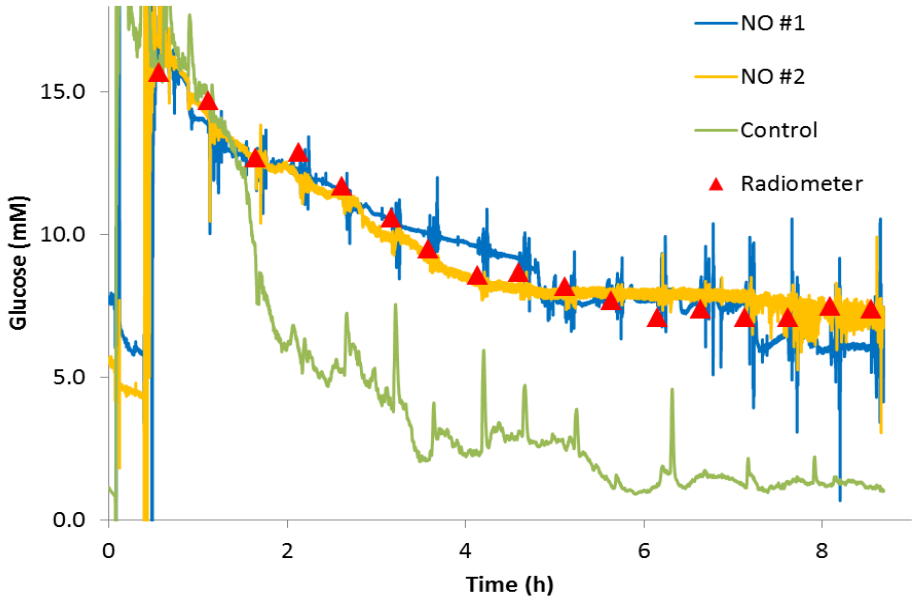

Figure 3.14. Continuous glucose monitoring results from implanted NO releasing and control sensors with comparison to the bench-top Radiometer readings.

To evaluate the accuracy of both NO release and control glucose sensors from a statistical view, the Clarke error grid analysis method was carried out [39]. The x axis (reference concentration) shows the control blood glucose readings from the bench-top Radiometer and the y axis shows the concentration readings from the implanted sensors. From the Clarke error grid shown in Figure 3.15, the NO releasing glucose sensors exhibited more accurate detection of glucose in the blood stream than the control sensors. Nitric oxide releasing sensors had 97.5% of data points in Zone A (clinically accurate zone) and Zone B (benign error zone with no clinical consequences) (Fig. 3.15 (a)), where measurement results are accepted as accurate, while control sensors had 86.7% of data points in these zones (Fig. 3.15 (b)). This is likely due to the fact that the thrombus formation on the implanted control sensors disturbed local glucose diffusion, leading to

false current output for a given level of glucose in the blood stream. Indeed, control sensors had significantly more data points in the upper zone C (leading to unnecessary treatment) than NO release sensors. This was likely due to the one-point calibration after 1 h of implantation when control sensors might already have developed thrombus on their surfaces which lowered the sensors' apparent sensitivity, thus leading to higher blood glucose readings during the first hour of implantation. The NO releasing sensors remained relatively accurate in reporting blood glucose levels as a result of NO down-regulating the platelet activity, thus eliminating thrombus formation. Furthermore, the thrombus formed on the surface of the implanted control devices could block blood flow within the vessel, which would have a negative effect on the local implant site, and ultimately be dangerous for the patient.

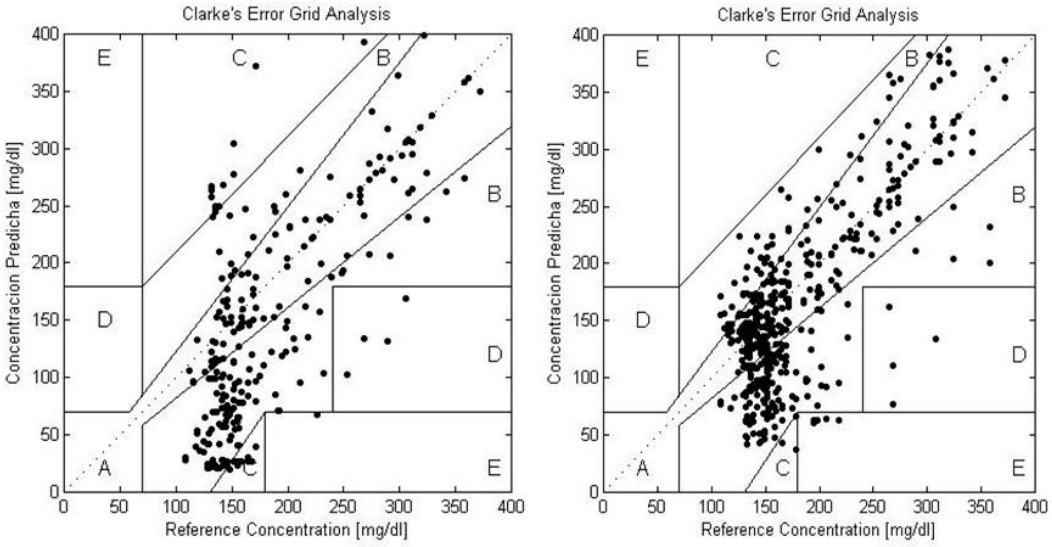

(a) (b)

Figure 3.15. Comparison of glucose measurement results for (a) control (n=15) and (b) NO releasing glucose sensors (n=30) when implanted in rabbit veins for 8 h using the Clarke error grid.

3.4 Conclusions

Nitric oxide releasing glucose and lactate sensing catheters have been successfully fabricated that exhibit NO release for more than one week at levels that attenuate thrombus formation using a new PLGA-based coating containing a lipophilic diazeniumdiolate NO donor species. The analytical performance of both the glucose and lactate sensors is not influenced significantly by the NO release or PLGA degradation products. The sensors exhibit relatively stable amperometric response over a one-week period with high selectivity over interferences, making them suitable for blood monitoring applications. An *in vivo* study (intravenous) of glucose sensors prepared in this manner showed that this coating exhibits a very good anti-thrombotic property for the implanted sensors, while not disturbing the glucose sensing function. Nitric oxide releasing glucose sensors implanted in the veins of rabbits for 8 h showed greatly reduced thrombus formation on their surfaces compared to corresponding controls. Further, improved accuracy in reporting blood glucose levels of NO release glucose sensors is achieved vs. controls as evaluated using a Clarke error grid type analysis. Although the lactate sensor reported here has not yet been evaluated for *in vivo* performance, the data on this sensor reported herein marks the first time that a lactate sensor has been formulated with an NO release coating. Thus, the data presented in this chapter for the lactate sensor demonstrates that NO release chemistry does not interfere with the lactate oxidase chemistry. While used here only for preparing glucose and lactate catheter style electrochemical sensors, the new NO release coating using PLGA

has prospective applications as a coating for many other blood-contacting biomedical devices.

3.5 References

1. Kondepati, V.R.; Heise, H.M. *Anal. Bioanal. Chem.* **2007**, 388(3), 545-563.

2. Bochicchio, G.V.; Scalea, T.M. *Serono. Sym.* **2008**, 42, 261-275.

3. Lonergan, T.; Le Compte, A.; Willacy, M.; Chase, J.G.; Shaw, G.M.; Wong, X.W.; Lotz, T.; Lin, J.; Hann, C.E. *Diabetes Technol. The.* **2006**, 8(2), 191-206.

4. Vanhorebeek, I.; Langouche, L.; Van den Berghe, G. *Chest* **2007**, 132(1), 268-278.

5. Schetz, M.; Vanhorebeek, I.; Wouters, P.J.; Wilmer, A.; van den Berghe, G. *J. Am. Soc. Nephrol.* **2008**, 19(3), 571-578.

6. Holloway, P.; Benham, S.; St John, A. *Clin. Chim. Acta* **2001**, 307(1-2), 9-13.

7. Shapiro, N.I.; Howell, M.D.; Talmor, D.; Nathanson, L.A.; Lisbon, A.; Wolfe, R.E.; Weiss, J.W. *Ann. Emerg. Med.* **2005**, 45(5), 524-528.

8. Shapiro, N.I.; Howell, M.D.; Talmor, D. *Ann. Emerg. Med.* **2005**, 46(6), 562-562.

9. Shapiro, N.I.; Fisher, C.; Donnino, M.; Cataldo, L.; Tang, A.; Trzeciak, S.; Horowitz, G.; Wolfe, R.E. *J. Emerg. Med.* **2010**, 39(1), 89-94.

10. Arnold, R.C.; Shapiro, N.I.; Jones, A.E.; Schorr, C.; Pope, J.; Casner, E.; Parrillo, J.E.; Dellinger, R.P.; Trzeciak, S.; Emergency Med Shock Res Network, E.M. *Shock* **2009**, 32(1), 35-39.

11. Valenza, F.; Aletti, G.; Fossali, T.; Chevallard, G.; Sacconi, F.; Irace, M.; Gattinoni, L. *Crit. Care* **2005**, 9(6), 588-593.

12. Meyerhoff, M.E. *Trac-Trend. Anal. Chem.* **1993**, 12(6), 257-266.

13. Wilson, G.S.; Gifford, R. *Biosens. Bioelectron.* **2005**, 20(12), 2388-2403.

14. Frost, M.C.; Batchelor, M.M.; Lee, Y.M.; Zhang, H.P.; Kang, Y.J.; Oh, B.K.; Wilson, G.S.; Gifford, R.; Rudich, S.M.; Meyerhoff, M.E. *Microchem. J.* **2003**, 74(3), 277-288.

15. Frost, M.C.; Reynolds, M.M.; Meyerhoff, M.E. *Biomaterials* **2005**, 26(14), 1685-1693.

16. Wu, Y.D.; Zhou, Z.R.; Meyerhoff, M.E. *J. Biomed. Mater. Res. A* **2007**, 81A(4), 956-963.

17. Wu, B.; Gerlitz, B.; Grinnell, B.W.; Meyerhoff, M.E. *Biomaterials* **2007**, 28(28), 4047-4055.

18. Frost, M.C.; Rudich, S.M.; Zhang, H.P.; Maraschio, M.A.; Meyerhoff, M.E. *Anal. Chem.* **2002**, 74(23), 5942-5947.

19. Fleser, P.S.; Nuthakki, V.K.; Malinzak, L.E.; Callahan, R.E.; Seymour, M.L.; Reynolds, M.M.; Merz, S.I.; Meyerhoff, M.E.; Bendick, P.J.; Zelenock, G.B.; Shanley, C.J. *J. Vasc. Surg.* **2004**, 40(4), 803-811.

20. Frost, M.C.; Meyerhoff, M.E., **2004**, in *Oxygen Sensing*, Vol. 381, pp. 704-715.

21. Skrzypchak, A.M.; Lafayette, N.G.; Bartlett, R.H.; Zhou, Z.R.; Frost, M.C.; Meyerhoff, M.E.; Reynolds, M.M.; Annich, G.M. *Perfusion-Uk* **2007**, 22(3), 193-200.

22. Major, T.C.; Brant, D.O.; Reynolds, M.M.; Bartlett, R.H.; Meyerhoff, M.E.; Handa, H.; Annich, G.M. *Biomaterials* **2010**, 31(10), 2736-2745.

23. Oh, B.K.; Robbins, M.E.; Nablo, B.J.; Schoenfisch, M.H. *Biosens. Bioelectron.* **2005**, 21(5), 749-757.

24. Annich, G.M.; Meinhardt, J.P.; Mowery, K.A.; Ashton, B.A.; Merz, S.I.; Hirschl, R.B.; Meyerhoff, M.E.; Bartlett, R.H. *Crit. Care Med.* **2000**, 28(4), 915-920.

25. Gifford, R.; Batchelor, M.M.; Lee, Y.; Gokulrangan, G.; Meyerhoff, M.E.; Wilson, G.S. *J. Biomed. Mater. Res. A* **2005**, 75A(4), 755-766.

26. Batchelor, M.M.; Reoma, S.L.; Fleser, P.S.; Nuthakki, V.K.; Callahan, R.E.; Shanley, C.J.; Politis, J.K.; Elmore, J.; Merz, S.I.; Meyerhoff, M.E. *J. Med. Chem.* **2003**, 46(24), 5153-5161.

27. Bindra, D.S.; Zhang, Y.N.; Wilson, G.S.; Sternberg, R.; Thevenot, D.R.; Moatti, D.; Reach, G. *Anal. Chem.* **1991**, 63(17), 1692-1696.

28. Geise, R.J.; Adams, J.M.; Barone, N.J.; Yacynych, A.M. *Biosens. Bioelectron.* **1991**, 6(2), 151-160.

29. Zhang, Y.N.; Hu, Y.B.; Wilson, G.S.; Moattisirat, D.; Poitout, V.; Reach, G. *Anal. Chem.* **1994**, 66(7), 1183-1188.

30. Choleau, C.; Klein, J.C.; Reach, G.; Aussedat, B.; Demaria-Pesce, V.; Wilson, G.S.; Gifford, R.; Ward, W.K. *Biosens. Bioelectron.* **2002**, 17(8), 641-646.

31. Choleau, C.; Klein, J.C.; Reach, G.; Aussedat, B.; Demaria-Pesce, V.; Wilson, G.S.; Gifford, R.; Ward, W.K. *Biosens. Bioelectron.* **2002**, 17(8), 647-654.

32. Vaughn, M.W.; Kuo, L.; Liao, J.C. *Am. J. Physiol.-Heart Circul. Physiol.* **1998**, 274(6), H2163-H2176.

33. Shin, J.H.; Marxer, S.M.; Schoenfisch, M.H. *Anal. Chem.* **2004**, 76(15), 4543-4549.

34. Lillis, B.; Grogan, C.; Berney, H.; Lane, W.A. *Sensor. Actuat. B-Chem.* **2000**, 68(1-3), 109-114.

35. Hu, Y.B.; Zhang, Y.N.; Wilson, G.S. *Anal. Chim. Acta* **1993**, 281(3), 503-511.

36. http://www.surmodicsbiomaterials.com/products-stock-polymers.html.

37. Manowitz, P.; Stoecker, P.W.; Yacynych, A.M. *Biosens. Bioelectron.* **1995**, 10(3-4), 359-370.

38. Furie, B.; Furie, B.C. *N. Engl. J. Med.* **2008**, 359(9), 938-949.

39. Girardin, C.M.; Huot, C.; Gonthier, M.; Delvin, E. *Clin. Biochem.* **2009**, 42(3), 136-142.

CHAPTER 4

IMPLANTABLE GLUCOSE/LACTATE SENSORS WITH NITRIC OXIDE GENERATION COATINGS

4.1 Introduction

As discussed in Chapter 1, the lifetime of the NO release method is limited by the amount of NO donors (diazeniumdiolates) doped within the polymer matrix, which cannot be increased without a limit in the function of the implantable sensor. To take the advantage of the perpetual reservoir of endogenous RSNOs in blood, there is interest in the method of catalytically generating NO from such RSNO species as an alternative to the NO release method in order to further prolong the effective NO release time frame.

Copper(II) is reported as the most efficient metal ion catalyst in generating NO from RSNOs [1]. Recent research in this group has successfully incorporated this catalytic mechanism into synthesized polymers, including polyurethane (PU) that possesses covalently immobilized Cu(II)-ligand complexes as catalytic sites [2-4]. It has also been demonstrated that micro and nano particles of Cu^{o} that naturally corrode to produce trace levels of Cu(II/I) ions can also generate NO via endogenous RSNOs [5]. In this chapter, the application of both synthesized Cu(II)-cyclen-PU (Fig. 4.1) and Cu^{0}

nanoparticle-doped polyurethane as the outer coatings for implantable glucose/lactate sensors is demonstrated. The Cu(II) sites within the polymers can catalytically generate NO *in situ* from RSNOs existing in the blood stream or subcutaneous fluids and potentially enhance the biocompatibility of such implantable devices.

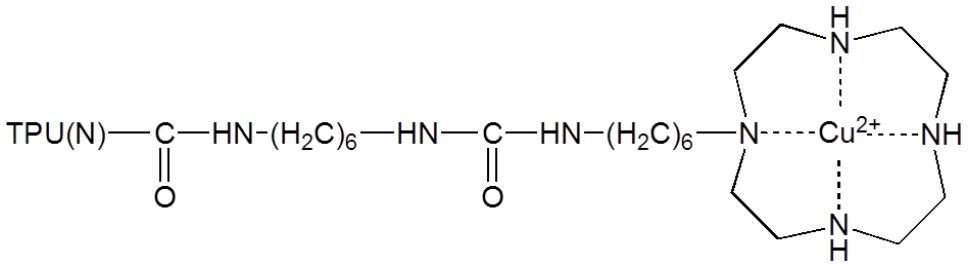

Figure 4.1. Structure of Cu(II)-cyclen-PU. TPU = Tecophilic SP-93A-100 or Tecophilic SP-60D-60 polyurethanes.

Beyond Cu(II), organoselenium (RSe) species have also been shown to be catalysts for generating NO from RSNOs [6]. While the synthesis of PU materials with covalently linked RSe sites intended for the use as the outer coatings for glucose/lactate sensors can be complicated, our lab has developed a generic and simple layer-by-layer (LbL) deposition approach to incorporate the RSe catalytic sites for NO generation on almost any surface, including PU [7]. Such LbL NO generating coatings are created from alternate layers of polycationic RSe-linked polyethyleneimine (SePEI) and polyanionic alginate (Alg). Figure 4.2 shows the idea of depositing such LbL coatings onto implantable sensors with NO generation. Enhanced biocompatibility of such implantable devices can be expected.

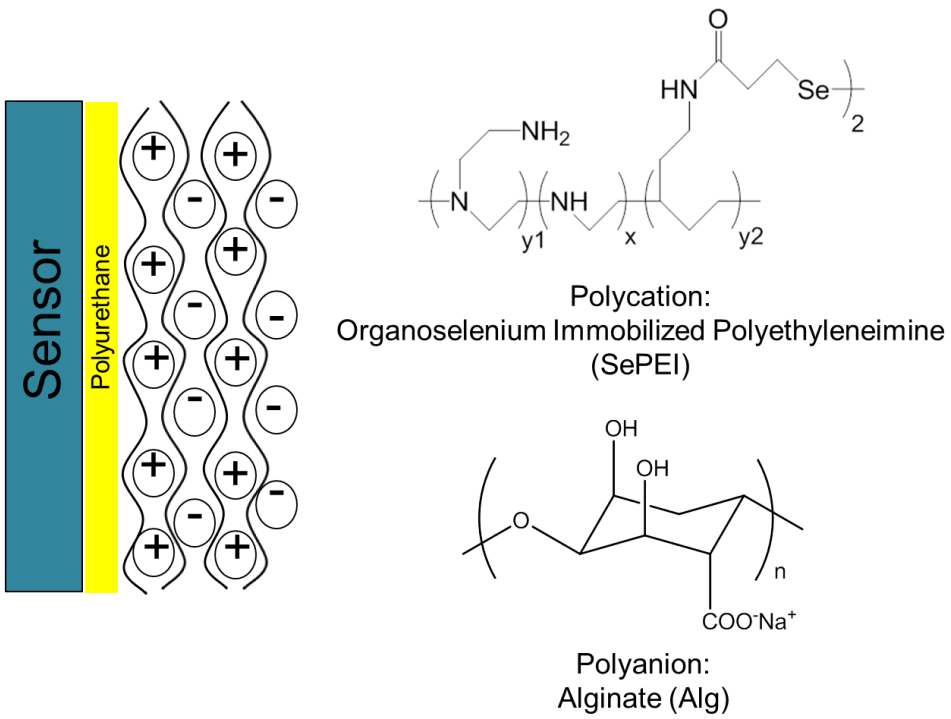

Figure 4.2. Schematic of an implantable sensor coated with SePEI/Alg via LbL deposition.

Apart from the NO generation efficiency of the catalysts, the NO flux from the implantable device surface will also be dependent on the RSNO levels in the blood stream or within the subcutaneous fluid. Thus the development of implantable glucose and lactate sensors using outer coatings with NO generation to improve biocompatibility is dependent on the levels of endogenous RSNO species. However, much debate remains on the actual levels of endogenous RSNOs, ranging from as low as 10 nM to as high as 7 μM [8]. The research described in this chapter is aimed at exploring and optimizing the chemistries required for the fabrication of implantable amperometric glucose/lactate sensors with outer polymeric films that can slowly generate low levels of

NO from endogenous RSNO species that are present in the blood stream and likely present in the interstitial fluid.

4.2 Experimental

4.2.1 Materials

Glucose oxidase (Type VII, From Aspergillus niger), d-(+)-glucose, glutaraldehyde, bovine serum albumin (BSA), iron (III) chloride ($FeCl_3$), 37 % hydrochloric acid (HCl), sulfuric acid (H_2SO_4), sodium nitrite ($NaNO_2$), reduced L-glutathione (GSH), L-lactate, L-ascorbic acid, uric acid, Nafion (5 wt % solution in lower aliphatic alcohols/H_2O mix), 1,3-diaminobenzene, resorcinol, l-(3-dimethylaminopropyl)-3-ethylcarbodiimide (EDC), sodium borohydride ($NaBH_4$), *N*-hydroxysuccinimide (NHS), 2-(*N*-morpholino)ethanesulfonic acid (MES), ethylenediaminetetraacetic acid (EDTA) and polyethylenimine (PEI, M_w 25 kD) were purchased from Sigma-Aldrich (St. Louis, MO). Sodium chloride (NaCl), potassium chloride (KCl), sodium phosphate dibasic (Na_2HPO_4), potassium phosphate monobasic (KH_2PO_4), tetrahydrofuran (THF) and dimethylformamide (DMF) were from Fisher Scientific (Pittsburgh, PA). Platinum/iridium (Pt/Ir) and silver (Ag) wires were products of A-M Systems (Sequim, WA). Lactate oxidase was obtained from Genzyme (Cambridge, MA). Copper nanoparticles (80 nm) were from Inframat Advanced Materials (Farmington, CT). Polydimethylsiloxane (PDMS) was purchased from NuSil (Metamora, MI). Polyurethane (PU) Tecoflex SG-80A, Tecophilic SP-93A-100 and

Tecophilic SP-60D-60 were from the Polymer Technology Group (Berkeley, CA). Cu(II)-cyclen-PU of Tecophilic SP-93A-100 was synthesized as described previously [2]. Cu(II)-cyclen-PU of Tecophilic SP-60D-60 was provided by Accord Biomaterials (Ann Arbor, MI). 3,3'-Diselenidedipropionic acid (SeDPA) and *S*-nitrosoglutathione (GSNO) were synthesized as described elsewhere [6].

4.2.2 Fabrication of Implantable Glucose/Lactate Sensors Coated with Cu(II)-Cyclen-PU or Cu^0 Nanoparticle-Doped PU

The fabrication of the needle-type glucose/lactate sensors was based on previous publications [9-11] and the details are described in Chapter 3. Sensors with NO generation were loop cast with 10 μL of 4% (w/v) of Cu(II)-cyclen-PU dissolved in THF. Both Tecophilic SP-93A-100 (100% water uptake) and Tecophilic SP-60D-60 (60% water uptake) derivatized Cu(II)-cyclen-PUs were tested as the outer coatings for glucose and lactate sensors. To obtain sensors with the desired linear range for glucose or lactate measurements, multiple layers were coated onto sensors by drying for 30 min in between.

For coatings of PU doped with Cu^0 nanoparticles, 20 % (w/w) of 80 nm Cu^0 nanoparticles were dispersed in ca. 4% (w/v) of 3:1 PU and PDMS dissolved in THF with 2% DMF. The suspension was sonicated for 1 h before being loop cast onto glucose sensors. Figure 4.3 shows the configuration of NO generating glucose/lactate sensors with Cu(II)-cyclen-PU or PU doped with Cu^0 nanoparticles.

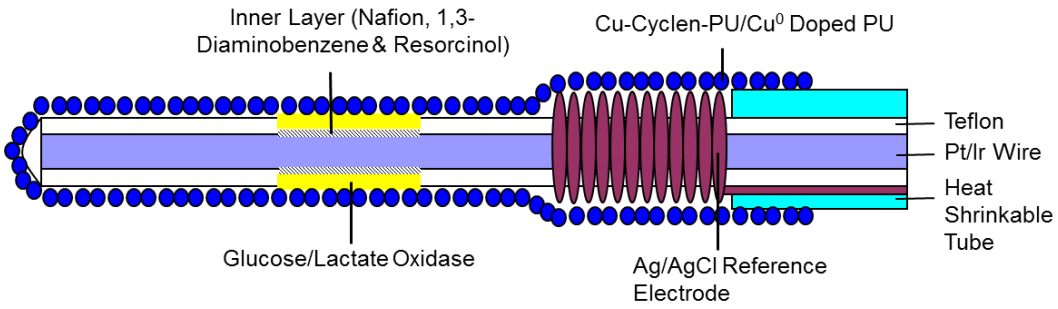

Figure 4.3. Configuration of glucose/lactate sensors with Cu(II)-based NO generation coatings.

4.2.3 Preparation of Organoselenium Immobilized PEI (SePEI)

The SePEI polyelectrolyte was synthesized according to the procedure proposed earlier [6, 7]. Briefly, 28 mg of SeDPA was first activated with 143 mg of EDC and 58 mg of NHS. The mixture was then allowed to react with PEI in MES buffer (pH = 6.0) for 2 h. The reaction solution was then centrifuged in an Amicon® centrifugal filter unit (MWCO = 3 kD, Millipore Corp., Billerica, MA) at 4,000 rpm for 40 min to remove any unreacted reagents. Afterwards, $NaBH_4$ was used to reduce the resulting yellow SePEI solution to break any diselenide crosslinking bonds to free selenol (RSeH) sites. The resulting mixture was then exhaustively dialyzed using dialysis membrane (Spectra/Por® 7, MWCO = 3.5 kD, Spectrum Laboratories Inc., Rancho Dominguez, CA) in 50 mM NaCl for 3 d to liberate any unreacted $–SeC_2H_4COOH$ functional groups. The NaCl solution was changed every 12 h. During the dialysis process, the reduced RSeH sites were oxidized back to diselenide (RSe-SeR) by ambient oxygen thus crosslinking PEI chains. The product solution was centrifuged and concentrated into a

yellow viscous solution and then stored at 4 ℃ until future use. Figure 4.4 illustrates the entire synthesis route.

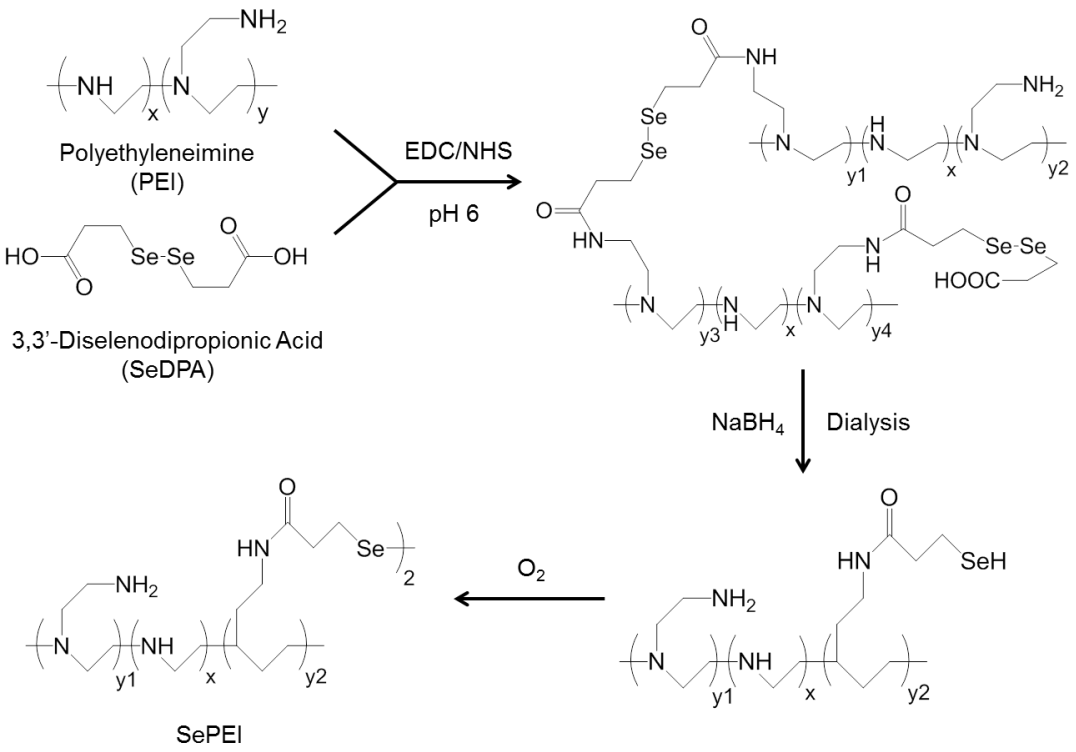

Figure 4.4. Schematic of SePEI synthesis by an EDC/NHS coupling reaction between SeDPA and PEI.

4.2.4 LbL Deposition of SePEI/Alg Bilayers onto Glucose Sensor

A glucose sensor was first fabricated and coated with ca. 4% 3:1 PU and PDMS solution in THF with 2% of DMF, and finally 100 bilayers of SePEI/Alg were deposited via the LbL method. Both SePEI and Alg polyelectrolytes were made into 1 mg/mL solutions in PBS (0.01 M, pH 7.4). The LbL deposition process was carried out with a homemade Lego automatic robot system (Fig. 4.5). The glucose sensors were

alternatingly immersed into SePEI and Alg solutions for 10 min each. In between the polycation and polyanion layers, the sensors were extensively washed 3 times by immersing into 3 beakers of PBS for 1 min. Figure 4.5 shows the LbL deposition process of coating bilayers of SePEI/Alg onto glucose sensors. The arm rotates and immerses sensors into beakers one by one. After each cycle, the arm turns half a circle and starts by dipping sensors into the SePEI solution again. One hundred SePEI/Agl bilayers were coated onto glucose sensors, taking about 2 days to complete. Figure 4.6 shows the configuration of the NO generating SePEI/Alg coated glucose sensor.

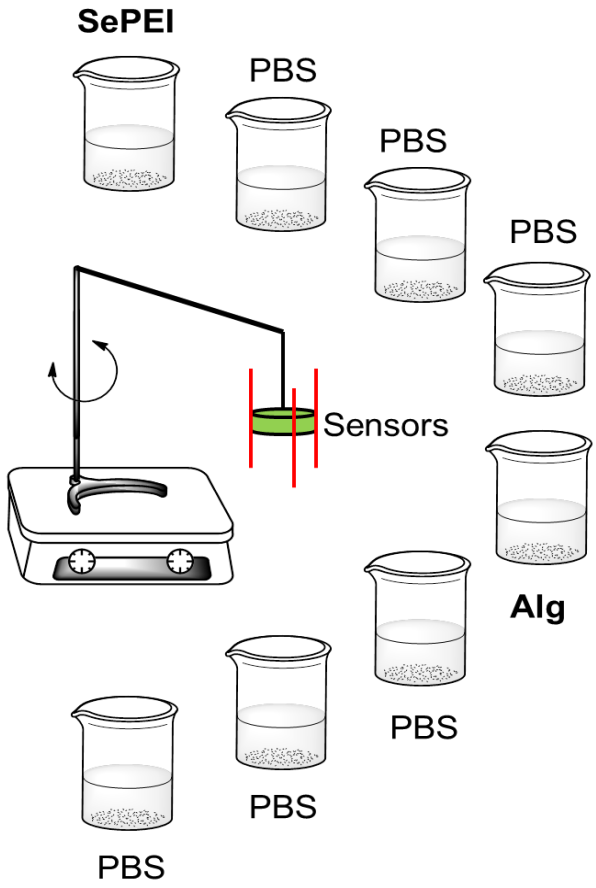

Figure 4.5. Schematic of the automatic LbL deposition of SePEI/Alg bilayers onto glucose sensors.

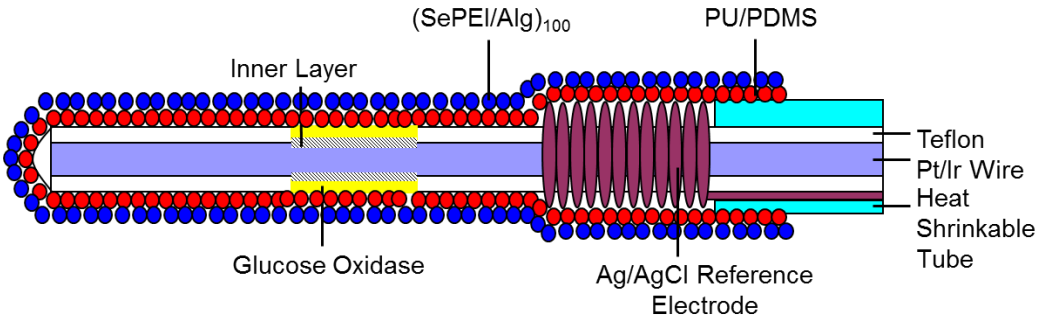

Figure 4.6. Configuration of NO generating glucose sensor with SePEI/Alg bilayers on the outermost surface.

4.2.5 NO Generation Measurements

Nitric oxide generated from coated sensors was monitored via a chemiluminescence method with a Sievers Nitric Oxide Analyzer (NOA) 280i (Boulder, CO). A stock solution of GSNO was prepared by mixing 5 mM of GSH and 5 mM of $NaNO_2$ in the presence of 60 mM of H_2SO_4, as previously described [6]. GSNO was used as a representative example of all the endogenous RSNO species. The sensors with NO generating coatings were immersed in PBS (pH 7.4) with 5, 10 or 50 μM of GSNO and the NO flux data were collected. The high GSNO concentration of 50 μM was used to observe the overall NO generation ability of different catalysts, and lower concentrations were used to mimic the endogenous RSNO levels. EDTA was added in the solution in order to bind with any trace metal ions so that they cannot catalytically decompose GSNO in the solution. The sensors were taken out of the solution after the NO flux reached a steady-state. After the signal returned to the baseline, the sensors were immersed again into the solution. Such up-and-down measurements were taken three times to obtain an average of the generated NO flux from the Cu- or Se-based

polymers. The stability of NO generation coatings was monitored by collecting NOA data over a 7-day period.

4.2.6 *In Vitro* and *In Vivo* Testing of NO Generating Glucose/Lactate Sensors

The calibration of NO generating glucose and lactate sensors was similar to the method described in Chapter 3. The sensors were calibrated on a 4-channel BioStat potentiostat (ESA Biosciences Inc., Chelmsford, MA). A potential of +600 mV vs. Ag/AgCl reference was applied onto the sensors in 0.1 M PBS, pH 7.4, at 37 ℃ and the output current was measured. The stability of NO generating glucose/lactate sensors was tested by calibrating the sensors over one week and monitoring the sensitivity change.

Preliminary *in vivo* experiments of NO generating glucose sensors coated with SePEI/Alg bilayers were carried out following the protocol described in Chapter 3. One NO generating glucose sensor with 100 bilayers of SePEI/Alg, one control glucose sensor with 100 bilayers of PEI/Alg without any Se species linked to the PEI and one control sensor with only PU were implanted in rabbit veins for 8 h. The accuracy of the continuous glucose response was monitored and at every 30 min interval, when 0.6 mL of blood was drawn and the blood glucose level was measured by a 700 Series Radiometer blood analyzer (Radiometer America Inc., Westlake, OH). All three sensors were explanted after 8 h of implantation and the thrombus formation was observed and compared.

4.3 Results and Discussion

4.3.1 NO Generating Glucose Sensors with Cu(II) Polymeric Coatings

Figure 4.7 shows the typical NO generation profile of glucose sensors coated with PU doped with 20 wt% of Cu^0 nanoparticles in 0.1 M PBS, pH 7.4, in the presence of 50 μM GSH, GSNO and EDTA. When the sensor was immersed into the solution, there was an increase in the NO flux, and when the sensor was taken out of the solution the NO flux dropped nearly to baseline. The repeated insertion/removal of the sensor demonstrates that the outer polymer can generate a comparable steady-state NO flux after each immersion and removal from the test solution. As a result, such glucose sensors are potentially able to generate NO from endogenous RSNO species when implanted in blood or subcutaneously. Improved biocompatibility of the implantable sensors from NO generation can be expected, provided there are adequate levels of RSNOs in the blood.

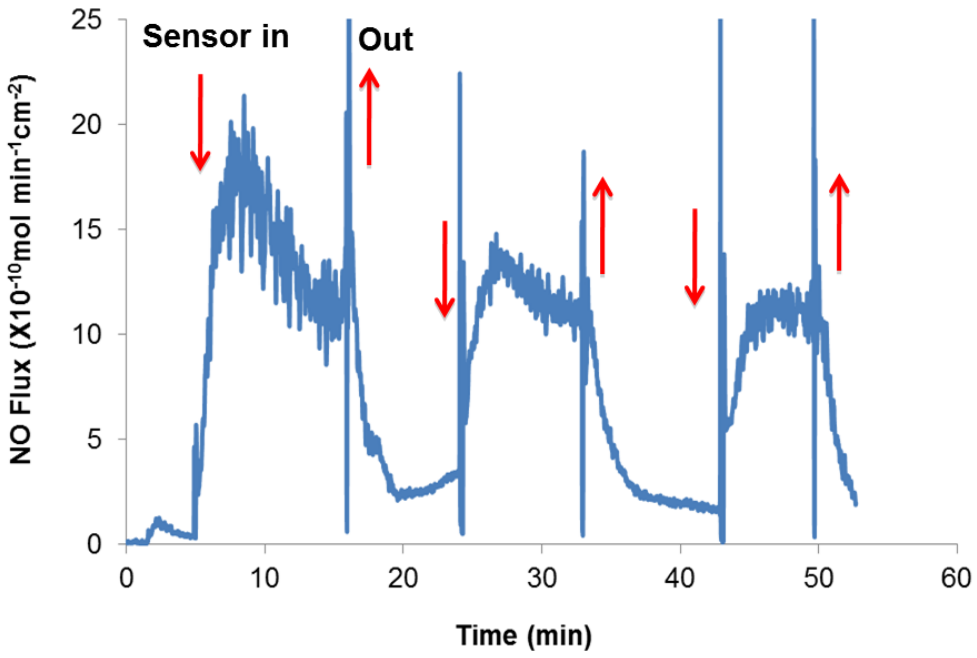

Figure 4.7. NO generation profile of glucose sensors coated with 20 wt% Cu^0 nanoparticles in 0.1 M PBS, pH 7.4, with 50 μM of GSH, GSNO and EDTA.

Table 4.1 summarizes the NO generation properties of the Cu(II)-cyclen-PU (both derived from Tecophilic SP-93A-100 and SP-60D-60) and Cu^0 nanoparticle-doped PU materials as sensor coatings. Firstly, it was noticed that the amount of NO generated was proportional to the RSNO levels in the solution, as the higher concentrations of GSNO elicited greater NO fluxes than lower GSNO levels. Secondly, the NO flux increased when the amount of Cu catalyst increased, and the Cu^0 nanoparticle-doped PU had the highest NO flux with a much greater Cu content than Cu(II)-cyclen-PUs. Two layers of Cu(II)-cyclen-PU also resulted in a higher NO flux than a single layer, which also showed that incresed Cu content results in a greater NO flux. However, the Cu(II)-cyclen-PU derived from Tecophilic SP-60D-60 showed the lowest NO flux, although it had a slightly higher Cu content (based on elemental analysis) than the

Cu(II)-cyclen-PU derived from Tecophilic SP-93A-100. This result also indicated that the Cu(II)-cyclen-PU derived from Tecophilic SP-93A-100 was more hydrophilic which allowed for more GSNO in the solution to diffuse into the polymer and be effectively decomposed by all the Cu(II) sites. Unfortunately, this hydrophilic property contradicts the requirement of a hydrophobic polymer to limit glucose/lactate diffusion, and this will be discussed later in this section. As described above, the Cu^0 nanoparticle-doped PU proved to be the most effective catalyst to generate the highest amount of NO from the tested RSNO concentrations.

Table 4.1. NO generation flux comparison of different types of Cu polymers.

Cu Polymer	**Cu Content (wt%)**	**Layers**	**NO Flux with 50 µM GSNO ($\times10^{-10}$ mol $min^{-1}cm^{-2}$)**	**NO Flux with 5 µM GSNO ($\times10^{-10}$ mol $min^{-1}cm^{-2}$)**
Cu(II)-cyclen-PU (Tecophilic SP-93A-100)	0.08 – 0.4	1	~ 0.7	~ 0.2
		2	~ 3	~ 0.8
Cu(II)-cyclen-PU (Tecophilic SP-60D-60)	0.64	1	~ 0.5	~ 0.1
Cu^0 80 nm doped PU (Tecoflex SG-80A)	20	1	~ 15	~ 2.5

Figure 4.8 shows a typical calibration curve of the NO generating glucose sensor using the Cu(II)-cyclen-PU derived from Tecophilic SP-60D-60 as the coating. Unfortunately, this Cu(II)-cyclen-PU had little catalytic ability in generating NO from RSNOs, possibly due to the hydrophobicity of Tecophilic SP-60-D-60, thus limiting the diffusion of RSNO species into the polymer to react with the Cu(II) sites, resulting in a low NO flux.

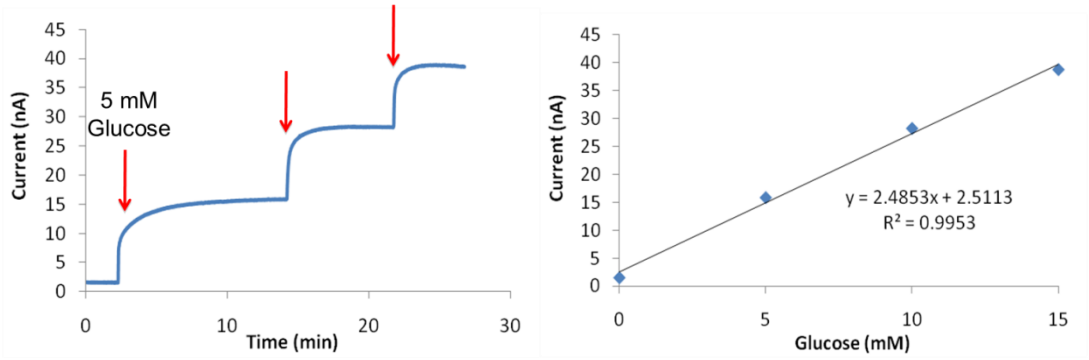

(a) (b)

Figure 4.8. Calibration curve of the NO generating glucose sensor with Cu(II)-cyclen-PU (SP-60D-60) in 0.1 M PBS, pH 7.4, at 37 ℃.

Table 4.2 summarizes the analytical performance of glucose sensors coated with the three different types of polymers containing Cu catalytic sites. It was observed that the glucose sensors did not have as wide of a linear range when coated with Cu(II)-cyclen-PU derived from Tecophilic SP-93A-100, compared to sensors coated with more hydrophobic PUs (see Chapter 3). This was largely due to the hydrophilicity of Tecophilic SP-93A-100, which did not limit glucose diffusion well enough to achieve the required linear range for high blood glucose detection. Thus, multiple layers of such polymer coatings were deposited onto glucose sensors, in the hope that a thicker membrane can further limit the glucose diffusion. Indeed, the linear range was wider when more than one layer of Cu(II)-cyclen-PU derived from SP-93A-100 was coated on the glucose sensors. However, the glucose response time also doubled with this increased thickness of the membrane. As a result, Cu(II)-cyclen-PU was not the optimal NO generating coating for glucose sensors because of the conflict between the need for

hydrophilicity to achieve more efficient NO generation and that of hydrophobicity to achieve a wider linear response range toward glucose. In the case of Cu^0 nanoparticle-doped PU, the glucose sensors preserved normal analytical performance, as well as excellent NO generation capability. As a result, this polymer coating seems to be optimal for fabricating Cu-based NO generating glucose sensors.

Table 4.2. Comparison of NO generating glucose sensors with different Cu polymers.

Cu Polymer	Layers	Linear Range (mM)	Response Time (min)
Cu(II)-cyclen-PU (Tecophillic SP-93A-100)	1	0 – 5	~ 5
	2	0 – 10	~ 10
Cu(II)-cyclen-PU (Tecophilic SP-60D-60)	1	0 – 15	~ 10
20 wt% Cu^0 80 nm-doped PU (Tecoflex SG-80A)	1	0 – 15	~ 5

4.3.2 NO Generating Lactate Sensors with Cu(II) Polymeric Coatings

The Cu(II)-cyclen-PU derived from Tecophilic SP-93A-100 was coated onto lactate sensors. Figure 4.9 shows the NO generation profile of the lactate sensor coated with four layers of such Cu(II)-cyclen-PU in 0.1 M PBS, pH 7.4, in the presence of 50 μM each of GSH, GSNO and EDTA. When the sensor was inserted into the buffer solution, there was an increase in the NO flux and this flux reached a steady-state. When the sensor was taken out of the solution, the NO flux decreased but a much higher baseline was observed, which might be due to the leaching of Cu species into the solution. The higher baseline was not observed on glucose sensors coated with Cu(II)-cyclen-PU

because the number of coated layers was smaller, so the leaching of Cu species was less. This up-and-down of the NO flux signal demonstrates that the outer polymer coatings can generate NO after each immersion in the solution with GSNO. However, the actual leaching of Cu species needs to be minimized for *in vivo* applications.

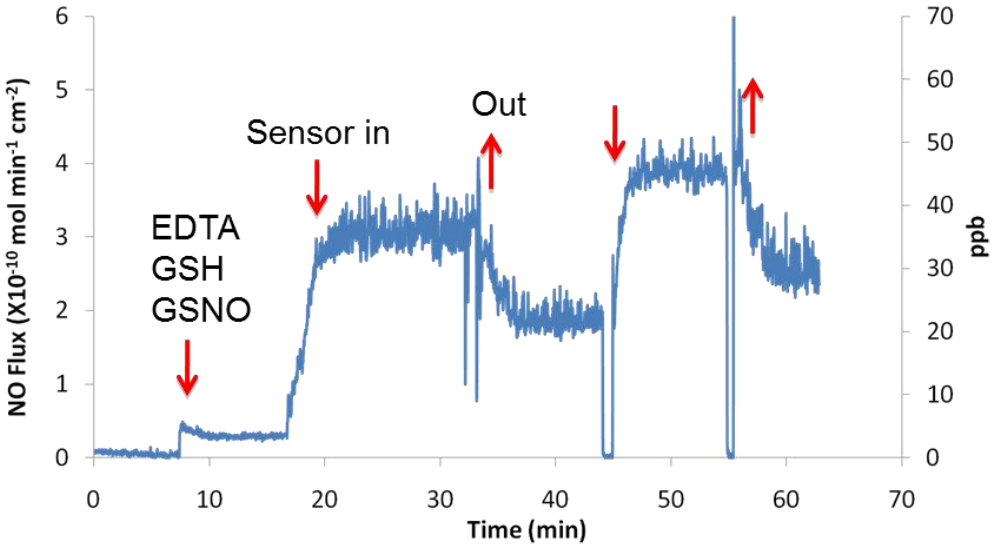

Figure 4.9. NO generation of lactate sensors coated with four layers of Cu(II)-cyclen-PU (SP-93A-100) in 0.1 M PBS, pH 7.4, with 50 μM each of GSH, GSNO and EDTA at 37 ℃.

Figure 4.10 shows an example of the calibration curve of the NO generating lactate sensor and Table 4.3 shows the analytical performance as well as the NO flux of lactate sensors with varying numbers of Cu(II)-cyclen-PU layers. Unlike glucose, lactate seems to be more permeable in the Tecophillic SP-93A-100 PU matrix, so as many as four layers of PU coatings did not change the response time significantly, with negligible effect on the linear range. On the other hand, the goal for the detection range for lactate in blood is up to around 5 mM, which is much lower than that of glucose. As

a result, the linear range of lactate sensors with Cu(II)-cyclen-PU Tecophillic SP-93A-100 is acceptable for future *in vivo* studies. However, the NO flux of such Cu(II)-cyclen-PU coatings, in the presence of high concentrations (50 μM) of GSNO, barely reached the NO levels required to eliminate thrombus formation from the *in vivo* experiment results as described in Chapter 3. To make such coatings anti-thrombotic as expected, additional infusions of RSNO species are likely needed for future biomedical applications.

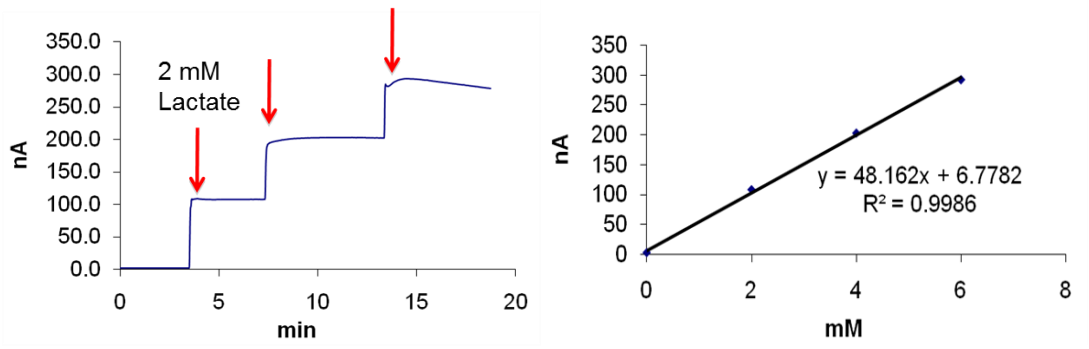

(a) (b)

Figure 4.10. Calibration curve of the NO generating lactate sensor.

Table 4.3. Characteristic comparison of NO generating lactate sensors with multiple layers of Cu(II)-cyclen-PU.

Cu Polymer	**Layers**	**NO Flux with 50 μM GSNO ($\times 10^{-10}$ mol min^{-1}cm^{-2})**	**Linear Range (mM)**
Cu(II)-cyclen-PU (Tecophillic SP-93A-100)	2	~ 1.7	0 – 5
	4	~ 3.2	0 – 6

4.3.3 NO Generating Glucose Sensors with SePEI/Alg LbL Coatings

NO generating coatings of SePEI/Alg via LbL deposition were successfully applied to glucose sensors with a PU/PDMS outer coating. As shown in Figure 4.11, when the glucose sensor with 100 SePEI/Alg bilayers was placed into a pH 7.4 PBS solution with 10 μM each of GSNO, GSH and EDTA, a burst of NO was detected and the flux reached a steady-state NO level (approximately 2×10^{-10} mol cm^{-2} min^{-1}). When the sensor was removed from the solution, the NO signal returned close to the original baseline, demonstrating the catalytic property of the bilayers with Se sites to liberate NO from GSNO. The repeated insertion/removal of the sensor demonstrated that the SePEI/Alg bilayers can generate a comparable steady-state NO flux after each immersion and removal from the test solution. The stability of such 100 bilayers of SePEI/Alg coatings was also examined and the results are shown in Figure 4.12. It can be seen from the graph that 100 bilayers exhibited excellent NO generating properties such that the generated NO remained relatively stable over a one week period, with a slight increase in the NO flux likely due to the conditioning of the bilayers. Compared to the Cu^0 nanoparticle-doped PU coatings, the 100 bilayers of SePEI/Alg can generate similar levels of NO at a relatively low GSNO concentration. As a result, the SePEI/Alg bilayer is a promising candidate coating to enhance the biocompatibility of implantable glucose sensors via NO generation from endogenous RSNO species.

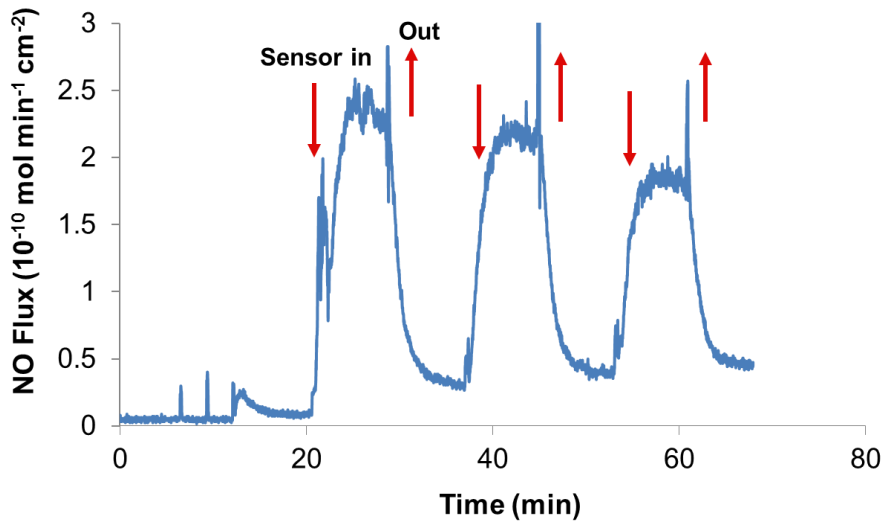

Figure 4.11. Nitric oxide generation profile of glucose sensors with 100 bilayers of SePEI/Alg in 0.01 M PBS with 10 μM each of EDTA, GSH and GSNO at 37 ℃.

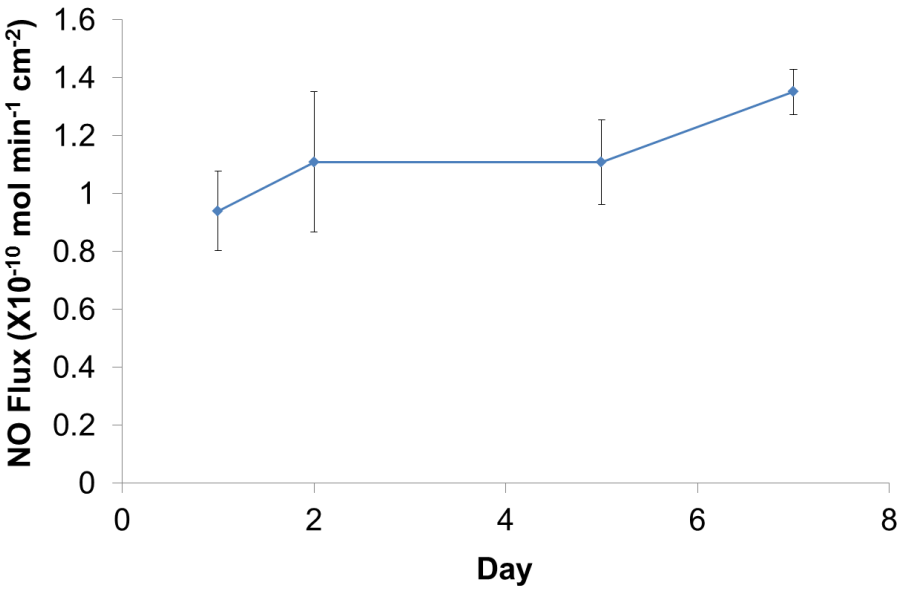

Figure 4.12. Stability of NO generation from glucose sensors with 100 bilayers of SePEI/Alg over one week (n=4).

Fortunately, this new NO generating chemistry is compatible with glucose sensing. Figure 4.13 shows an example of the calibration curve of the NO generating

glucose sensor prepared with the LbL coating. At the same time, the entire sensor can generate reasonable levels of NO at the surface in the presence of GSH and GSNO. The NO generating glucose sensors showed excellent analytical performance in comparison to control sensors without any NO LbL generating coatings, indicating that the SePEI/Alg bilayers did not have any negative influence on the glucose sensing chemistry. Such NO generating glucose sensors also remained relatively stable in their sensitivity to glucose over a one week period, as shown in Figure 4.14, with two individual sensor examples.

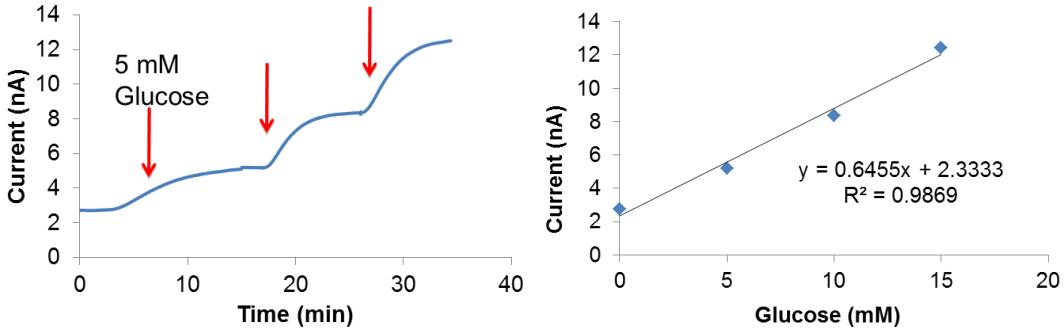

(a) (b)

Figure 4.13. Amperometric response (a) and corresponding calibration curve (b) of the NO generating glucose sensor prepared with 100 bilayers of SePEI/Alg.

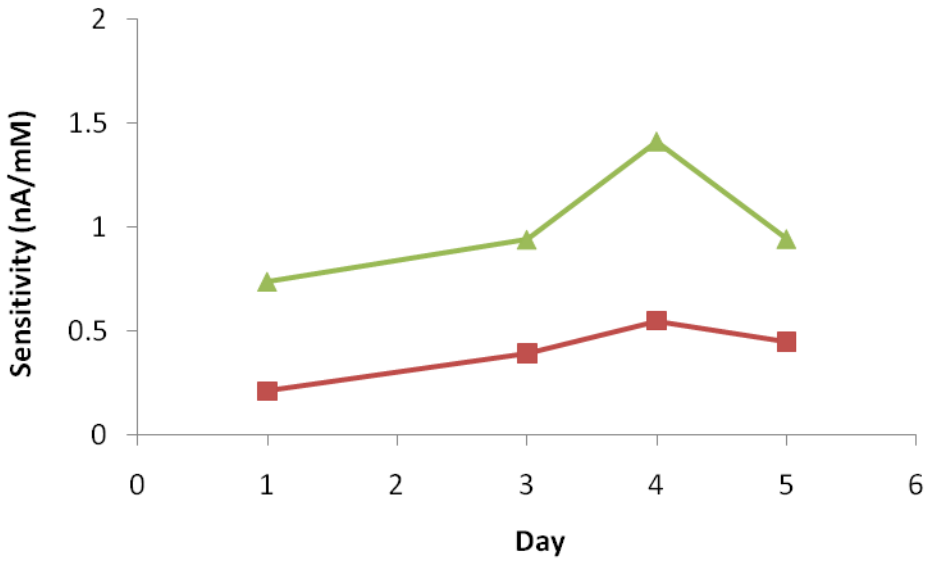

Figure 4.14. Stability of two individual NO generating glucose sensors prepared with 100 bilayers of SePEI/Alg over one week in terms of sensitivity.

4.3.4 *In Vivo* Testing of NO Generating Glucose Sensors with SePEI/Alg Bilayers

Preliminary animal studies of this new NO generating glucose sensor design were carried out by implanting one sensor with 100 bilayers of NO generating SePEI/Alg, one control with 100 PEI/Alg bilayers without NO generating Se sites and another control with bare PU/PDMS into rabbit veins for 8 hours and two separate rabbit experiments of this type were carried out. The animal experiment protocol was followed as described elsewhere [12] and in Chapter 3. Every 30 min, 0.6 mL of blood samples were drawn and the blood glucose concentration was measured using a bench-top Radiometer instrument and compared to the continuous output from implanted glucose sensors. Unfortunately, as shown in Figure 4.15, the expected thrombus resisting property from NO generated by Se from endogenous RSNO species was not observed from the explanted sensors after the 8 h implantation. All of the implanted sensors in both rabbit

experiments formed obvious thrombus after the 8 h of implantation in rabbit veins. This might be due to the low endogenous RSNO concentrations in the micromolar range or less in the rabbit blood stream. In accordance with the thrombus formation results, all the glucose sensors showed deviations from the *in vitro* measurements by the Radiometer, as shown in Figure 4.16. The deviation might be due to the thrombus formation with time which disturbed local glucose diffusion into the sensor within blood vessels so that the implanted sensors were not reporting the glucose levels in the bulk of the blood stream. As a result, this SePEI/Alg coating might realize expected anti-thrombus function only in the situation where infusions of RSNO species into blood stream is feasible, in order to generate high enough fluxes of NO on implanted sensor surfaces. This would be possible only in limited biomedical situations.

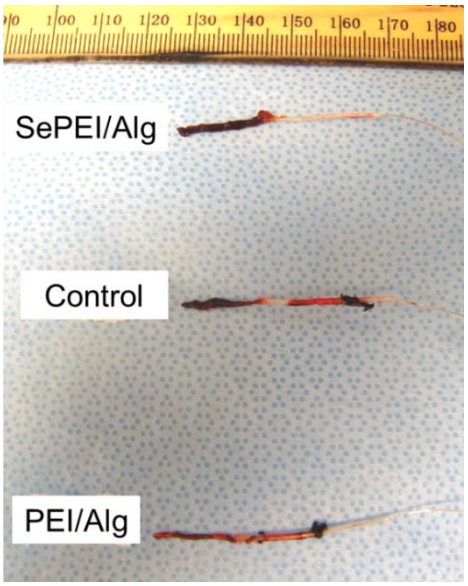

Figure 4.15. Picture of thrombus formation on the surface of glucose sensors implanted in rabbit veins for 8 h.

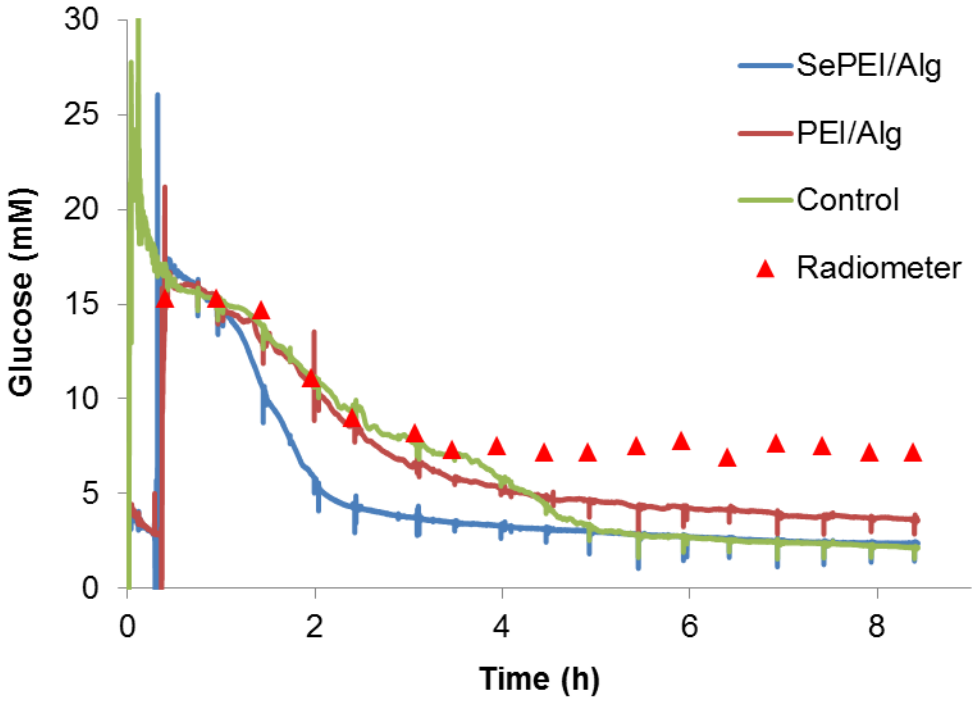

Figure 4.16. Continuous glucose monitoring results from implanted NO generating and control sensors with comparison to the bench-top Radiometer readings, from one of the *in vivo* rabbit experiments.

4.4 Conclusions

Implantable glucose/lactate sensors have been fabricated with various NO generating coatings, including Cu(II)-cyclen-PUs, PU doped with Cu^0 nanoparticles and SePEI/Alg bilayers. All of the coatings exhibited NO generation properties via catalytically generating NO from RSNO species. Both SePEI/Alg bilayers and PU doped with Cu^0 nanoparticles showed the best NO generation efficiency. Coatings of Cu(II)-cyclen-PUs on glucose sensors did not provide the sensor with a wide enough linear range, while the same coating on lactate sensors maintained an acceptable lactate detection range. Coatings of PU doped with Cu^0 nanoparticles and SePEI/Alg bilayers

did not have any negative influence on the glucose sensing performance, thus enabling the potential biomedical applications of such sensors with anticipated anti-thrombus property. However, preliminary *in vivo* experimental results of glucose sensors coated with 100 bilayers of SePEI/Alg indicated that thrombus occurs, suggesting that generated levels of NO were inadequate, likely because of low endogenous levels of RSNO species. Only two animal experiments were conducted, so it is impossible to make conclusions, since if more animals were tested, and they had higher endogenous RSNO levels, results could be more encouraging.

4.5 References

1. Williams, D.L.H. *Accounts Chem. Res.* **1999**, 32(10), 869-876.

2. Oh, B.K.; Meyerhoff, M.E. *J. Am. Chem. Soc.* **2003**, 125(32), 9552-9553.

3. Hwang, S.; Cha, W.; Meyerhoff, M.E. *Angew. Chem. Int. Edit.* **2006**, 45(17), 2745-2748.

4. Hwang, S.; Meyerhoff, M.E. *Biomaterials* **2008**, 29(16), 2443-2452.

5. Wu, Y.D.; Rojas, A.P.; Griffith, G.W.; Skrzypchak, A.M.; Lafayette, N.; Bartlett, R.H.; Meyerhoff, M.E. *Sensor. Actuat. B-Chem.* **2007**, 121(1), 36-46.

6. Cha, W.; Meyerhoff, M.E. *Biomaterials* **2007**, 28(1), 19-27.

7. Yang, J.; Welby, J.L.; Meyerhoff, M.E. *Langmuir* **2008**, 24(18), 10265-10272.

8. Giustarini, D.; Milzani, A.; Colombo, R.; Dalle-Donne, I.; Rossi, R. *Clin. Chim. Acta* **2003**, 330(1-2), 85-98.

9. Bindra, D.S.; Zhang, Y.N.; Wilson, G.S.; Sternberg, R.; Thevenot, D.R.; Moatti, D.; Reach, G. *Anal. Chem.* **1991**, 63(17), 1692-1696.

10. Gifford, R.; Batchelor, M.M.; Lee, Y.; Gokulrangan, G.; Meyerhoff, M.E.; Wilson, G.S. *J. Biomed. Mater. Res. A* **2005**, 75A(4), 755-766.

11. Hu, Y.B.; Zhang, Y.N.; Wilson, G.S. *Anal. Chim. Acta* **1993**, 281(3), 503-511.

12. Major, T.C.; Brant, D.O.; Reynolds, M.M.; Bartlett, R.H.; Meyerhoff, M.E.; Handa, H.; Annich, G.M. *Biomaterials* **2010**, 31(10), 2736-2745.

CHAPTER 5

GLUCOSE MEASUREMENT IN HUMAN TEARS USING THE NEEDLE-TYPE GLUCOSE SENSOR

5.1 Introduction

Glucose monitoring technologies have drawn significant attention over the past several decades to help in the management of diabetes, which afflicts about 5% of the world's population [1]. Tight glycemic control is critical to the care of patients with diabetes especially to prevent complications such as cardiovascular disease [2]. It is recommended that blood glucose levels be measured several times a day, which usually requires finger pricking coupled with measurement using a strip-test type glucometer (with either optical or electrochemical readout). However, in practice, patients may not follow these recommendations, and this might be largely due to the accumulated pain from the repeated finger pricks and blood collection.

A number of studies have been carried out to find a less invasive means to monitor blood glucose levels, including the use of infrared spectroscopy [3, 4], a GlucoWatch design that is based on electro-osmotic flow of subcutaneous fluid to the surface of the skin and detection of glucose with enzyme-electrode system [5], and

measurement of tissue metabolic heat conformation [6], but none of these techniques have yielded the quality of analytical results required to become a full substitute for blood glucose measurements [7]. Other investigations have suggested testing glucose in tear fluid as a substitute for blood, and this concept dates back to the 1950's [8]. This approach provides a unique possibility of developing a relatively simple non-invasive method of detecting glucose, if it can be clearly shown that tear glucose levels correlate closely with blood glucose values. If a good correlation between the two types of samples can be established, measurement of tear glucose levels could provide an attractive indirect measurement method for blood glucose levels within the normal as well as hyperglycemic and hypoglycemic ranges. For such a method to be effective, tear fluid needs to be collected using a non-stimulating method [9] so that increases in tear production do not further dilute out the naturally present glucose. At the same time, it is important to sample the tear fluid without inflicting any damage to blood capillaries within the eye, which might result in tear samples with much higher levels of glucose than actually present in the neat tear fluid sample (see below).

Research has been conducted by a number of groups to develop detection methods for measuring the levels of glucose in tears. The requirements of tear glucose detection include a low detection limit (i.e., μM range), high selectivity over interferences such as ascorbic acid and uric acid, and the ability to measure small sample volumes as tear fluid can only be collected via a few microliters at a time. Published methods include capillary electrophoresis (CE) coupled with laser-induced fluorescence (LIF) [10], fluorescence sensors [11], liquid chromatography (LC) coupled with

electrospray ionization mass spectrometry (ESI-MS) [12], holographic glucose sensors [13], a miniaturized flexible thick-film flow-cell detector [14], and a strip-type flexible biosensor [15]. Badugu et al. [16, 17] also reviewed the feasibility of using disposable contact lenses to monitor glucose through ophthalmic detection. They suggested that this new approach can be considered as a significant alternative to diabetes care and management because many diabetics require vision correction and already wear contact lenses.

Using an enzymatic method, it was found in the 1980's that tear glucose levels were significantly higher in diabetic patients with higher blood glucose levels than normal patients [18]. However, levels of glucose in tears have been found to be typically 30-50 times lower than in blood. Baca et al. recently reviewed studies of the correlation between blood and tear glucose levels using different detection methods [9], and concluded that there is evidence of a correlation between average tear and blood glucose concentrations, but further characterization and justification is needed from animal and human studies to determine the potential utility of tear glucose measurements to help achieve glycemic control. In a recent paper, the correlation between the tear glucose concentrations and the average blood glucose concentrations was found to be stronger for non-contact lens wearers than for participants wearing contact lenses by using an LC-MS glucose detection method [12]. However, previous studies of critically ill patients using a high performance liquid chromatography method with pulse amperometric detection (HPLC-PAD) to monitor tear glucose showed no significant correlation between tear and blood glucose concentrations [19]. As a result, further

research is needed to evaluate whether measuring tear glucose concentrations can be considered a reasonable substitute for blood glucose monitoring.

In this chapter, a relatively simple needle-type amperometric enzyme electrode for glucose is described that is capable of measuring the levels of glucose in tear fluid down to 1.5 μM, within a capillary tube containing ca. 5 μl of tear fluid. The sensor is utilized to assess the correlation between tear glucose levels and blood glucose concentrations in anesthetized rabbits. It will be shown that measurements with the electrochemical device suggest reasonably good correlation between the two types of samples within a given animal; however, the ratio between tear glucose and blood glucose is found to vary considerably from animal to animal.

5.2 Experimental

5.2.1 Materials

Glucose oxidase (Type VII, From Aspergillus niger), d-(+)-glucose, glutaraldehyde, bovine serum albumin (BSA), sodium chloride (NaCl), potassium chloride (KCl), sodium phosphate dibasic (Na_2HPO_4), potassium phosphate monobasic (KH_2PO_4), iron (III) chloride ($FeCl_3$), 37 % hydrochloric acid (HCl), L-ascorbic acid, uric acid, Nafion (5 wt % solution in a lower aliphatic alcohols/H_2O mix), 1,3-diaminobenzene, and resorcinol, were all purchased from Sigma-Aldrich (St. Louis,

MO). Platinum/iridium (Pt/Ir) and silver (Ag) wires were products of A-M Systems (Sequim, WA).

5.2.2 Fabrication of Tear Glucose Sensor

The design of the tear glucose biosensor (see Figure 5.1) was based on previous configurations used to prepare electrochemical sensors suitable for subcutaneous measurements of glucose [20, 21]. Briefly, a 10-cm long Teflon-coated Pt/Ir wire of 0.2 mm outer diameter was cut and a 1 mm cavity was created (by stripping the Teflon) at 4 mm from one tip. Starting 1.5 mm above the opening, a 15 cm, 0.1 mm o.d. silver/silver chloride (Ag/AgCl) wire was tightly wrapped around the sensor covering a length of 4 mm. The Ag/AgCl wire was prepared by dipping the Ag wire into a 1 M $FeCl_3$ in 0.1 M HCl solution. The straight section above the wrapped Ag/AgCl wire was then covered with a 5 cm long, 0.4 mm o.d., heat shrink polyester tubing (Advanced Polymers, Salem, NH).

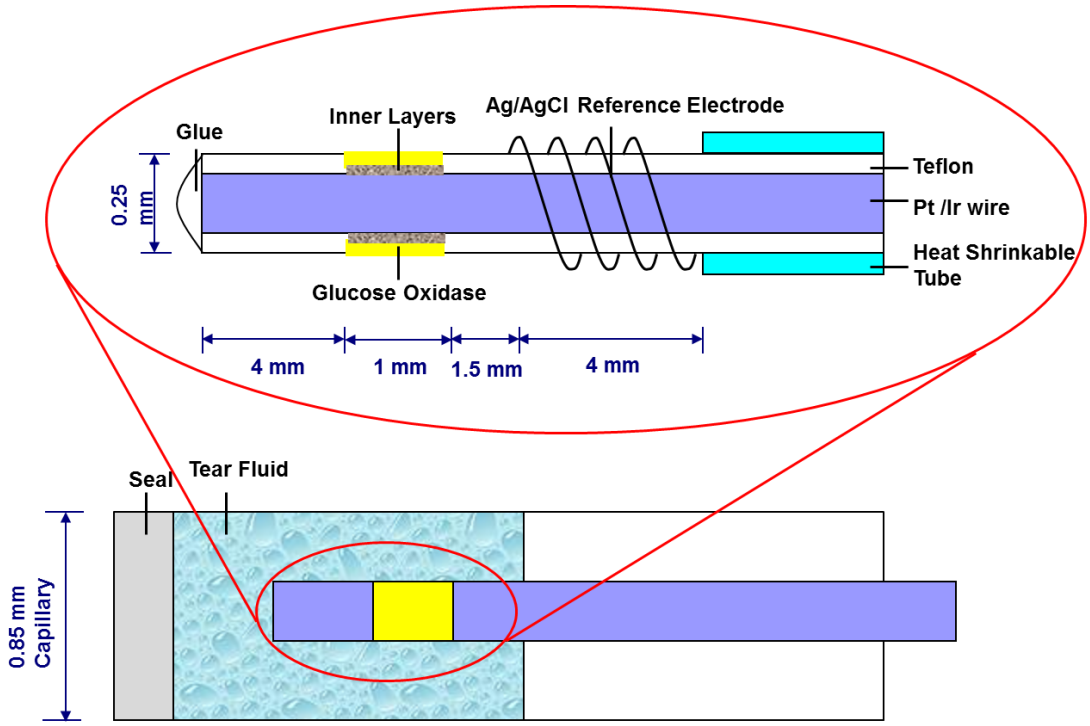

Figure 5.1. Configuration of the tear glucose sensor in capillary.

Inner polymeric layers deposited on the Pt electrode were used to eliminate interferences from ascorbic acid and uric acid. First, the cavity was coated with a thin layer of Nafion (ca. 5 μm thick). Then, electropolymerization of a solution containing 1.5 mM 1,3-diaminobenzene and a similar concentration of resorcinol in PBS buffer (0.1 M, pH 7.4) was initiated using a Voltammograph potentiostat (Bioanalytical Systems Inc., West Lafayette, IN) with a cycling voltage of 0 to +830 mV at a scan rate of 2 mV/s for 18 h [22]. The enzyme layer was created by first dropping 1 μL of a 3 wt% glucose oxidase solution containing also 3 wt% BSA in the cavity along the wire and drying this layer for 30 min. Then, the enzyme was crosslinked by adding 1 μl of 2% (vol/vol) glutaraldehyde solution and cured in air for 1 h. The sensor was then rinsed with deionized water and stored in 0.1 M PBS (pH 7.4) buffer for future use.

5.2.3 Calibration of Tear Glucose Sensor

The amperometric tear glucose sensors were calibrated using a 4-channel BioStat potentiostat (ESA Biosciences Inc., Chelmsford, MA). The sensors were first polarized at a potential of +600 mV vs. Ag/AgCl reference in a vial containing 10 mL of PBS buffer solution. Five microliters of glucose standard solutions (100, 200, 500, 800 and 1000 μM) prepared in PBS were collected by individual 0.85 mm i.d. glass capillaries (World Precision Instruments, Sarasota, FL) and sealed with Critoseal (McCormick Scientific, Richmond, IL). The sensor was then taken out of the PBS, blotted briefly with Kimwipes (Kimberly-Clark, GA) to remove excess solution and inserted into the capillary so that the solution completely covered the sensing region containing the immobilized enzyme (see Figure 5.1). After a stable current was achieved (typically within 2 min), the sensor was rinsed with water three times and then put back into the stock PBS buffer to reach the steady-state baseline value in preparation for the next measurement within the capillary tubes. To test the sensor selectivity over interferences, standard solutions containing potential interferent species at their maximum possible levels in tear fluid [23, 24] (i.e., 100 μM of ascorbic acid, 100 μM of uric acid and 10 μM of acetaminophen (based on the dilution factor blood ratio)) were collected in capillaries, and the response current for each interferent species was measured. Based on the sensitivity of the sensor to glucose, and the amperometric signal observed for these interferent speices, the % error that would occur for samples containing these levels of interferences and 100 μM tear glucose were calculated. To test the repeatability of such tear glucose sensor, the device was inserted into five separate capillaries containing 5 μL

of 100 μM glucose, with washing and baseline stabilization in PBS buffer in between the multiple measurements. The average reported glucose concentration was determined from a prior calibration curve made in capillary tubes using 100, 200, 500, 800 and 1000 μM glucose standards.

5.2.4 Protocol to Assess Correlation between Tear and Blood Glucose Concentrations in Rabbits

Twelve white rabbits (Myrtle's Rabbitry, Thompson's Station, TN) were used in this study to test the correlation between tear glucose measured with the needle-type sensor and blood glucose measured with a Radiometer. An anesthesia protocol as described elsewhere in detail [25] was followed for the experiments with the exception that the maintenance fluid rate was adjusted to 3.3 mL/kg/min. All rabbits were under anesthesia for 8 h. The tear glucose sensor was polarized at +600 mV in PBS buffer through the duration of the entire experiment. The sensor was calibrated in capillary tubes with 100 μM glucose in the middle of the 8 hour experiment. Every 30 min, 0.6 mL blood was drawn and the blood glucose level was measured using a 700 Series Radiometer blood analyzer (Radiometer America Inc., Westlake, OH) that employs a macro-electrochemical enzyme electrode to quantitate blood glucose. At the same time, 5 μL of rabbit tear fluid was collected in the capillary and the current from the glucose in the tear fluid was recorded using the tear glucose sensor. The tear glucose level was calculated from the one point calibration result. Statistical data analysis was carried out to examine the correlation between the blood and tear glucose values within a given animal and across all 12 animals involved in the study.

5.3 Results and Discussion

5.3.1 The Analytical Performance of Tear Glucose Biosensor

The typical calibration curve for the tear glucose biosensor in capillary tubes is shown in Figure 5.2. The detection limit is 1.5 ± 0.4 μM of glucose (S/N=3). It should be noted that this low detection limit is achieved by not coating the outer surface of the sensor with an additional membrane that restricts diffusion of glucose to the enzymatic layer. Such an additional coating is required for blood and subcutaneous glucose sensing in order to ensure that oxygen is always present in excess compared to glucose in the enzymatic layer to achieve linear response to high glucose concentrations. However, given the much lower levels of glucose in tear fluid, no outer membrane is needed to retard glucose diffusion, since oxygen levels will be always in excess in such samples. This ultimately enables the very low detection limit of the sensor. The glucose sensor design employed in this work has an average sensitivity of 0.019 ± 0.009 nA/μM of glucose (n=4). The linear range can reach to 1000 μM which is nearly 10-fold greater than the average normal value of 138 μM found previously for tear glucose levels in humans [10]. From the repeatability test of the tear glucose sensors, they showed an acceptable repeatability with an average of 102.5 ± 3.2 μM measured for the 5 measurements in individual capillaries containing ca. 5 μl of 100 μM glucose solution, each (Figure 5.3).

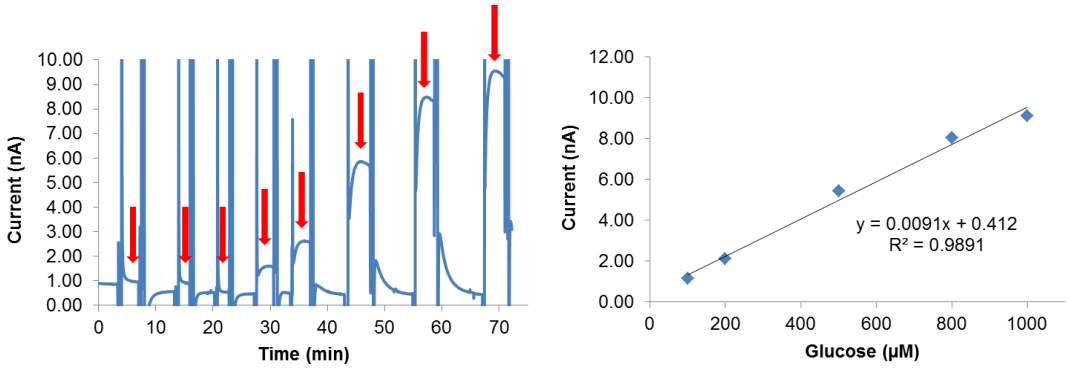

(a) (b)

Figure 5.2. Amperometric response of tear glucose sensor using 5 µL solution in capillary. (a) Solutions in the order of 100 µM ascorbic acid, 100 µM uric acid, 10 µM acetaminophen, 100 µM, 200 µM, 500 µM, 800 µM and 1000 µM glucose solution. (b) Calibration curve of tear glucose sensor.

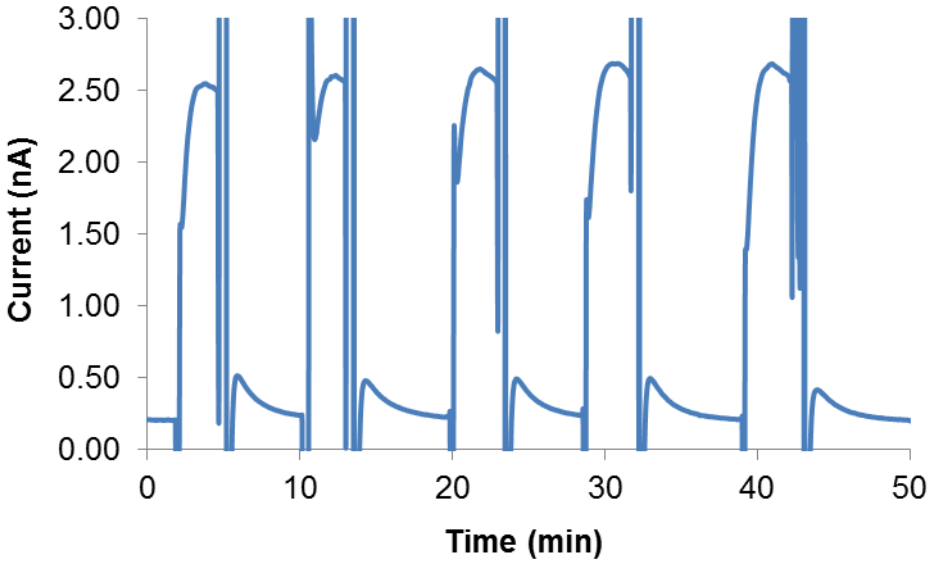

Figure 5.3. Repeatability test of 5 measurements in individual capillaries containing ca. 5 µl of 100 µM glucose solution, each.

Any glucose sensor designed for measurements in physiological tear fluid must exhibit acceptable selectivity over existing electroactive species typically present in tears. At the potential of +600 mV vs. Ag/AgCl reference electrode, those interferences might

also be oxidized at the working electrode used to detect the hydrogen peroxide generated from glucose oxidase reaction with glucose, adding error to the output current. It has been reported in the literature that ascorbic and uric acid concentrations in tear fluid are ca. 20 and 70 μM, respectively [23, 24]. As a result, 100 μM of both ascorbic acid and uric acid were used to test the selectivity of the tear glucose sensor. For small neutral molecule interferences, 10 μM of acetaminophen was employed for testing, assuming that this species would be present in tear fluid at levels similar to the relative dilution ratio of blood glucose levels. The error percentage was calculated by dividing the current of certain interference by that observed for a 100 μM standard of glucose. The presence of the Nafion and electropolymerized 1,3-diaminobenzene/resorcinol inner layer enabled the sensor to exhibit excellent exclusion of interferences with the % errors for ascorbic acid, uric acid and acetaminophen of 6.45 ± 4.06, 3.75 ± 2.88 and 3.55 ± 1.76%, respectively (n=4). These results indicate that the tear glucose biosensor has acceptable selectivity over major electroactive interferences found in tear fluid and that results obtained for tear samples will likely reflect the true level of glucose present in such samples.

5.3.2 Correlation of Tear Glucose and Blood Glucose from the Rabbit Model

Figures 5.4(a) and (b) show the Pearson's correlation between tear and blood glucose from 2 individual rabbit experiments. The determined r^2 values are 0.9126 and 0.8894, respectively ($p<<0.05$), indicating significant correlation between tear and blood glucose concentrations. Both examples show excellent fitting to the linear regression model. Figure 5.4(c) shows all the blood-tear glucose values from the twelve rabbit

experiments. There seems to be a low correlation between blood and tear glucose concentrations when the data from all animals tested are combined, based on the results obtained using Pearson's correlation analysis (r^2=0.4867, p<<0.05). Furthermore, it is difficult to establish a simple mathematic function model, such as a linear relationship, between the tear and blood values for the entire data set. This is due to the fact that there was a significant difference in the correlations for individual rabbits. This implies that even though the tear and blood glucose levels in each rabbit demonstrate a reasonable linearity in correlation, the variation among individual animals undermines this general trend as a whole, and this resulted in a low global tear-blood glucose correlation.

It should be noted that there is a common trend of blood and tear glucose concentration decay from the beginning of the 8 h experiment for all the rabbits tested. As a result, average values of both blood and tear glucose values can be taken at each half-hour time point. The shared trend of glucose decay in both blood and tear glucose values, indicates that the blood and tear glucose levels increase or decrease in tandem. Figure 5.4(d) shows the average of blood-tear glucose levels at thirty minute increments. A Pearson's correlation analysis reveals a significant relationship between tear and blood glucose concentrations (r^2=0.9475, p<<0.05) and a linear regression shows excellent fitting. Using a 2nd order polynomial correlation, the fitting model between tear and blood glucose levels is even better (r^2=0.9835) (Figure 5.4(e)). Although this fitting shows a slightly higher correlation coefficient, it makes the model one order more

complex, with only slight gains. As a result, in future applications, the linear model can still be used with acceptable accuracy.

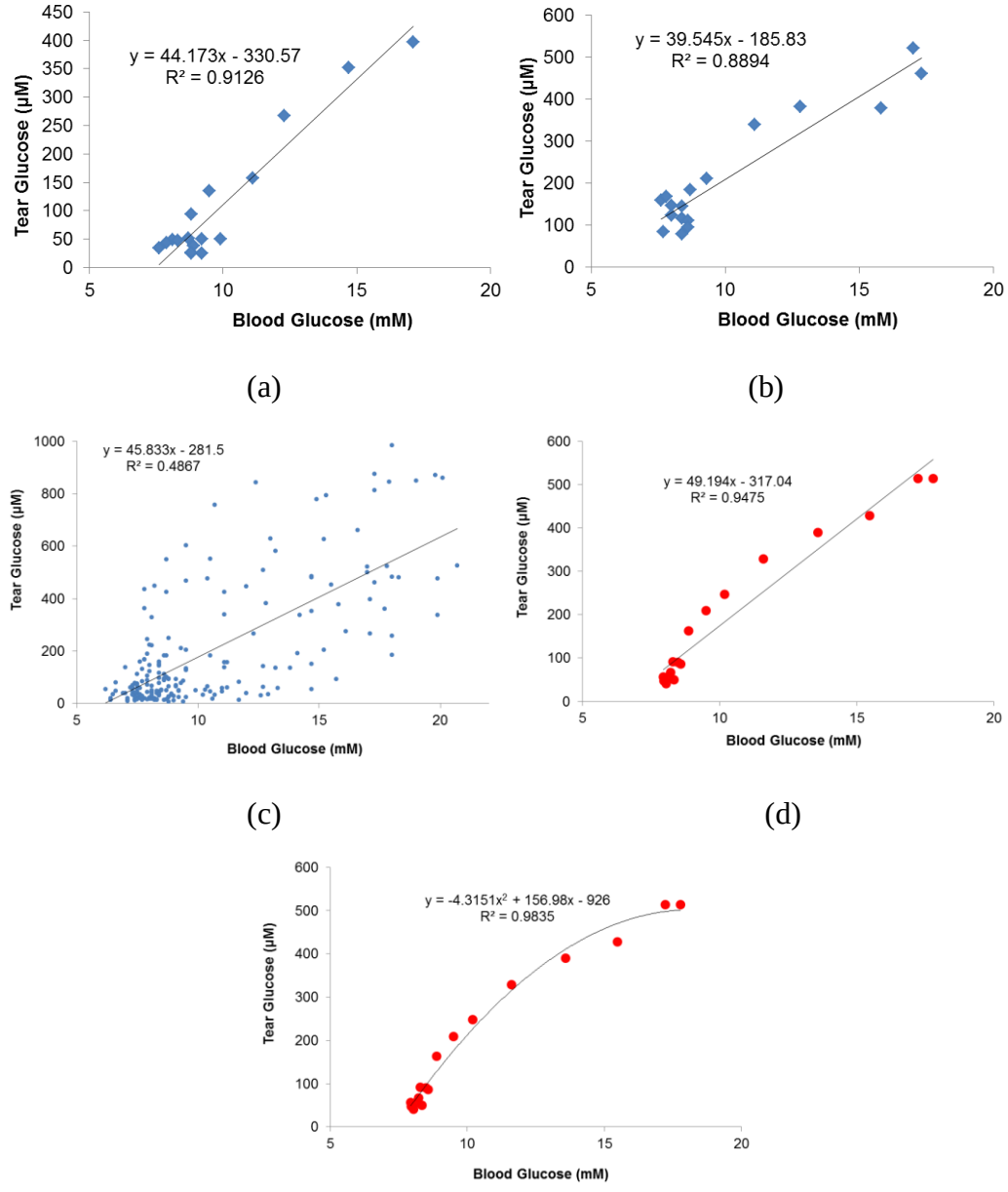

Figure 5.4. Correlation between tear and blood glucose levels using a rabbit model. (a) & (b) Results from two individual rabbit experiments. (c) All the data points of tear and blood glucose values for the total of 12 rabbits. (d) The average values of both tear and blood glucose levels for all animals in study at every half hour time point. (e) A 2nd order polynomial correlation between average tear and blood glucose levels.

In the potential real-world application of the biosensor method for monitoring glucose levels of diabetic patients, after the correlation between tear and blood glucose levels for each individual is established (presuming, like rabbits, the exact correlation and dilution factor from patient to patient may vary), an abnormal tear glucose concentration range can be set up to detect dangerous blood glucose levels from the correlation. Thus, tear glucose levels can be measured multiple times per day to monitor blood glucose changes without the potential pain from the repeated invasive blood drawing method. Indeed, blood glucose levels can still be measured using the traditional blood collection method in order to trigger proper therapy when tear glucose detection suggests that blood glucose levels are out of the normal range.

5.4 Conclusions

A simple electrochemical tear glucose biosensor coupled with a tear fluid collection capillary configuration has been used to monitor glucose levels in tears from rabbits. The needle-type amperometric sensor exhibits excellent selectivity over known electroactive interferences, a low detection limit, a wide dynamic range, excellent repeatability and at present requires a 4-5 microliter sample volume. With further miniaturization of the sensor diameter, it is likely that measurements in as little as 1-2 μL of fluid should be possible, a volume more suitable for routine tear glucose measurements in humans. The correlation between tear and blood glucose levels has been established in a rabbit model and data analysis suggests that a significant correlation between tear and blood glucose levels does exist, but that the exact correlation varies from animal to

animal. Hence, the use of tears as an alternate sample to assess blood glucose in human subjects will likely require that the ratio of glucose in tears and blood be established first for a given individual, so that the appropriate algorithm can be employed to report values that more closely reflect the true blood levels present.

5.5 References

1. http://www.worlddiabetesfoundation.org/composite-35.htm.

2. Mattila, T.K.; de Boer, A. *Drugs* **2010**, 70(17), 2229-2245.

3. Maruo, K.; Oota, T.; Tsurugi, M.; Nakagawa, T.; Arimoto, H.; Hayakawa, M.; Tamura, M.; Ozaki, Y.; Yamada, Y. *Appl. Spectrosc.* **2006**, 60(12), 1423-1431.

4. Mueller, M.; Grunze, M.; Leiter, E.H.; Reifsnyder, P.C.; Klueh, U.; Kreutzer, D. *Sensor. Actuat. B-Chem.* **2009**, 142(2), 502-508.

5. Potts, R.O.; Tamada, J.A.; Tierney, M.J. *Diabetes-Metab. Res.* **2002**, 18, S49-S53.

6. Cho, O.K.; Kim, Y.Y.; Mitsumaki, H.; Kuwa, K. *Clin. Chem.* **2004**, 50(10), 1894-1898.

7. do Amaral, C.E.F.; Wolf, B. *Med. Eng. Phys.* **2008**, 30(5), 541-549.

8. Lewis, J.G. *Br. Med. J.* **1957**, 1(MAR9), 585-585.

9. Baca, J.T.; Finegold, D.N.; Asher, S.A. *Ocul. Surf.* **2007**, 5(4), 280-293.

10. Jin, Z.; Chen, R.; Colon, L.A. *Anal. Chem.* **1997**, 69(7), 1326-1331.

11. Badugu, R.; Lakowicz, J.R.; Geddes, C.D. *Talanta* **2005**, 65(3), 762-768.

12. Baca, J.T.; Taormina, C.R.; Feingold, E.; Finegold, D.N.; Grabowski, J.J.; Asher, S.A. *Clin. Chem.* **2007**, 53(7), 1370-1372.

13. Yang, X.P.; Pan, X.H.; Blyth, J.; Lowe, C.R. *Biosens. Bioelectron.* **2008**, 23(6), 899-905.

14. Kagie, A.; Bishop, D.K.; Burdick, J.; La Belle, J.T.; Dymond, R.; Felder, R.; Wang, J. *Electroanal.* **2008**, 20(14), 1610-1614.

15. Chu, M.X.; Kudo, H.; Shirai, T.; Miyajima, K.; Saito, H.; Morimoto, N.; Yano, K.; Iwasaki, Y.; Akiyoshi, K.; Mitsubayashi, K. *Biomed. Microdevices* **2009**, 11(4), 837-842.

16. Badugu, R.; Lakowicz, J.R.; Geddes, C.D. *Journal of Fluorescence* **2004**, 14(5), 617-633.

17. Badugu, R.; Lakowicz, J.R.; Geddes, C.D. *Current Opinion in Biotechnology* **2005**, 16(1), 100-107.

18. Sen, D.K.; Sarin, G.S. *Br. J. Ophthalmol.* **1980**, 64(9), 693-695.

19. LeBlanc, J.M.; Haas, C.E.; Vicente, G.; Colon, L.A. *Intens. Care Med.* **2005**, 31(10), 1442-1445.

20. Bindra, D.S.; Zhang, Y.N.; Wilson, G.S.; Sternberg, R.; Thevenot, D.R.; Moatti, D.; Reach, G. *Anal. Chem.* **1991**, 63(17), 1692-1696.

21. Gifford, R.; Batchelor, M.M.; Lee, Y.; Gokulrangan, G.; Meyerhoff, M.E.; Wilson, G.S. *J. Biomed. Mater. Res. A* **2005**, 75A(4), 755-766.

22. Geise, R.J.; Adams, J.M.; Barone, N.J.; Yacynych, A.M. *Biosens. Bioelectron.* **1991**, 6(2), 151-160.

23. Choy, C.K.M.; Benzie, I.F.F.; Cho, P. *Invest. Ophthalmol. Vis. Sci.* **2000**, 41(11), 3293-3298.

24. Choy, C.K.M.; Cho, P.; Chung, W.Y.; Benzie, I.F.F. *Optom. Vis. Sci.* **2003**, 80(9), 632-636.

25. Major, T.C.; Brant, D.O.; Reynolds, M.M.; Bartlett, R.H.; Meyerhoff, M.E.; Handa, H.; Annich, G.M. *Biomaterials* **2010**, 31(10), 2736-2745.

CHAPTER 6

CONCLUSIONS

6.1 Summary of Results for Dissertation Research

Tight glycemic control is beneficial not only for diabetic patients to reduce occurrences of complications, but also for non-diabetic critically ill patients to potentially achieve improved outcomes [1-5]. Continuous monitoring of blood lactate levels also plays an important role in the critical care medical setting. While the development of implantable glucose/lactate sensors has been the focus of many investigators over many years, success in this area has been hindered by biocompatibility problems, either thrombus formation when sensors are implanted within blood vessels, or encapsulation by immune cells when the sensors are implanted subcutaneously.

Nitric oxide (NO) has been found as a potent anti-thrombus and anti-inflammatory agent which naturally exists in many cells in the human body [6-10]. In this dissertation research, efforts have been made to develop intravascular glucose/lactate sensors with polymeric coatings capable of releasing NO from doped diazeniumdiolates or from generating NO from endogenous blood *S*-nitrosothiols (RSNOs), in the hope of improving the *in vivo* biocompatibility of the implantable

devices.

In Chapter 2, relatively thin NO releasing coatings for potential use as sensor coatings were developed using poly(lactide-*co*-glycolide) (PLGA) as the polymer matrix with *N*-diazeniumdiolated dibutylhexanediamine (DBHD/N_2O_2) doped as the NO donor. Such coatings with a top layer of PurSil can release NO for over one week at physiological levels (> 1×10^{-10} mol min^{-1} cm^{-2}), which is much longer than previously published coatings applied to implantable glucose sensors [11]. The most appropriate PLGA type, 50:50 RG 502 H, was chosen for future sensor studies due to its optimal NO release characteristics. The PLGA polymer to DBHD/N_2O_2 weight ratio was also optimized as 2:1.

In Chapter 3, intravascular glucose/lactate sensors with NO release were fabricated using the polymeric coatings examined in Chapter 2. *In vitro*, the NO release sensors showed excellent analytical performance required for real blood sample detection, in terms of having stable sensitivity over one week and high selectivity over major interferences, such as ascorbic acid. With the PLGA-based polymer coatings, the sensors can release NO on the surfaces at physiologically relevant levels for over 7 days. *In vivo* hemocompatibility of NO releasing glucose sensors was studied by implanting the sensors in rabbit veins for 8 hours. From digital pictures of explanted sensors, control sensors without NO release showed obvious thrombus formation on the surfaces while NO releasing sensors exhibited much cleaner surfaces, indicating enhanced biocompatibility. A quantitative method to analyze thrombus formation was applied by

using Image J software to measure the red pixel area of the pictures of the explanted sensors, and this imaging confirmed the enhanced biocompatibility of NO release sensors (vs. controls) with statistically significantly less thrombus formation on their surfaces. The NO releasing glucose sensors also showed greater accuracy in reporting blood glucose levels in comparison to the control sensors as seen in the Clarke error grid analysis of the *in vivo* data, where more glucose values fell into the accurate zones when correlated to readings from a bench-top instrument on drawn blood samples from the test animals.

In addition to releasing from doped donors, NO can also be catalytically generated from endogenous RSNO species. The NO generating chemistry was applied to implantable glucose/lactate sensors and the chemical compatibility was evaluated in Chapter 4. For the copper type catalysts, Cu(II)-cyclen-polyurethanes did not provide glucose sensors with a wide enough linear range due to their hydrophilicity, but they did not have any negative effects on the analytical performance of lactate sensors. However, the NO flux generated from endogenous levels of RSNOs was low and may not be enough to eliminate thrombus formation as expected. Copper nanoparticle-doped polyurethane was compatible with the glucose sensing chemistry and this coating exhibited the highest efficiency of catalytically generating NO from RSNOs. For the selenium catalyst, 100 bilayers of organoselenium immobilized polyethyleneimine (SePEI) and alginate (Alg) deposited on glucose sensor surfaces also showed a similar NO generation capability to that of Cu^0 nanoparticle-doped polyurethane while maintaining the analytical performance of the glucose sensors. Such coated sensors

were implanted in rabbit veins for 8 hours, but the preliminary results did not show the expected anti-thrombus property, likely due to the low RSNO levels in blood [12, 13]. However, since only two rabbits were tested, clear cut conclusions cannot be drawn at this point. Certainly, additional animal testing is needed to make a definitive assessment regarding the prospects of using the NO generating coatings on intravascular sensors. However, it is possible that the NO generating chemistry can only be applied in the situation where infusion of additional RSNOs is feasible in order to generate a high enough NO flux so that enhanced biocompatibility can be best realized.

Beyond implantable glucose sensors, tear glucose measurements have shown potential as a non-invasive method of monitoring blood glucose levels based on the correlation between glucose levels in blood and in tear fluids. In Chapter 5, a new and simple amperometric tear glucose biosensor coupled with a tear fluid collection capillary configuration was studied. The sensor exhibited excellent selectivity over major interferences, a low detection limit in the micromolar range, a wide dynamic range (up to one millimolar) and only requires ca. 5 μL of sample volume. The sensors were used to monitor glucose levels in tears from rabbits and the correlation between tear and blood glucose levels was established. The data analysis showed a significant correlation between tear and blood glucose levels, but the exact mathematic ratio between the two values varied from animal to animal. Hence, the use of tear fluids as an alternate sample to monitor blood glucose in human subjects is promising only if the appropriate algorithm of glucose in tears and blood can be established first for a given individual.

6.2 Future Work

The NO releasing coatings proposed in Chapter 2 showed promising anti-thrombotic applications onto other blood-contacting medical devices from the *in vivo* experiment results of NO releasing glucose sensors implanted in rabbit veins for 8 hours described in Chapter 3. Although the first lactate sensor was also formulated with an NO releasing coating, it has not yet been evaluated for *in vivo* performance. The chemistry of NO release using DBHD/N_2O_2-doped in PLGA did not interfere with the lactate sensing chemistry from the data presented in Chapter 3. As a result, the NO releasing lactate sensors implanted in blood vessels are expected to exhibit anti-thrombus forming surfaces, similar to NO releasing glucose sensors. Improved accuracy in continuously reporting blood lactate levels from sensors with NO release can also be expected compared to control sensors without any NO release.

In Chapters 2 and 3, PLGA was used as the matrix to sustain prolonged NO release from doped diazeniumdiolates, taking advantage of the slow hydrolysis process of PLGA to control the pH in the polymer. There are other polymers with anionic sites that can also be considered as appropriate matrices for long term NO release including the sulfonated polyurethane (PU-SO_3), based on the mechanism similar to the use of borate additives described in Chapter 2 [14]. The sulfonate anionic groups tethered to the PU backbones can also function as counter anions to the ammonium sites formed after NO is released from DBHD/N_2O_2 (Fig. 6.1). The advantage of using sulfonated PUs is that no additives are needed in the polymeric coatings and there are no additional species being

introduced to the system which might potentially influence the sensor performance. Tecoflex-SO_3 was successfully derivatized previously in our group according to a method described earlier [15]. Preliminary data of NO release from 33 wt% of DBHD/N_2O_2 doped in such a polymer coated on glucose sensors showed a prolonged NO release for 4 days (Fig. 6.2). Tecoflex-SO_3 is also promising because it did not show any negative effect on glucose sensing. In the future, the optimization of such polymer coatings on glucose sensors need to be further studied and such coatings can also be applied onto other implantable sensors as well. Enhanced biocompatibility of those sensors can also be expected from *in vivo* experiments.

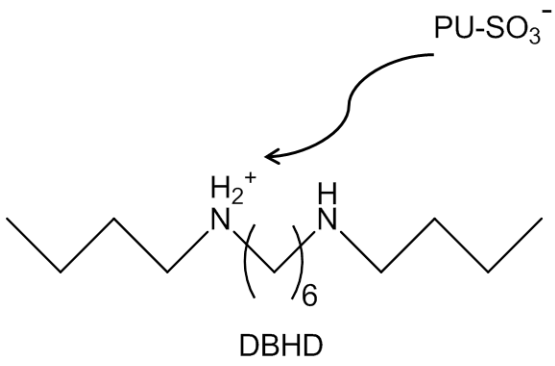

Figure 6.1 Schematic of sulfonated anionic sites in PU backbones working as counter anions to the ammonium groups of DBHD after NO is released.

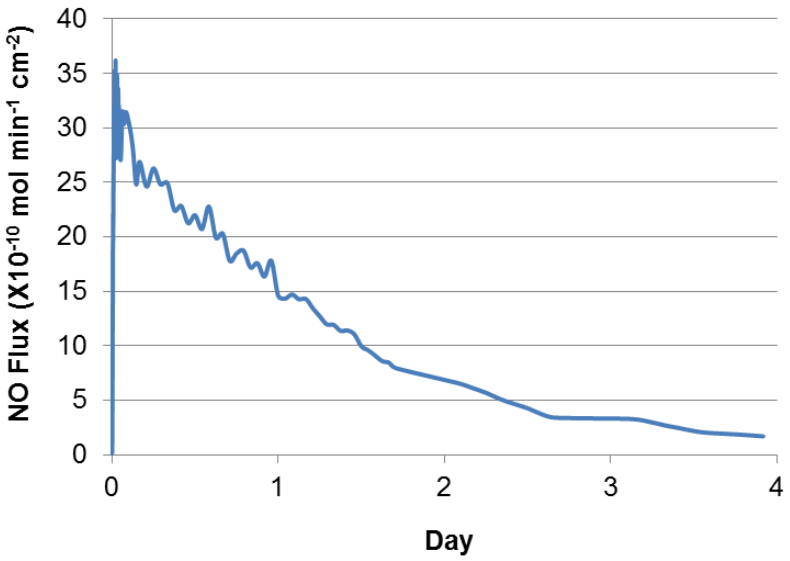

Figure 6.2. Nitric oxide release of glucose sensors coated with 33 wt% doped DBHD/N_2O_2 in Tecoflex-SO_3 over 4 days.

Considering the possibility that low endogenous RSNO levels might not generate adequate levels of NO to eliminate thrombus formation when using sensor coatings described in Chapter 4 that catalytically generate NO from RSNOs, alternate approaches based on using RSNO reservoirs in polymer materials may be needed. Indeed, RSNO species can also be considered as prospective NO donors for long-term NO release/generation purposes. It has been already reported in the literature that RSNO-modified xerogel films are able to release physiological levels of NO induced by thermal, photolytic, and copper ions [16]. These films also resisted platelet and bacterial adhesion because of the NO release. Thus it should be also be possible to dope RSNOs into PLGA films so that NO release can be well controlled for various biological applications. The advantage of using RSNOs is that they are naturally occurring species in the human body and hence the combination of NO release via embedded RSNOs and

the PLGA matrix will not form any toxic residuals after the NO is released, in comparison to the residual DBHD that exists when using diazeniumdiolates as the NO donors. DBHD may ultimately cause some toxicity issues if it is leaches out to any degree from the polymer [17]. As a result, PLGA films with doped RSNOs can be coated onto many medical devices with expected anti-thrombus and anti-inflammatory biological properties, without any concern about potential toxicity.

The glucose sensor proposed in Chapter 5 for tear glucose measurement needs to be further miniaturized so that only one microliter of tear fluid is needed for real applications. In that case, it might be difficult to obtain a steady-state amperometric current within the capillary due to the small amount of glucose in tear fluid which could potentially increase the error of reporting tear glucose concentrations. One alternative approach is to use a coulometric method to measure the total amount of hydrogen peroxide (H_2O_2) generated from the enzyme reaction that would deplete all the glucose in the tear sample. This can be accomplished by making the surface area of the sensing region larger relative to the volume of tear sample. In this way, the total amount of glucose contained in the tear fluid sample is measured by countying charge, instead of reaching some steady state current that can be influenced by thickness of membrane coatings, etc. Indeed, it is likely that the coulometric approach would yield a greater degree of accuracy for measuring tear glucose values and such an approach should be pursued.

6.3 References

1. Kondepati, V.R.; Heise, H.M. *Anal. Bioanal. Chem.* **2007**, 388(3), 545-563.

2. Bochicchio, G.V.; Scalea, T.M. *Serono. Sym.* **2008**, 42, 261-275.

3. Lonergan, T.; Le Compte, A.; Willacy, M.; Chase, J.G.; Shaw, G.M.; Wong, X.W.; Lotz, T.; Lin, J.; Hann, C.E. *Diabetes Technol. The.* **2006**, 8(2), 191-206.

4. Vanhorebeek, I.; Langouche, L.; Van den Berghe, G. *Chest* **2007**, 132(1), 268-278.

5. Schetz, M.; Vanhorebeek, I.; Wouters, P.J.; Wilmer, A.; van den Berghe, G. *J. Am. Soc. Nephrol.* **2008**, 19(3), 571-578.

6. Riddell, D.R.; Owen, J.S., **1999**, in *Vitamins and Hormones - Advances in Research and Applications*, Vol. 57, Academic Press Inc, San Diego, pp. 25-48.

7. D'Atri, L.P.; Malaver, E.; Romaniuk, M.A.; Pozner, R.G.; Negrotto, S.; Schattner, M. *Curr. Med. Chem.* **2009**, 16(4), 417-429.

8. Bogdan, C. *Nat. Immunol.* **2001**, 2(10), 907-916.

9. Moncada, S.; Palmer, R.M.J.; Higgs, E.A. *Pharmacol. Rev.* **1991**, 43(2), 109-142.

10. Guzik, T.J.; Korbut, R.; Adamek-Guzik, T. *J. Physiol. Pharmacol.* **2003**, 54(4), 469-487.

11. Gifford, R.; Batchelor, M.M.; Lee, Y.; Gokulrangan, G.; Meyerhoff, M.E.; Wilson, G.S. *J. Biomed. Mater. Res. A* **2005**, 75A(4), 755-766.

12. Giustarini, D.; Milzani, A.; Colombo, R.; Dalle-Donne, I.; Rossi, R. *Clin. Chim. Acta* **2003**, 330(1-2), 85-98.

13. Wu, Y.D.; Cha, W.S.; Zhang, F.H.; Meyerhoff, M.E. *Clin. Chem.* **2009**, 55(5), 1038-1040.

14. Batchelor, M.M.; Reoma, S.L.; Fleser, P.S.; Nuthakki, V.K.; Callahan, R.E.; Shanley, C.J.; Politis, J.K.; Elmore, J.; Merz, S.I.; Meyerhoff, M.E. *J. Med. Chem.* **2003**, 46(24), 5153-5161.

15. Grasel, T.G.; Cooper, S.L. *J. Biomed. Mater. Res.* **1989**, 23(3), 311-338.

16. Riccio, D.A.; Dobmeier, K.P.; Hetrick, E.M.; Privett, B.J.; Paul, H.S.; Schoenfisch, M.H. *Biomaterials* **2009**, 30(27), 4494-4502.

17. http://www.chemcas.com/msds/cas/msds62/4835-11-4.asp.